Fakultät für Medizin

Novel treatment options for chronic hepatitis B: Therapeutic vaccination and interferon-mediated cccDNA degradation

Martin Kächele

Vollständiger Abdruck der von der Fakultät für Medizin der Technischen Universität München zur Erlangung des akademischen Grades eines

Doktors der Naturwissenschaften (Dr. rer. nat.)

genehmigten Dissertation.

Vorsitz: Prof. Dr. Susanne Kossatz

Prüfer*innen der Dissertation:

1. Prof. Dr. Ulrike Protzer
2. Prof. Dr. Michael Sattler

Die Dissertation wurde am 26.07.2021 bei der Technischen Universität München eingereicht und durch die Fakultät für Medizin am 12.10.2021 angenommen.

Table of contents

Abbreviations

Adeno-associated virus	AAV
Adenovirus	AV
Adverse events	AE
Alanine aminotransferase	ALT
Apolipoprotein B mRNA editing enzyme, catalytic polypeptide-like 3A	APOBEC3A, A3A
Apolipoprotein B mRNA editing enzyme, catalytic polypeptide-like 3B	APOBEC3B, A3B
Chicken embryo fibroblast	CEF
Chorioallantois vaccinia virus Ankara	CVA
Covalently closed circular DNA	cccDNA
Cullin 4	CUL4
Cytomegalovirus	CMV
Cytotoxic T lymphocyte	CTL
Dendritic cell	DC
Dengue virus	DENV
DNA damage-binding protein 1	DDB1
Duck hepatitis B virus	DHBV
Endoplasmatic reticulum	ER
Endosomal sorting complex	ESCRT
Entecavir	ETV
Heparin sulfate proteoglycans	HSPG
Hepatitis B virus	HBV
Hepatitis B virus core protein	HBc
Hepatitis B virus e antigen	HBeAg
Hepatitis B virus s antigen	HBsAg
Hepatitis B virus X protein	HBx
Hepatitis C virus	HCV
Hepatocellular carcinoma	HCC
Histone 3	H3
Histone 4	H4

Histone acetyl transferase	HAT
Histone deacetylase	HDAC
Human immunodeficiency virus	HIV
Human papilloma virus	HPV
IFN-inducible RNA-dependent protein kinase	PKR
IFN-regulated factor 9	IFN9
IFN-stimulated gene factor 3	ISGF3
IFNγ-activated sites	GAS
Immunofluorescence	IF
Infectious units	IFU
Interferon alpha	IFNα
Interferon beta	IFNβ
Interferon gamma	IFNγ
Interferon stimulated gene	ISG
Interferon-stimulated response elements	ISRE
Intracellular cytokine staining	ICS
Janus activated kinase	JAK
Japanese encephalitis virus	JEV
Lymphotoxin beta receptor	LTβR
Lysine demethylase	KDM
Lysine methyltransferase	KMT
Major histocompatibility complex I	MHC I
Major histocompatibility complex II	MHC II
Modified vaccinia Ankara	MVA
Multiplicity of infection	MOI
Multi-vesicular body	MVB
Natural killer cells	NK cells
NEDD8-activating enzyme	NAE
Nucleos(t)ide analogue	NUC
Open reading frame	ORF

Interferon stimulated gene 20 protein	ISG20
Pathogen associated molecular pattern	PAMP
Pattern recognition receptor	PRR
Pegylated interferon alpha	pegIFNα
Post-translational modification	PTM
Pre-genomic RNA	pgRNA
Primary human hepatocytes	PHH
Professional antigen presenting cell	APC
Promyelocytic leukiaemia	PML
Relaxed-circular DNA	rcDNA
Retinoic acid inducible gene	RIG-I
Sendai virus	SeV
Severe acute respiratory syndrome coronavirus	SARS-CoV
Sodium taurocholate cotransporting polypeptide	NTCP
Toll-like receptor	TLR
Trichostatin A	TSA
Tripartite motif-containing	TRIM
Tumor necrosis factor alpha	TNFα
Tyrosine kinase 2	TYK2
Vesicular stomatitis virus	VSV
Wildtype	WT
Woodchuck hepatitis virus	WHV
Yellow fever virus	YFV

Abstract

With around 257 million chronically infected people and 887.000 deaths per year, hepatitis B virus (HBV) infection is a major global health problem. Treatment with nucleos(t)ide analogues, which interfere with viral transcription, requires long term medication due to the persistence of the viral covalently closed circular DNA (cccDNA) in the nucleus of infected cells. Therefore, the aim of this thesis was the development of a therapeutic vaccine against chronic hepatitis B, which supports the induction of a strong, polyclonal T-cell response capable of killing infected hepatocytes as well as mediating cccDNA degradation via interferon secretion.

The first part of the thesis describes the establishment of a viral vaccine vector termed MVA HBVac under GMP-like conditions. The vector supported the expression of five different HBV atigens from a polycistronic insert while retaining the growth, stability and safety hallmarks necessary for industrial scale amplification. *In vivo* testing of MVA HBVac in conjunction with an adjuvanted protein prime led to the induction of strong antibody and T-cell responses in naïve C57BL/6 mice. Most importantly, when used in the AAV-HBV mouse model, administration of the therapeutic vaccine strategy resulted in the loss of viral antigens from the serum as well as transient elevation of ALT levels, indicating the killing of infected hepatocytes. Due to the promising results, the vaccine was approved for evaluation in clinical trials and is expected to enter a phase I trial in the fourth quarter of 2021.

The second part of this thesis aimed at clarifying potential connections between the conformation of cccDNA and its susceptibility towards T-cell cytokine mediated degradation. The results demonstrated that active transcription from cccDNA was required to allow targeting of the molecule by interferon induced deaminase APOBEC3A. Shifting the cccDNA into a closed conformation by blocking virus mediated SMC5/6 degradation completely abrogated interferon mediated cccDNA decay. On the other hand, changing the cccDNA conformation by targeting its epigenetic state did not affect the interferon mediated loss of cccDNA despite effectively regulating viral transcription.

The final part of the thesis was focused on interferon stimulated gene 20 protein (ISG20), which plays a crucial role in the cytokine mediated loss of cccDNA. ISG20 was demonstrated to accumulate in the nucleoli of interferon stimulated hepatocytes, a mechanism still active after infection with HBV. Although HBVcore also accumulated in nuclei there was no direct interaction detectable between ISG20 and the viral core protein. However, analysis of nucleoli isolated from HBV transgenic cells detected a high amount of viral DNA which was further increased upon treatment with interferon indicating that the process of ISG20 mediated cccDNA degradation, at least partially, occurs inside of the nucleoli.

Overall, the results from this thesis demonstrated the establishment of a novel viral vaccine vector capable of inducing strong and polyclonal T-cell responses. Activated T cells were shown to efficiently kill infected hepatocytes while simultaneously causing non-cytolytic loss of cccDNA via the secretion of type II interferon. In contrast, infected cells harboring inactive cccDNA molecules could not be efficiently targeted by either of these mechanisms, offering a potential explanation for the persistence of cccDNA in hepatocytes of patients with resolved HBV infection and at the same time providing a starting point for potential therapy improvements towards an HBV cure.

Zusammenfassung

Mit etwa 257 Millionen chronisch infizierten Menschen und 887.000 Todesfällen pro Jahr ist das Hepatitis B Virus (HBV) weiterhin ein großes Problem für die weltweite Gesundheit. Zur Behandlung werden momentan verschiedene Nukleos(t)id Analoga verwendet, die zwar die virale Transkription blockieren, aber keinen Einfluss auf die persistente virale cccDNA haben. Dies macht eine langfristige Medikamenteneinnahme erforderlich. Das Ziel dieser Arbeit war die Entwicklung eines therapeutischen Impfstoffs, der eine starke, polyklonale T-Zell Antwort induziert, welche einerseits infizierte Hepatozyten abtötet und gleichzeitig via Interferonsekretion den nicht zytotoxischen Abbau viraler cccDNA induziert.

Im ersten Teil der Arbeit wurde die Herstellung eines viralen Impfstoffvektors mit dem Namen MVA-HBVac unter GMP-ähnlichen Bedingungen gezeigt. Der Vektor erlaubte die Expression aller fünf gewünschten HBV Antigene aus einem polycistronischen Insert unter Beibehaltung der Wachstums-, Stabilitäts- und Sicherheitsmerkmale, die für eine Vervielfältigung im industriellen Maßstab und die anschließende Anwendung im Menschen erforderlich sind. Bei *in vivo* Testung in naiven C57BL/6 Mäusen verursachte MVA-HBVac im Zusammenspiel mit einem adjuvantierten Protein Prime die Induktion starker Antikörper- und T-Zell Antworten. Die Verwendung der therapeutischen Impfstrategie in einem AAV-HBV Mausmodell führte zum Verlust viraler Antigene im Serum sowie einer vorübergehenden Erhöhung der ALT-Werte, was auf die gezielte Abtötung infizierter Hepatozyten hinweist. Aufgrund dieser vielversprechenden Ergebnisse wurde MVA-HBVac zur Testung im Rahmen einer klinischen Studie zugelassen, welche voraussichtlich im vierten Quartal 2021 starten wird

Der zweite Teil dieser Arbeit konzentrierte sich auf mögliche Zusammenhänge zwischen der Konformation der cccDNA und ihrer Anfälligkeit gegenüber Interferon vermittelter Degradation. Die Ergebnisse zeigten, dass cccDNA transkriptionell aktiv sein musste, um durch die Interferon-induzierte Deaminase APOBEC3A angegriffen werden zu können. Die Verschiebung der cccDNA in eine geschlossene Konformation durch die Blockade der virusvermittelten SMC5/6-Degradation negierte die Interferon-vermittelte cccDNA Degradation vollständig. Eine Änderung der cccDNA Konformation mittels epigenetischer Modifikation zeigte jedoch keinerlei Einfluss auf den Interferon-vermittelten Verlust von cccDNA obwohl die virale Transkription effektiv reguliert wurde.

Der letzte Teil der Arbeit konzentrierte sich auf das Interferon-stimulierte Gen 20-Protein (ISG20), das eine entscheidende Rolle beim Interferon-vermittelten Verlust von cccDNA spielt. Wir konnten zeigen, dass sich ISG20 in den Nukleoli von Interferon-stimulierten Hepatozyten anreicherte, ein Mechanismus der durch HBV nicht beeinflusst wurde. Des Weiteren konnten wir zeigen, dass keine direkte

Interaktion zwischen ISG20 und dem viralen Kapsidprotein nachweisbar war. Die Analyse von Nukleoli isoliert aus HBV transgenen Zellen zeigte jedoch größere Mengen an viraler DNA, die bei Behandlung mit Interferon weiter erhöht wurden. Dies deutet darauf hin, dass zumindest ein Teil des Interferon-vermittelten cccDNA Abbauprozesses in den Nukleoli stattfindet.

Zusammengefasst demonstrieren die Ergebnisse dieser Arbeit die Schaffung eines neuartigen viralen Impfstoffvektors, der in der Lage ist, starke und polyklonale T-Zell-Antworten zu induzieren. Diese aktivierten T-Zellen sind sowohl in der Lage infizierte Hepatozyten zu erkennen und abtöten als auch einen nicht zytotoxischen Interferon-vermittelten Abbau von cccDNA zu induzieren. Infizierte Zellen, die transkriptionell inaktive cccDNA beherbergen, können jedoch durch keinen der beiden Mechanismen effizient bekämpft werden. Diese Ergebnisse bieten eine mögliche Erklärung für das Vorhandensein von cccDNA in Hepatozyten von Patienten, welche die Ifnektion erfolgreich überwunden haben und stellen gleichzeitig einen Ansatzpunkt für mögliche Therapieverbesserungen dar.

1.   Introduction

Hepatitis B virus (HBV) is a widespread, major human pathogen that infects the hepatocytes of its host. Depending on age and immune status of the affected individual, infection with HBV can lead to either acute or chronic disease progression. There are currently around 257 million people chronically infected with HBV and these individuals have an increased risk to develop severe health conditions like liver cirrhosis or hepatocellular carcinoma (HCC) resulting in around 887,000 deaths per year [1]. Treatment of chronic hepatitis B using pegylated interferon alpha (pegIFNα) or nucleos(t)ide analogues (NUCs) is possible, however cure rates are low and most patients require life-long medication to prevent viral resurgence [2]. Novel treatment approaches for chronic hepatitis B are therefore urgently needed. The first part of this theses is focused on the development and testing of a novel vaccine vector for therapeutic application in chronic hepatitis B while the second part takes a closer look at one of the cytokine-mediated antiviral mechanisms which can be induced by activated T-cells.

1.1.   The hepatitis B virus

Since this thesis is focused on the development of a therapeutic vaccine and the understanding of cytokine-mediated mechanisms against the hepatitis B virus, the following chapters will introduce the basic biology of HBV.

1.1.1.   Hepatitis B virus taxonomy and global distribution

Hepatitis B virus is a member of the *Orthohepadnavirus* genus which contains several other species such as the woodchuck hepatitis virus (WHV) or the duck hepatitis B virus (DHBV). All members of this genus differ from each other by a whole genome sequence divergence of at least 20%. *Orthohepadnavirus* together with five other genera (*Avihepadnavirus*, *Herpetohepadnavirus*, *Metahepadnavirus*, *Parahepadnavirus*) form the family of *Hepadnaviridae* where each genus differs from each other by a nucleotide sequence divergence of roughly 55 % [3]. All members of this virus family are hepatotropic and can cause acute as well as chronic infections. They are enveloped, possess a small, partially double-stranded DNA genome and replicate via reverse transcription. On a megataxonomy scale, the *Hepadnaviridae* are a member of the realm of *Riboviria* and belong to the order of *Blubervirales* [4].

HBV encompasses nine different genotypes (A, B, C, D, E, F, G, H, I) which are set apart by differences in their nucleotide sequence. Each genotype differs from each other by at least 7.5 %, in addition sub-genotypes have been defined which show at least 4 % intragenotype divergence [5, 6]. Furthermore,

HBV can be subdivided into nine different serotypes (*ayw1, ayw2, ayw3, ayw4, ayr, adw2, adw4q-, adrq, adrq-*) based on amino acid variations in the viral surface proteins [7].

The genotypes differ in their behavior as well as in their responsiveness towards treatment [8]. For example, patients infected with HBV genotype C showed an increased chance to develop a chronic infection when compared to individuals infected with genotype B [9]. Similar effects can also be observed when analyzing the antiviral response rates in patients receiving pegIFNα. Persistent clearance of viral hepatitis B virus e antigen (HBeAg) and hepatitis B virus s antigen (HBsAg) upon treatment is more likely to be achieved in patients infected with serotype A than serotype E [10, 11].

Hepatitis B virus occurs in basically every country worldwide and around 3.6 % of the total global population show HBsAg seroprevalence, which serves as a marker of HBV infection. When looking at the six different WHO regions, the highest number of incidences can be found in the African (8.83 %) and Western Pacific (5.26 %) regions. However, variability within these groups can be quite large, such as between the Seychelles (0.48 %) and South Sudan (22.38 %) which are both members of the African region [12].

Similar to the number of infections, the different HBV genotypes are not evenly spread around the world. Instead their distribution is based on ancient human migration and subsequent divergent evolution [13, 14].
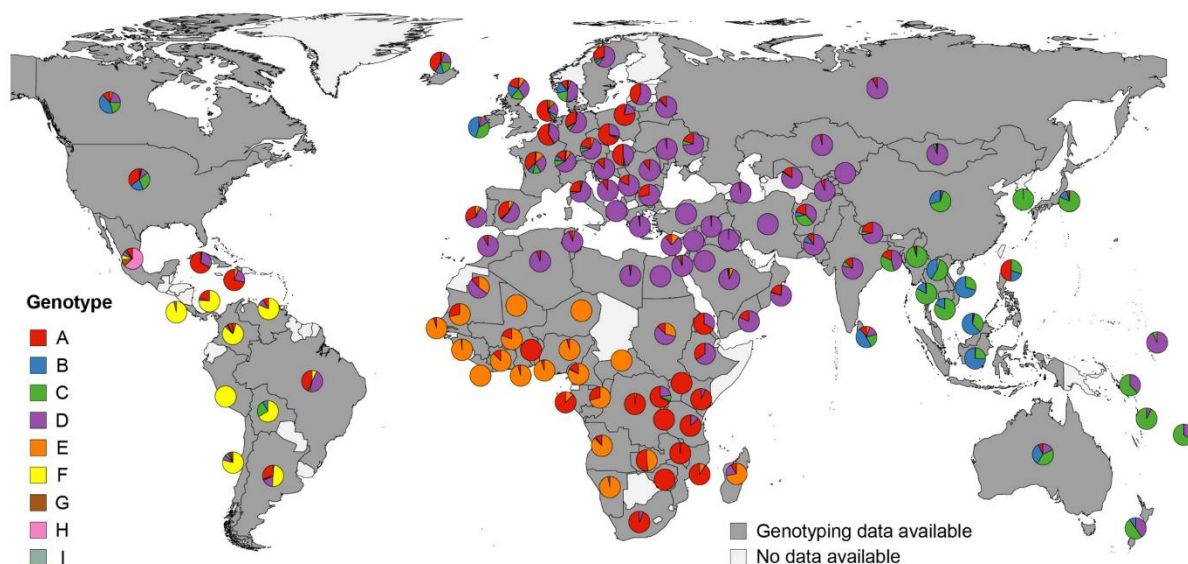
Figure 1: Global frequency of the different HBV genotypes. Genotype distribution per country is indicated by the colored pie charts. Countries where only insufficient data are available are shown in white. Adapted from Velkov et al. [15].

For example, genotype F exists nearly exclusively in southern America and is responsible for the majority of infections in countries like Chile, Peru or Colombia. In Brazil on the other hand most cases

of hepatitis B are caused by either genotype A or D, a distribution very similar to the one observed in most of the Western European countries. The African continent can be roughly divided into three areas: HBV genotype D circulates in northern Africa, genotype E in Western Africa and genotype A can be found mostly in the eastern parts of the African continent. Genotypes B and C are prevalent in many Asian countries such as China or Indonesia (Figure 1). Taken together the five major genotypes A (16.9 %), B (13.5 %), C (26.1 %), D (22.1 %) and E (17.6 %) are estimated to be responsible for about 96.2 % of global HBV infections [15]. The information outlined above is especially relevant in the context of drug development, since global applicability of any future treatment options against chronic hepatitis B is dependent on its ability to efficiently target as many genotypes as possible [16].

1.1.2. Composition of the viral particle

Infectious viral particles of HBV were first discovered in 1970 and are also referred to as Dane particles, named after their discoverer D. SA. Dane [17]. They appear as 42 nm sized particles, consisting of an outer lipid envelope containing a capsid structure. The viral envelope contains three different surface proteins (S, M, and L) which are encoded on the same ORF and share a common C terminus, but vary in their N termini due to different transcription and translation initiation sites (Figure 2).

L protein	preS1 domain	preS2 domain	S domain

M protein		preS2 domain	S domain
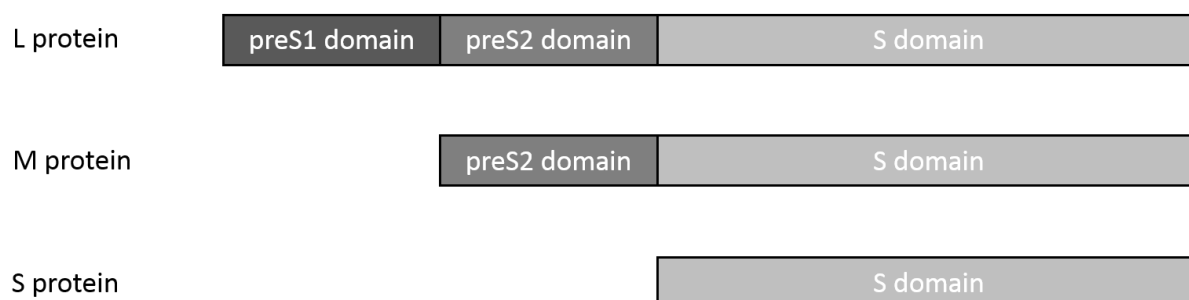
S protein			S domain

Figure 2: The three viral surface proteins of HBV. The L protein contains three domains: PreS1, preS2 and S and has a size of 389 aa or 400 aa, depending on the genotype. The M protein contains only the preS2 as well as the S domain and consist out of 281 aa. The smallest of the three, the S protein contains only the S domain and is 226 aa long [18].

The viral capsid is a homomultimer consisting of viral core proteins. Those proteins first form dimers through di-sulfide linkage before their self-assembly into complete viral capsids [19, 20]. Two distinct forms of HBV capsids are described which differ in their symmetry: The T3 symmetric capsid which contains 90 as well as the T4 symmetric capsid which contains 120 core dimers [21]. So far, only T4 capsid containing viral particles have been shown to be infectious [22]. Inside the capsid the partially double-stranded DNA genome of HBV, which is also called relaxed-circular DNA (rcDNA), is packaged (Figure 3). The viral polymerase is covalently attached to the 5' end of the rcDNA [23].
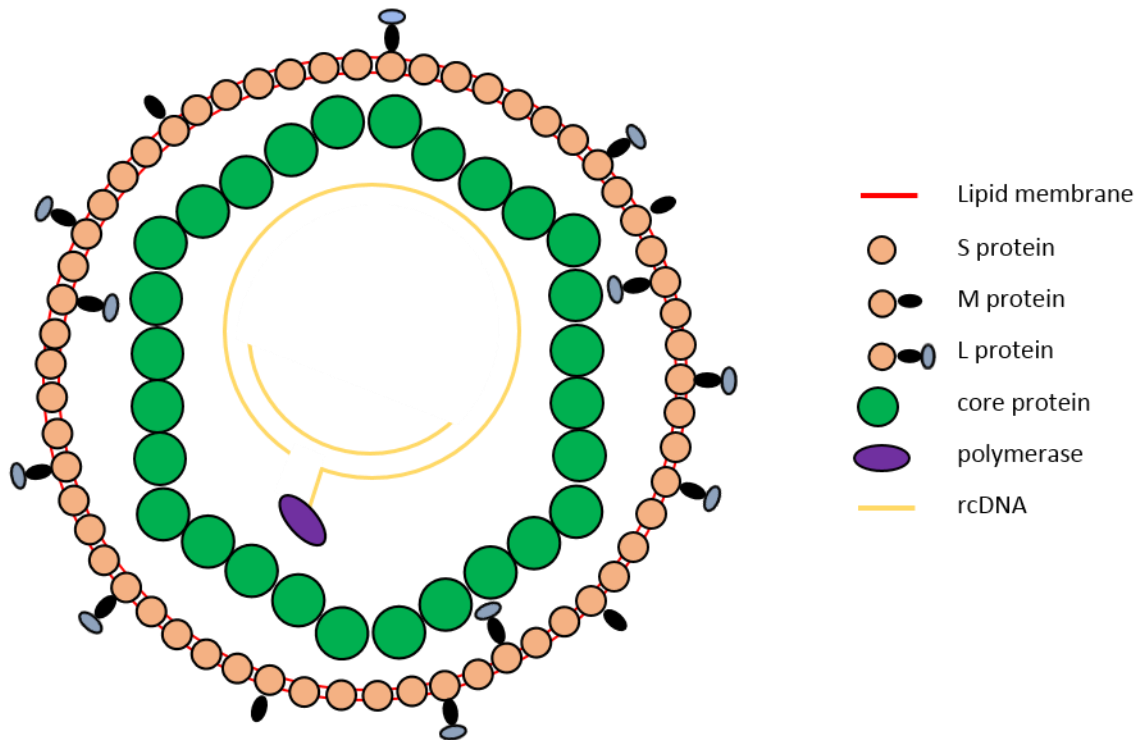
Figure 3: Structure of an infectious HBV particle. The envelope of the particle is formed by a lipid bilayer containing the viral surface proteins S, M and L. It contains the viral capsid which is formed by disulfide-linked core protein dimers. Inside of the capsid, the viral rcDNA, which is covalently linked to the viral polymerase, is stored.

In addition to infectious virions, HBV infected cells also secrete non-infectious subviral particles (SVPs), which can be divided into two subgroups: Empty subviral particles that contain only the viral surface proteins and appear in the forms of spheres and filaments or genome free viral particles containing a capsid but no viral genome [24, 25].

1.1.3. The viral replication cycle

During the first step of the viral replication cycle, an infectious HBV particle unspecifically attaches to the heparin sulfate proteoglycans (HSPG) on the cell surface, followed by a specific interaction with the receptor sodium taurocholate cotransporting polypeptide (NTCP) [26].This receptor is expressed exclusively on hepatocytes, located on their basolateral membrane and is one of the factors responsible for HBVs highly selective hepatotropsim [26, 27]. The virion binds to NTCP via the L proteins preS1 domain and triggers endocytosis, leading to the uptake of the viral particle into the cell [28]. After entering the cell, the viral particle escapes the endosome using an unknown mechanism. During this endosomal escape, the viral capsid is released from its envelope and then transported to the nuclear membrane. Upon arrival, the capsid interacts with one of the nuclear pore complexes and dissociates, thereby supporting rcDNA internalization into the nucleus [29, 30]. After entering the

nucleoplasm, the viral genome is repaired by cellular DNA repair enzymes to the covalently closed circular DNA (cccDNA), forming an episomal minichromosome (Figure 4) [31].
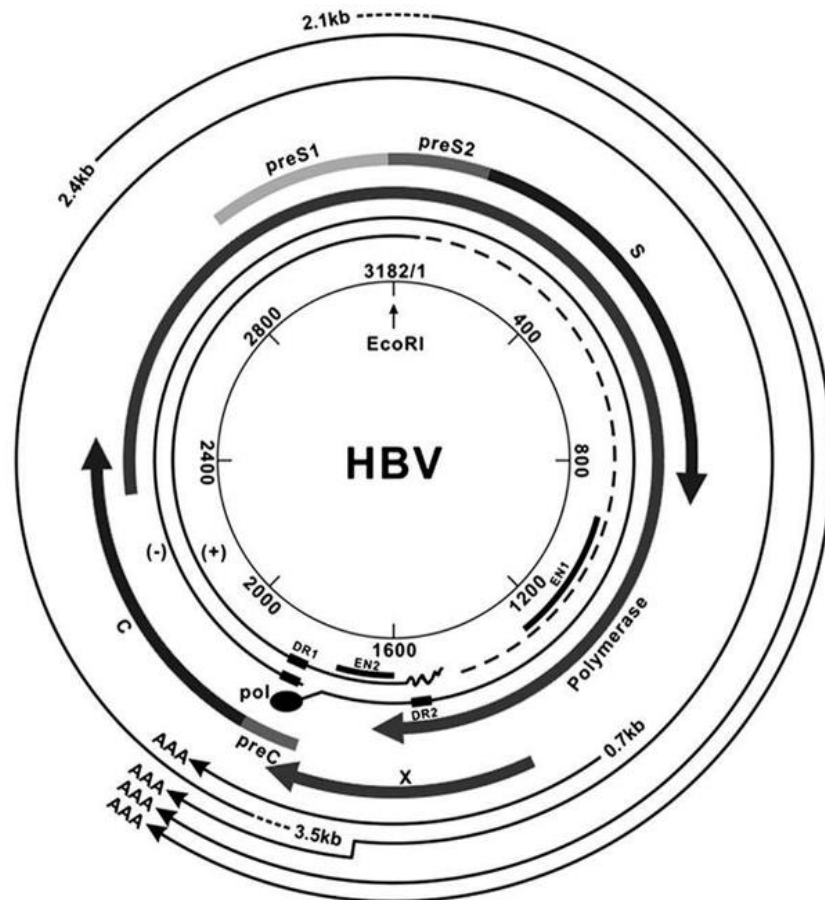
Figure 4: Structure of the viral rcDNA genome. The four outer circles depict the four types of viral RNAs which can be transcribed from cccDNA. Pre-core mRNA and pgRNA (3.5 kb), L mRNA (2.4 kb), S/M mRNA (2.1 kb) and X mRNA (0.7 kb) share a common poly-A tail as indicated. The four protein coding open reading frames (ORFs) are indicated by big arrows. The two innermost circles represent the viral rcDNA and show the viral enhancer regions (EN1/ EN2), the direct repeats DR1/2 as well as the covalently bound viral polymerase (pol). Adapted from Protzer, Schaller et al.[32].

The cccDNA molecule functions as the viral persistence form and is extremely stable. Results obtained from the woodchuck hepatitis virus and duck hepatitis B virus models indicate an average half-life approximately between 33 and 57 days [33, 34]. Similar timeframes are observed in the human HepG2-NTCP cell line were a half-life of 40 days was determined [35]. After establishment, the cccDNA serves as transcription template for all viral RNAs: the 3.5 kb pre-core and pre-genomic RNAs (pgRNA) coding for the pre-core, core and polymerase proteins, two RNAs (2.4 kb and 2.1 kb) coding for L, M and S and a 0.7 kb RNA coding for the hepatitis B virus X protein (HBx). Upon expression of the viral proteins, the viral polymerase binds to free pgRNA molecules in the cytoplasm and triggers encapsidation by core proteins followed by reverse transcription into rcDNA [36]. These matured, rcDNA containing, cytoplasmic capsids are now able to follow two different pathways: intracellular recycling to the

nucleus or release. The first leads to the transport of mature viral capsids back to the nuclear pore. Similar to incoming capsid from HBV particles, this causes rcDNA release and establishment of new cccDNA molecules. Alternatively, viral capsids can interact with the viral surface proteins embedded into the endoplasmatic reticulum (ER) membrane [35, 37]. Currently, it is not known why exclusively matured capsids are able to interact with the surface proteins. One explanation could be the influence of different phosphorylation patterns [38]. During the budding process, L proteins which are located on the cytosolic side of the ER membrane directly interact with the viral capsid while the L proteins on the cisternal side will be responsible for NTCP binding later on [39]. The exact mechanism, leading to the release of viral and subviral particles from the ER is still under investigation, but involvement of the endosomal sorting complex (ESCRT) as well as the formation of multi-vesicular bodies (MVB) has been suggested [40, 41].
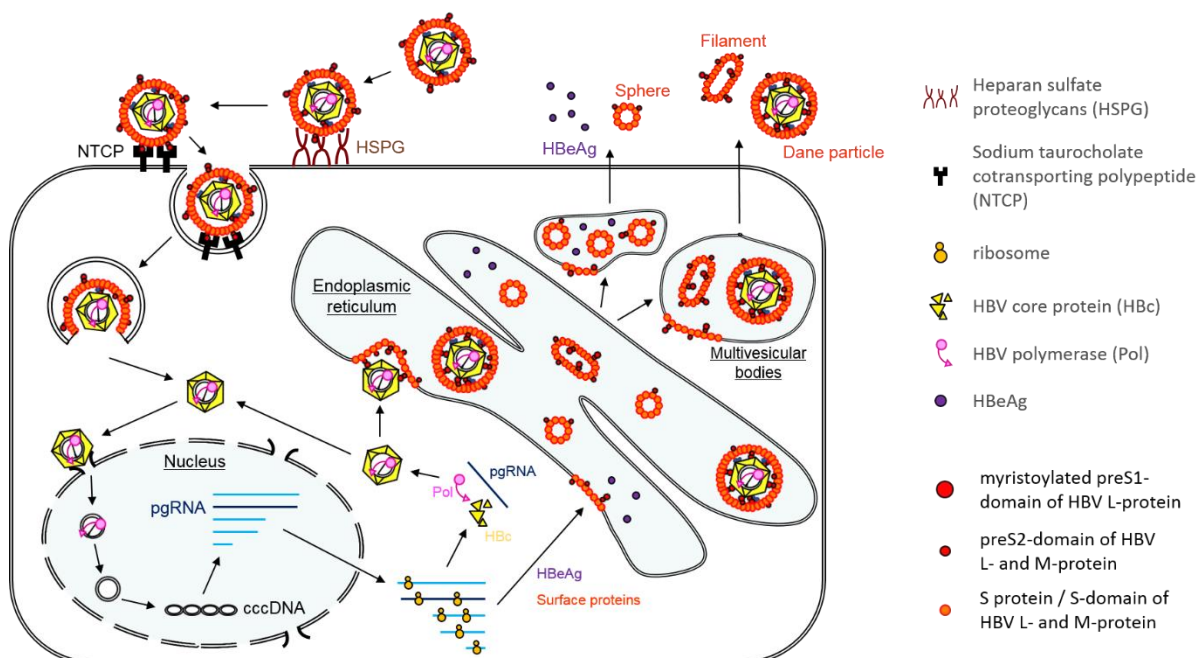
Figure 5: The replication cycle of hepatitis B virus. After unspecific attachment to the cell surface via HSPG, viral particles bind to their specific receptor NTCP and enter the cell via endocytosis. HBV virions lose their envelope during endosomal escape and the naked capsids get transported to the nuclear pore complex. Capsid disassembly happens inside of the nuclear pore, leading to release of rcDNA into the nucleoplasm followed by its conversion into cccDNA. The newly established viral episome serves as a viral persistence form as well as a transcription template for all viral RNAs. Expression of pgRNA and viral proteins leads to capsid assembly in the cytoplasm of infected cells followed by conversion of pgRNA into rcDNA. The mature capsids can now either be transported back to the nucleus to maintain the cellular cccDNA pool or be enveloped and secreted via the ER and multivescular bodies. Adapted from Ko et al. [42].

1.1.4. Episomal organization of cccDNA

In addition to changes in its base pair sequence, DNA can also be altered by mechanisms that induce non-permanent changes in its chromatin structure, a process that is collectively described as

epigenetics [43]. For example, modification of the N-terminal tails of DNA associated histones is a well-established fact for the human genome and has been shown to play an important role in the regulation of the transcriptional activity of certain DNA regions [44]. Histone tails can be modified by adding a variety of post-translational modifications (PTMs), with the most studied modifications being methylation and acetylation. Addition or removal of these groups is mediated by cellular enzymes like histone acetyl transferases (HAT), histone deacetylases (HDAC), lysine methyltransferases (KMT) or lysine demethylases (KDM). By targeting specific residues of the N-terminal histone tails the aforementioned enzymes create highly complex patterns of differently modified nucleosomes. The exact impact of these modifications is still under investigation; however, as a general rule, high numbers of acetylated histone 3 (H3) and histone 4 (H4) tails mark areas of high transcriptional activity, while areas without acetylated histones tend to be transcriptionally repressed. A similar rule exists for methylation, but in this case the position of the modified amino acid needs to be considered: Histone 3 tails which are polymethlyated at the lysine 4 (K4) position are associated with active transcription, while polymethylations at the positions K9 and K27 of histone 3 are associated with repressed transcription [44, 45].

Similar to cellular DNA, cccDNA adopts a chromosome-like structure by associating with a wide range of viral and cellular proteins including histones [46, 47]. Association of histones and the cccDNA does not occur randomly, instead certain sequences are preferentially protected by nucleosomes arguing for a level of epigenetic regulation of cccDNA activity (Figure 6) [48].
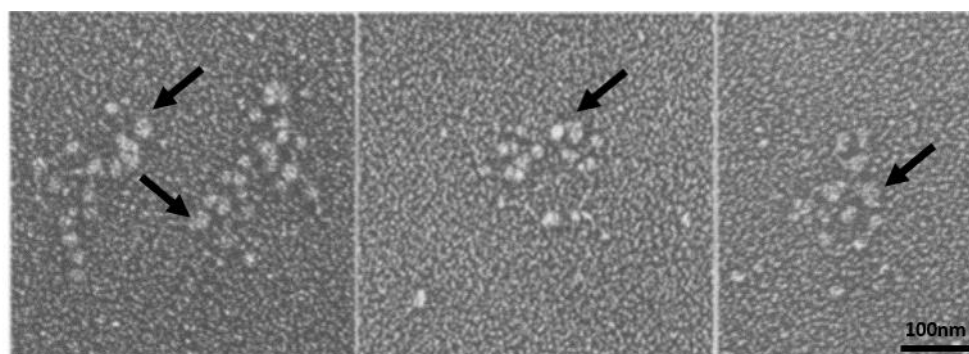
Figure 6 Nucleosomes attached to viral cccDNA. The nucleoprotein complexes were purified by sucrose gradient centrifugation and analyzed by electron microscopy. Arrows indicate nucleosomes bound to cccDNA. The bar represents 100nm. Adapted from Bock et al. [46].

Congruent to the situation in cellular DNA, data collected from patients shows that hyperacetylation of the cccDNA bound histones correlates with high viremia while HDAC recruitment and hypoacetylation are associated with low levels of viremia [49]. Similar results obtained *in vitro* indicate that the transcriptional activity of cccDNA is directly linked to its epigenetic state and that HBV specifically targets proteins necessary to maintain an active chromatin conformation [50]. The major

regulator of this process is the viral HBx, which was shown to recruit the HATs p300, PCAF/GCN5 and CBP to the cccDNA leading to hyperacetylation and transcriptional activity (Figure 7). Loss of HBx expression hinders recruitment of HATs, increases recruitment of HDACs and results in transcriptional repression [51]. However, changes in the epigenetic state of the cccDNA are not solely dependent on viral proteins and instead can be caused by a variety of signals. Type I interferons for example have been shown to repress viral transcription and reduce the number of acetyl PTMs by recruiting HDAC1 to the cccDNA [52-54].
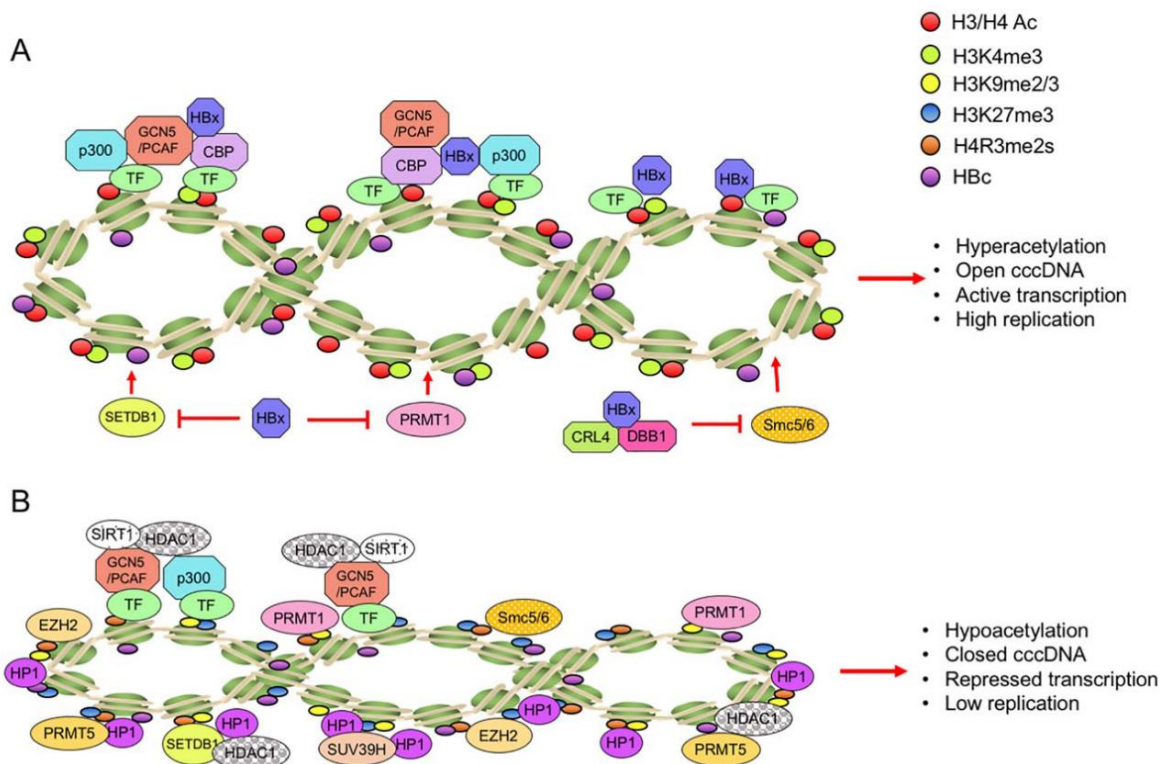
Figure 7: Regulation of the cccDNAs epigenetic state and structure by HBx and its influence on transcriptional activity. (A) HBx recruits HATs to the cccDNA leading to hyperacetylation while simultaneously blocking enzymes necessary for transcriptional inactivation of cccDNA. Under these circumstances, cccDNA shows an open conformation leading to increased expression of viral proteins as well as viral replication. (B) Lack of HBx protein leads to hypoacetylation of cccDNA as well as binding of repressive cellular proteins and results in a loss of viral transcription. Adapted from Hong et al. [50].

The influence of HBV infection on histone modification is not limited to the cccDNA and epigenetic changes in cellular chromosomes have been described as an important factor in HBV-induced carcinogenesis [55]. Drugs capable of changing the epigenetic state of cells by blocking HATS or HDACs are currently being tested in clinical trials against cancers and have shown viable results [56]. While originally developed to change the cellular chromatin, these drugs might also be able to efficiently influence cccDNAs epigenetic state. Compared to the currently available NA treatment, which fails to efficiently reduce production of viral proteins, silencing or enhancing transcription might offer

interesting new approaches towards direct targeting of cccDNA. Due to the mechanism of action, this will however only result in a silencing but not in a loss of cccDNA.

Except for histone modification, HBV uses several other additional mechanisms to influence the chromatin structure of cccDNA. For example, hepatitis B virus core protein (HBc), an important component of cccDNA minichromosome, has been shown to influence its structure by reducing nucleosome spacing by around 10% when comparing genomic and cccDNA. Similar observations have also been made for other viral minichromosomes and associated proteins, however their impact is still under investigation [51, 53].

1.1.5. Regulation of transcriptional activity

In addition to epigenetics and its chromosomal structure, transcription from cccDNA is regulated by the four different viral promoters as well as two viral enhancer sequences (see also Figure 4) [57]. Binding of different transcription factors such as COUP-TF1/2, TR2/4, and HNF4 can up-or down-regulate expression of viral RNAs, strongly affecting the progression of the viral infection [58, 59]. Another major regulator of transcriptional activity during natural infection is the viral X protein [60]. HBx deficient HBV is strongly attenuated *in vitro* and *in vivo* and infected cells show only very limited or no expression of viral RNAs and proteins [61, 62]. The observed pro-transcriptional activity of HBx is not limited to the cccDNA, and HBx induced activation of cellular genes has also been demonstrated [63, 64]. Besides its influence on epigenetic regulation (see also Figure 7), several different mechanisms have been described such as calcium signaling, changes in phosphorylation patterns as well as cell cycle regulation [65-67].

Direct interactions between HBx and different transcription factors such as AP-1 and NFκB have also been suggested. However these results were created in highly artificial systems and their relevance to natural HBV infection is still unclear [68]. Another direct interaction partner of HBx is the DNA damage-binding protein 1 (DDB1), one of the major components of the DDB1-containing E3 ubiquitin ligase complex which is capable of targeting proteins for degradation via ubiquitination (Figure 8) [69]. By highjacking this protein, HBx causes degradation of the cellular Smc5/6 complex whose physiological role is to bind and inactivate episomal DNA molecules [70]. HBx R96E mutants which lack the ability to efficiently bind to DDB1, fail to mediate Smc5/6 degradation and are unable to support efficient viral transcription *in vitro* [70].
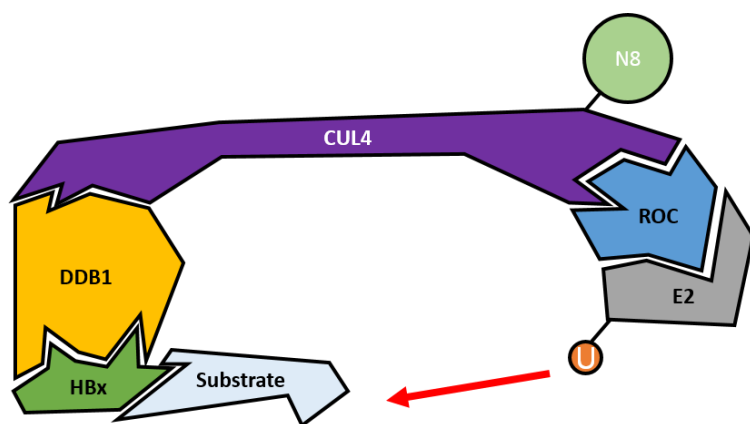
Figure 8: HBx highjacks a cullin-RING ligase complex. HBx can directly interact with the DDB1 adaptor protein and uses this interaction to degrade specific proteins using the ubiquitin-proteasome pathway. NEDD8-activating enzyme (NAE) mediates the neddylation of cullin 4 (CUL4, marked by N8 residue) which is necessary to activate its holoenzyme E3 ligase activity and serves as a regulatory mechanism [70, 71].

As the only accessory protein of HBV, HBx is a major regulator of viral transcription and represents an interesting target for therapeutic approaches. Lack of HBx activity causes reduced expression of viral RNAs as well as proteins and could lead to a reduced disease burden in patients by silencing viral transcription and preventing replication.

1.1.6. Maintenance and degradation of viral cccDNA

After successful infection of hepatocytes, HBV establishes a stable cccDNA pool in the nucleus of infected cells. The mechanisms behind this establishment process varies between model systems. For the human HepG2-NTCP cell line, recycling of rcDNA containing nucleocapsids has been described and DHBV can even accumulate large numbers of cccDNA in the nucleus [35, 72]. In contrast, the human HepaRG cell is described to acquire basically all of its cccDNA from incoming viral particles and maintains stable cccDNA levels without any recycling [73]. Despite these differences however, both cell lines show comparable amounts of cccDNA, ranging between 1-2.5 copies/cell [73, 74].The situation in patients is still under investigation and a range between 0.01 and 10 cccDNA molecules per hepatocyte has been described [75, 76].

Since cccDNA does not possess a centromere structure, cell division of infected hepatocytes can lead to its loss. The existence of several cccDNA molecules per infected cell minimizes this effect by enhancing the probability that at least one cccDNA molecule will be included into one of the newly formed nuclei [77]. cccDNA molecules which are located in the cytoplasm post mitosis step are rapidly destroyed by cellular nucleases [78]. Loss of cccDNA due to cell division appears to play an important role in the clearance of cccDNA during acute hepatitis B, however the exact mechanisms are still unclear [79].

Apart from cell division, loss of cccDNA can also be caused by the host immune system via different mechanisms which can be roughly divided into two groups: cytolytic and non-cytolytic. Loss of cccDNA

due to cytolysis is mainly based on cytotoxic T lymphocyte (CTL) mediated killing of infected hepatocytes [80]. This mechanism is well described in human HBV infection, where it plays a major role in resolving acute hepatitis B infection. Unfortunately, in rare cases, activation of this system can lead to fulminant hepatitis and the death of the host [81]. Besides direct targeting of infected cells, CTLs also secrete antiviral cytokines such as interferon gamma (IFNγ) which act in a more indirect, non-cytolytic manner. IFNγ stimulation of infected hepatocytes leads to the elimination of rcDNA carrying capsids in the cytosol of infected cells as well as repression of viral transcription [82]. Similar observations have been made for the cytokines interferon alpha (IFNα) and interferon beta (IFNβ) indicating a possible role for activated natural killer (NK) cells as well as CD4^{+} T cells [83, 84].

In addition to loss of rcDNA, cytokine stimulation can also cause non-cytolytic elimination of cccDNA [85]. Recent *in vitro* results indicate that enzymes called Apolipoprotein B mRNA editing enzyme, catalytic polypeptide-like 3A/3B (APOBEC3A, APOBEC3B, A3A, A3B) which can act as DNA cytidine deaminases are involved in this process [86]. Targeting of cccDNA by these enzymes leads to deamination of cytosine residues creating uracil. The exact mechanism of cccDNA loss is still under investigation. However the current theory is that these uracils can be detected by cellular enzymes resulting in uracil excision, the creation of apyrimidinic sites and finally degradation of the cccDNA (Figure 9) [87].
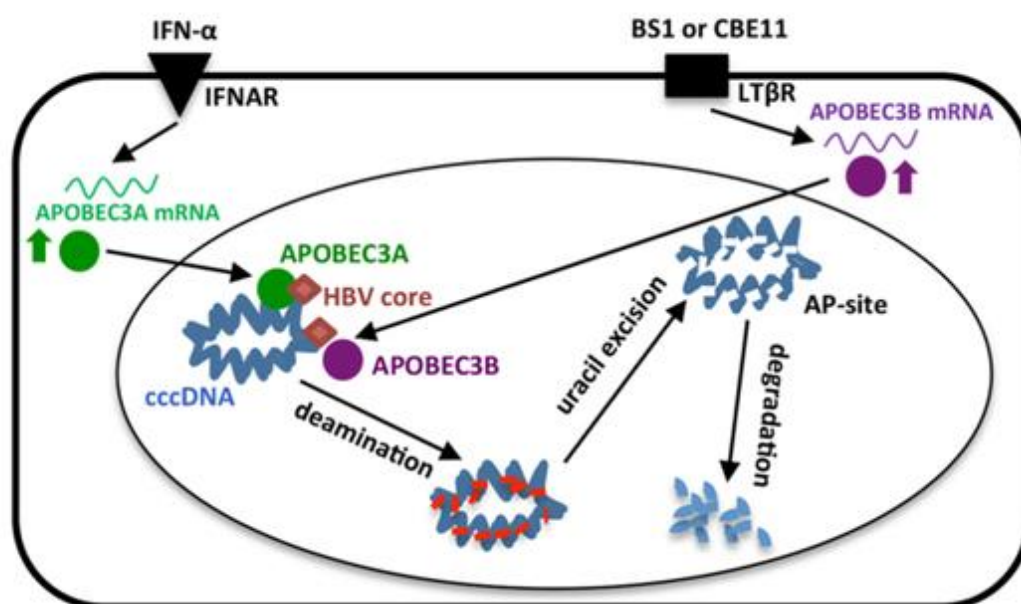
Figure 9: Model for IFNα mediated non-cytolytic cccDNA degradation. Stimulation by IFNα or the Lymphotoxin beta receptor (LTβR) agonist BS1 leads to induction of APOBEC3A or APOBEC3B respectively. The enzymes migrate to the nucleus, bind to cccDNA and start deaminating cytidine nucleotides leading to the formation of uridine. These residues can now be recognized by cellular repair mechanisms, which cause uracil excision and creation of apyrimidinic sites. Intracellular enzymes can now degrade the thusly-damaged cccDNA. Adapted from Lucifora, Xia et al. from [86].

The mechanisms described above can be utilized for treatment and administration of pegIFNα, which mimics the induction of an immune response, remains one of the most efficient treatment options to date [88]. Unfortunately systemic administration of interferon can cause severe sides effects and must be carefully considered and monitored in each patient [89]. A more advanced approach, that is currently undergoing clinical trials, is based on the induction of innate immunity by using small molecules capable of binding to key regulators of innate immunity called Toll-like receptors (TLR). These TLR binders lead to induction of innate immunity and subsequent secretion of interferons, however their side-effects are less severe when compared to pegIFNα [90].

Taken together, non-cytolytic reduction of cccDNA is a well described mechanism and based on induction of innate immunity by cytokines or small molecules [87, 91, 92]. Interferon-induced loss of viral DNA is a major contributor in the T cell mediated clearance of HBV and a better understanding of the underlying processes might help in the optimization of therapies based on immune activation as well as T cell based therapies [93].

1.2.   Antiviral immunity

The human body is protected against viruses, such as HBV, by a wide array of immune defense mechanisms, which can be sorted into two major groups: Innate immunity which is fast acting, hereditary and does not lead to generation of memory and adaptive immunity which is slower but highly pathogen specific and leads to development of long-lasting immune memory cells [94, 95]. The following text will give a short overview over the two different arms of antiviral immune responses and their functions in the context of hepatitis B.

1.2.1.   Innate immunity in the context of HBV

As mentioned above, innate immunity is the fast acting first line of defense against viral infections. The innate immune system senses infections by detecting pathogen associated molecular patterns (PAMPs) using a wide array of different receptors called pattern recognition receptors (PRRs). In the case of HBV, detection of the virus can be mediated either by Toll-like receptors, which detect the viral nucleic acids inside the endosome, or by the retinoic acid inducible gene (RIG-I) receptor which recognizes HBV dsRNA in the cytosol [96-98]. Published data suggests that HBV induces no or only very limited activation of innate immunity during the initial infection, however there are also reports that show significant induction of innate immunity as well as interferon in the case of HBV infection [99-102]. A possible explanation for these discrepancies could be that several HBV proteins have been shown to interfere with important pathways of the innate immune system such as interferon signaling

(Figure 10) [103, 104]. In addition, most data were generated *in vitro*, using cell lines originating from human hepatocellular carcinoma that differ significantly from primary human hepatocytes (PHH).
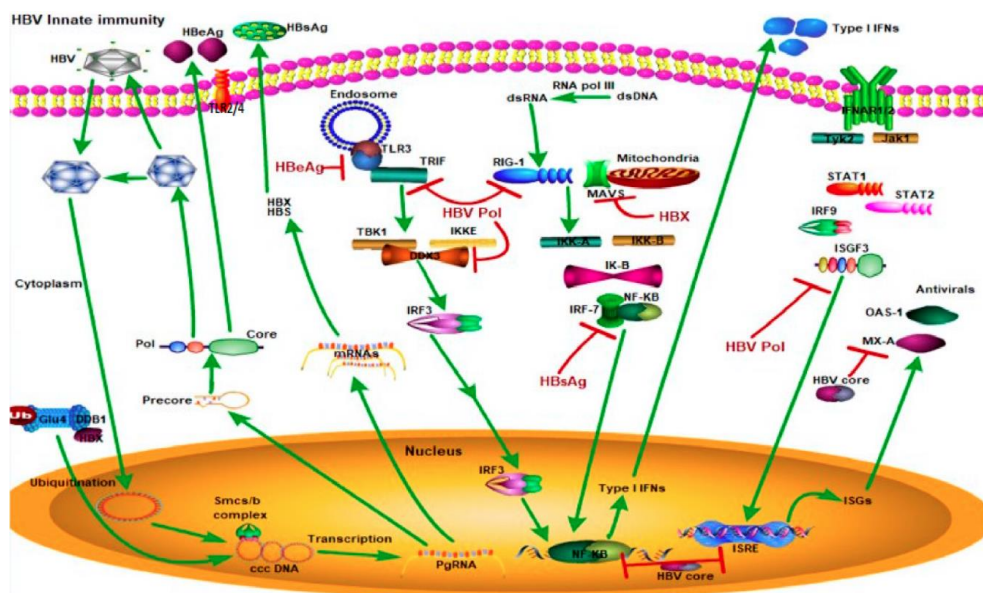
Figure 10: Induction and suppression of the type I interferon response. HBV infection is recognized by the innate immune system via TRL3 and RIG-I and results in the induction of type I interferons. HBV counteracts this mechanism by interfering with different steps of the pathway. For example, HBx protein has been shown to block RIG-I signaling by blocking the interaction between MAVS and the mitochondria. Similarly, HBeAg has been demonstrated to inhibit binding of TLR3 to TRIF, thereby blocking the TL3 mediated IFN induction. Adapted from Megahed et al. [97].

The impact of the cellular part of innate immunity on hepatitis B is also still under investigation. NK cells for example are contributing to the early control of HBV infection, however they also seem to exacerbate liver damage due to their cytotoxic functions while at the same time losing the ability to produce antiviral cytokines in a chronic setting [105-108]. Liver resident monocytes are important for liver inflammation during acute infection but their role during the establishment of chronicity remains unclear [109]. Liver resident macrophages, termed Kupffer cells have been shown to produce the anti-inflammatory cytokine IL10 upon contact with HBV core protein leading to suppression of CD8 T-cell responses [110]. Other data however suggests a proinflammatory effect of Kupffer cells in HBV infection mediated by production of inflammatory cytokines [111, 112].

In general the role of cellular innate immunity in HBV infection and chronic hepatitis B is still unclear and needs to be further investigated. Divergent results can be attributed to usage of different models, analysis of different sub-populations as well as the technical difficulties when studying localized innate immune responses.

1.2.2. Adaptive immunity in the context of HBV

In the second phase of the infection, HBV starts to replicate at high levels, infecting nearly every hepatocyte and leading to increased levels of viral markers in the serum of the patient. This spike in viral activity leads to activation of adaptive immunity and induces a strong and polyclonal T-cell response usually six to eight weeks after infection [113].

Depending on different receptors expressed on their surface, T lymphocytes can be subdivided into cytotoxic CD8$^+$, CD4$^+$ TH$_1$ or CD4$^+$ TH$_2$T cells. These T cell types differ in their behavior as well as in their activation pathways. CD8$^+$ T cells are focused on recognizing and killing infected cells, and get activated by endogenous peptides presented on the major histocompatibility complex I (MHC I). CD4$^+$TH$_1$ or TH$_2$ cells are activated by endogenous and exogenous peptides presented on major histocompatibility complex II (MHC II) and enhance the proliferation and activation of CD8$^+$ T or B cells respectively [95, 114, 115]. Activation of T cells mostly occurs in the lymph nodes and is mediated by activated dendritic cells (DC) which present antigenic material on their receptors [116].After priming in the lymph nodes, activated T cells then expand and migrate to the site of infection where, upon recognition of their respective antigens, they release proinflammatory cytokines such as IFNγ and tumor necrosis factor alpha (TNFα). In addition, CD8$^+$ T cells are also capable of directly killing infected cells via perforin/granzyme or the Fas pathway [117]. These activities enhance the inflammation, leading to the recruitment of additional cellular components of both adaptive as well as innate immunity and usually result in the clearance of the infection and formation of a long-lasting immune memory [118].

In the case of hepatitis B, HBV specific CD4$^+$ and CD8$^+$ T cells get activated in the lymph nodes and then migrate to the liver where they can target HBV infected hepatocytes using two different mechanisms: On the one hand activated lymphocytes release cytokines that inhibit viral expression and reduce the amount of viral DNA in the liver by around 90% without induction of liver damage [119, 120]. On the other hand, CD8$^+$ T cells recognize and kill hepatocytes infected by HBV leading to liver damage and increased alanine aminotransferase (ALT) levels in the serum of the patient [121, 122]. However, even in individuals that manage to resolve their acute HBV infection, a small group of infected hepatocytes remains [123]. This remaining virus can be efficiently suppressed by the immune system and helps to support a strong and long term anti-HBV memory T-cell response which can be detected for the next 20-30 years [124]. In patients with resolved acute infections, immunosuppression can lead to reactivation of these dormant hepatitis B virus infections [125].
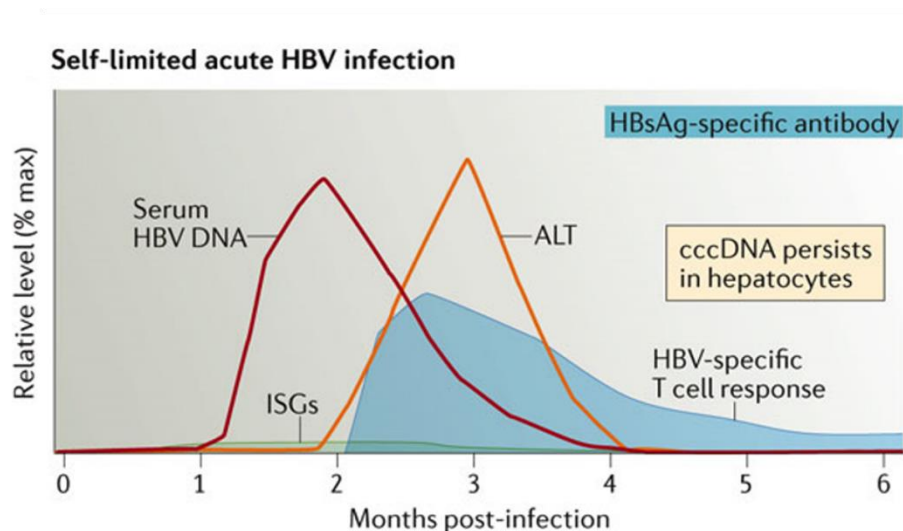
Figure 11: Time course of acute hepatitis B. In acute HBV infections, the virus can be efficiently controlled by the hosts T-cell response. Levels of viral DNA in the serum start to drop bevor alanine aminotransferase, a marker of liver damage which indicates death of hepatocytes, reaches its peak suggesting non-cytolytic elimination of HBV. Adapted from Shin et al. [126].

The course of disease outline in Figure 11 describes acute hepatitis B, where the infection can be resolved by a strong and polyclonal T-cell response. Unfortunately, up to 5% of infected adults and around 95% of children infected at less than one year of age do not manage to resolve the infection and instead progress to chronic hepatitis B (Figure 12). This age dependency could also be observed in the WHV and DHBV models, however the responsible mechanism is still unclear [127, 128].

A chronic hepatitis B can be classified into five phases (I – HBeAg-positive chronic infection, II – HBeAg-positive chronic hepatitis, III – HBeAg negative chronic infection, IV – HBeAg-negative chronic hepatitis, V – HBsAg negative phase) and patients suffering from this disease show significantly increased chances to develop liver cirrhosis or hepatocellular carcinoma [129, 130]. The currently available treatment options, peg-IFNα or nucleos(t)ide analogues can efficiently suppress viral replication, however only a minority of treated patients manages to clear the virus. Furthermore, patients under long-term NUC treatment still have an increased risk to develop potentially live threatening liver-related complications such as HCC [131].
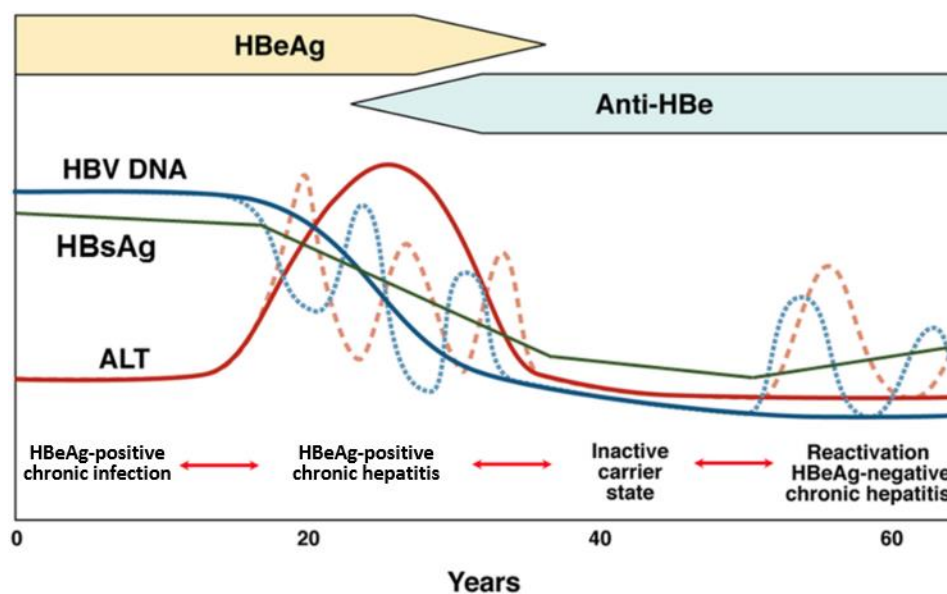
Figure 12: Time course of chronic hepatitis B. In chronic hepatitis B, the host T cell response fails to eliminate the viral infection. Seroconversion from HBeAg to anti-HBe often takes place, however many patients stay HBsAg positive and show frequent flares of viral reproduction and increased ALT values. Adapted from Suk-Fong Lok et al.[132].

As opposed to acute infection with HBV, the T-cell response in chronic hepatitis B is characterized by a narrow repertoire as well as low numbers [133]. Remaining HBV specific T cells show an exhausted phenotype and upregulation of inhibitory pathways effectively preventing T-cell function [134]. This dysfunctional T-cell response is still under investigation, however current results indicate that the long-lasting exposure of the CD8^{+} T cells to high antigen titers together with the tolerogenic liver environment might be responsible [133, 135, 136]. The suppressive effect of high viremia was also described in patients, where high titers of viral markers in the serum are inversely correlated with HBV specific T-cell activity [137]. Efficient induction of HBV specific CD8^{+} T cells is also strongly dependent on a sufficiently strong CD4^{+} T-cell response and lack of T-cell help might be another important factor in the development of chronic hepatitis B [138]. It has also been suggested that, while inflammation is necessary to attract T cells, long-term exposure to an inflammatory environment could inhibit T-cell function [139].

In summary, patients capable of resolving their HBV infection show the induction of a strong and polyclonal T-cell response, while chronically infected patients show only low levels of dysfunctional T cells. Therefore, the induction of an efficient, T-cell mediated antiviral response via vaccination represents a promising therapeutic approach for chronic hepatitis B.

1.2.3. Antiviral effects of type I and type II interferons

Interferons are small signaling molecules that can be produced by human cells in response to pathogens and play an important role in the host defense against viruses. Depending on their properties, they can be divided into three different subgroups: type I interferons (e.g. IFNα, IFNβ), type II interferons (IFNγ) and type III interferons (IFNλ1, IFNλ2, IFNλ3).

Production of type I interferons is induced upon stimulation of PRRs. After secretion, type I interferons act in a paracrine or autocrine fashion by binding to their shared receptor, an IFNAR1/IFNAR2 hetero-dimer located on the cell surface. Activation of the receptor induces phosphorylation of STAT proteins and finally leads to expression of so-called interferon stimulated genes (ISGs) (Figure 13). Activation of these ISGs results in the induction of an antiviral state, marked by high levels of antiviral proteins (e.g. IFN-inducible RNA-dependent protein kinase (PKR), tripartite motif-containing (TRIM) or interferon stimulated gene 20 protein (ISG20)) [140].
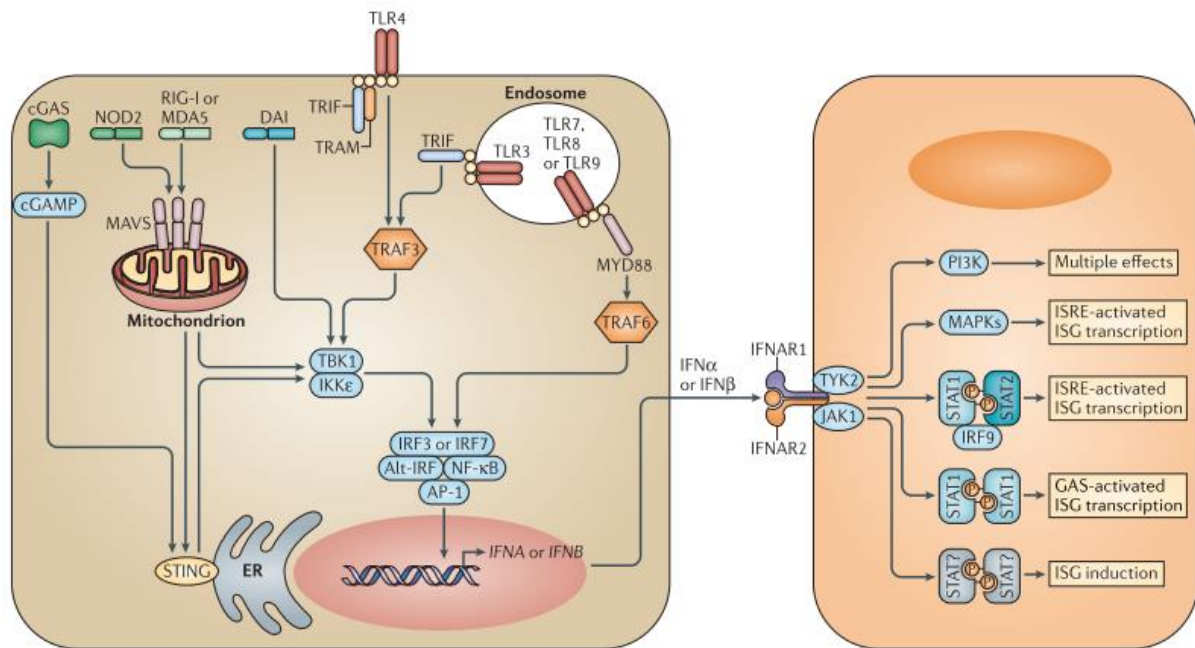
Figure 13: Induction and effects of type I interferons. Upon activation of one of the PRRs, expression and secretion of type I interferons is induced via TANK-binding kinase 1 (TBK1) and interferon regulatory factor 3 or 7 (IRF3/7). Binding of type I interferons to their corresponding receptor can cause induction of several different pathways such as the canonical signaling via STAT1-STAT2-IRF9. Alternatively, signaling via STAT1 homodimers is also possible although this pathway sis usually associated with IFNγ signaling. Adapted from McNab et al. [140]

In addition to inducing an acute antiviral state in the affected cells, type I interferons also play an important role in the activation and control of the innate cellular immune response. For example, IFNα is known to promote the differentiation of dendritic cell precursors, can activate mature DCs and increases their ability to stimulate T cells [141-143]. Connections between type I interferons and the adaptive immune system also exist, type I interferons have been shown to enhance CD4^{+} T-cell survival as well as differentiation into the T$_H$1 helper subset [144, 145]. Similarly, CD8^{+} T cells are also affected

by type I interferon and enhanced cytoxocity as well as IFNγ production have been reported [146, 147]. In the context of HBV infection, IFNα signaling induces APOBEC mediated cccDNA degradation, blocking of viral RNAs by 2'-5'-oligoadenylate synthetase (OAS) as well as regulation of viral promotor activity via TRIM22 [148]. Pegylated IFNα has been used to treat chronic infection for the last two decades. Unfortunately, IFNα can induce severe side effects, which limits the maximal treatment time and its efficacy varies strongly between genotypes [89].

As opposed to type I interferons, IFNγ, the only member of the type II interferons, is predominantly expressed by activated B and T cells as well as NK and professional antigen presenting cells (APCs)[149, 150]. Since IFNγ is structurally distinct from the type I interferons, it is unable to bind to the same receptor an instead binds to the functional IFNγ receptor (IFNGR) which is comprised from IFNGR1 and IFNGR2 proteins (Figure 14). The downstream signaling of IFNγ closely resembles the pathway observed for type I interferons, however while type I interferons can signal via different, distinct STAT combinations, IFNγ seems to signal purely via STAT1 homodimers [151].
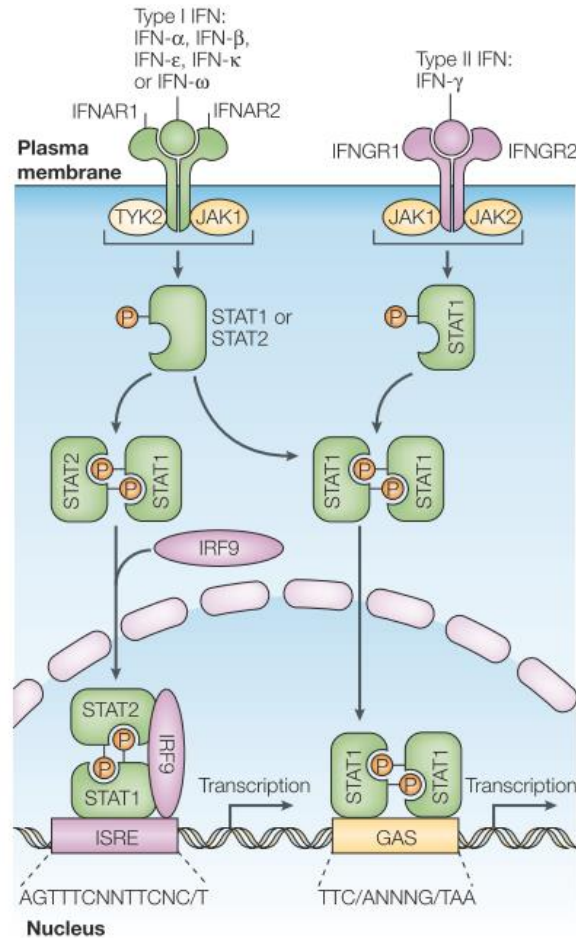
Figure 14: Signaling pathways of type I and type II interferons. Type I interferons signal via the Type I IFN receptor which is composed of two subunits, IFNAR1 and IFNAR2. The receptor is associated with two different Janus activated kinases (JAKs) called JAK1 and tyrosine kinase 2 (TYK2). Type II interferons signal via the type II IFN receptor which contains one IFNGR1 and one IFNGR2 protein. The two halves of this receptor associate with their respective JAKs called JAK1 and JAK2. Activation of the type I IFN receptor causes phosphorylation of STAT1 and 2. These two proteins interact with IFN-regulated factor 9 (IFN9) to form the so-called IFN-stimulated gene factor 3 (ISGF3) complexes. These complexes can enter the nucleus and bind to interferon-stimulated response elements (ISREs) to induce transcription of ISGs. Type II IFN receptors cause phosphorylation of STAT1, which then forms homodimers, enters the nucleus and binds IFNγ-activated sites (GAS) to initiate gene transcription. Type I interferon can also induce this pathway. Adapted from Platanias et al.[152].

Due to their close resemblance there is significant cross-talk between the pathways activated by type I and II interferons and many target genes can be regulated by both interferon types [153-155]. For example, the members of the APOBEC family can be induced using either IFNα or IFNγ [156]. The effects of IFNγ treatment against HBV are more or less identical to the ones observed when treating with type I interferons although their kinetics seem to differ [157, 158]. Use of pegIFNγ as a replacement for pegIFNα has been considered, however it suffers from the same drawbacks and so far data obtained from clinical trials are unconvincing [159].

1.3. Therapeutic vaccination against chronic hepatitis B

Patients chronically infected with HBV which are able to resolve their infection, either spontaneously or due to pegIFNα treatment, show development of a strong and polyclonal anti-HBV T-cell response similar to the one observed during acute infection [160]. This indicates that reconstitution of HBV specific T-cell immunity by therapeutic intervention represents a very promising approach towards curing chronic hepatitis B. The fact that chronically HBV infected patients who received bone marrow transplants from anti-HBsAg positive donors are sometimes able to spontaneously clear the infection further substantiates this idea [161]. Based on these observations different therapeutic vaccines were developed with the goal of evoking a strong enough HBV specific T-cell response to control the virus in chronic hepatitis B patients. Several such vaccines have been tested in human trials, however so far none was able to achieve a strong enough and sustained T-cell response sufficient for functional or sterile cure [162, 163].

1.3.1. State of the art

Development of therapeutic vaccines against chronic hepatitis B began in the 90s with the use of prophylactic vaccines, containing the viral S protein, in infected patients [164]. This approach led to decreased titers of HBV DNA in the serum of the patients but failed to induce any lasting reduction of viral antigens. Attempts to enhance vaccine efficacy by adding the viral L and M proteins or by combining the vaccination with NA treatment did not lead to improvement [165, 166]. However, when injected together with viral capsids, S protein based vaccines did induce normalization of ALT in all subjects, as well as a sustained suppression of viral DNA in approximately half of the participants [167]. Unfortunately, even these improved vaccines, similar to previous approaches, failed to cause any reduction in serum antigen.

In addition to protein-based approaches, DNA –based vaccines were also developed. Different vectors encoding different combinations of viral antigens were tested and proved to be superior to purely protein based approaches. Clinical studies using DNA vaccines reported induction of HBV-specific T-cell responses, decreases in viral titers as well as loss of HBeAg [168, 169]. However, HBsAg seroconversion, the indicator of achieving functional cure, was never observed. A possible explanation for this is that the observed T-cell responses, while HBV-specific, were relatively weak. Most likely due to the low immunogenicity of DNA-based vaccines in humans.

The latest development in the field of therapeutic vaccination is the use of viral vectors, since these are capable of inducing strong and long-lasting T-cell responses, as demonstrated in results from the HIV field [170, 171]. However, the results obtained when using vector-based therapeutic vaccines in

human trials were relatively similar to the ones seen when using DNA-based vaccines. The vectors succeeded in the induction of strong T-cell responses and, in some cases, caused loss of HBeAg but failed to induce a functional cure in the participants [172, 173].

In summary, previously developed therapeutic vaccines failed to induce a sufficiently strong and broad T-cell response to overcome the HBV-induced immunosuppression. Further research is required to improve vaccine immunogenicity and efficiently decrease the amounts of viral antigen in blood of treated patients.

1.3.2. Modified vaccinia Ankara as a vaccine vector

Modified vaccinia Ankara (MVA) belongs to the family of *poxviridae* and was originally developed as a safer alternative to the previously used, Chorioallantois vaccinia virus Ankara (CVA) based, smallpox vaccine [174]. The virus was created by serial passaging of the original CVA strain in chicken embryo fibroblasts (CEFs). This led to virus adaptation and loss of six genome regions (Deletions I – VI) amounting to approximately 30kb which corresponds to 15 % of the viral genome [175]. Compared to its progenitor, MVA lost the ability to productively infect cells of human origin as well as several important immunosupressive genes [176, 177]. This combination created a highly immunogenic virus with a strongly attenuated phenotype, suitable for use in immunocompromised patients [178]. When used *in vivo*, MVA causes efficient expression of viral and recombinant proteins in infected cells, resulting in high antibody titers as well as a strong T-cell response [179]. This high immunogenicity coupled with its excellent safety record made MVA an interesting candidate for the development of vector based vaccines and clinical trials targeting human immunodeficiency virus (HIV), human papilloma virus (HPV), melanoma, tuberculosis or malaria have been published [180]. In the context of chronic HBV infection, the combination of two protein priming steps followed by an MVA boost was sufficiently immunogenic to overcome the HBV induced immune tolerance in an *in vivo* model [181]. However, the vectors used in this publication each contained only one HBV transgene (either S or core) and *in vivo* vaccine efficacy was negatively impacted by high antigen titers in the serum of treated animals. A first phase I clinical trial using an MVA vector expressing S and core antigens is conducted since 2017 by GSK biologicals, however no results are publicly available so far [182].

Altogether, MVA is a safe and highly immunogenic vaccine vector suitable for use in healthy as well as immunosuppressed individuals. MVA-based therapeutic vaccines showed promising results in HBV *in vivo* models, however efficacy in humans has not been demonstrated yet.

1.3.3. From Bench to Bedside

In vivo experiments conducted in suitable animal models are an important step in vaccine development and can be used to establish a proof of principle. Unfortunately, transferring results gathered in animal models to the human situation is difficult at best [183]. Vaccine development therefore necessitates the use of human trials. To ensure the safety of trial participants, transitioning from animals into humans requires the approval of the proper regulatory authorities [184]. The applicant has to provide data pertaining to pharmacokinetics and dynamics as well as toxicity and safety and all substances intended for human use need to meet the standards prescribed by the "Good manufacturing practice" (GMP) regulations [185-187].
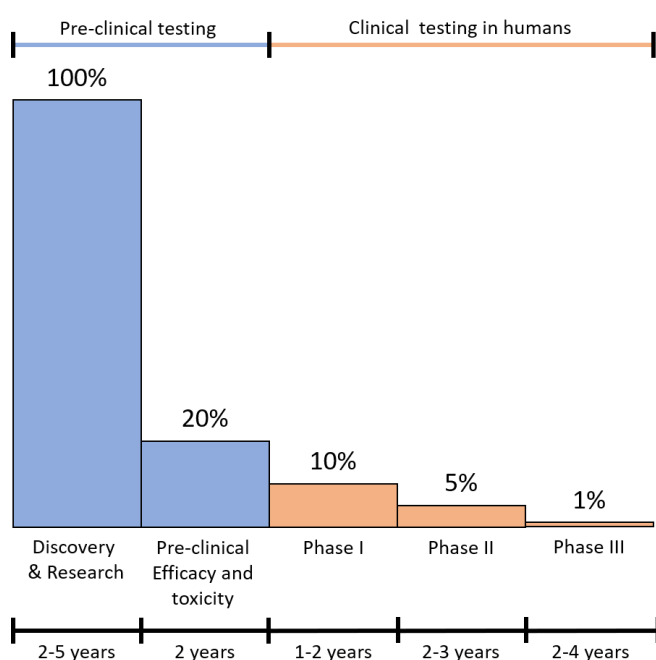
Figure 15: The vaccine development pipeline. Vaccine development is extremely time and labor intensive due to the high safety standards and only approximately 1% of vaccine candidates enters a phase III trial. Development time can vary however, it averages at around 10 years.

Clinical trials are conducted in different staggered phases (Figure 15). Phase I trials determine safety and dose ranging in a small number of participants and offer a first glimpse at indicators of immunogenicity. Should the obtained results be satisfactory, the trials progress into phase II. This phase includes an increased number of participants, usually between 100 and 1000, and its aim is the evaluation of safety, immunogenicity as well as efficacy in a small group. The final phase III studies usually use large, multi-center cohorts to evaluate safety, immunogenicity and efficacy and are necessary to detect rare side-effects of the developed vaccine. After successfully passing all three phases, the data can be entered for regulatory submission. In case of approval and licensure the vaccine can now be entered into the market, however post-licensure pharmacovigilance is required to detect potential adverse events (AEs) that were missed during clinical testing. This post-marketing surveillance phase of vaccine development is often termed phase IV.

1.4.   Aims of the study

Despite recent advance in the field, therapeutic vaccinations against chronic hepatitis B have, so far, failed to generate convincing efficacy data when tested in humans. This can be attributed to the inability of vaccines to induce sufficiently strong T-cell responses, which would be crucial to surmount the HBV mediated immune suppression. Overcoming this hurdle necessitates boosting the immunogenicity of therapeutic vaccines, for example by using novel adjuvants, viral vectors or even combination therapy with small molecules. Therefore, the first part of this thesis is focused on the creation and validation of a novel, highly immunogenic vaccine vector suitable for testing in a clinical trial, while the second part takes a closer look at the cytokine-mediated non-cytotoxic cccDNA degradation and possible ways to enhance this effect using small molecules. The final section of the thesis deals with one of the enzymes necessary for non-cytotoxic cccDNA loss and possible connections between its function and its intracellular localization.

The first objective of the project is the development and characterization of a novel MVA vector to analyze whether the designed virus can be created and efficiently produced under GMP-like conditions and if it meets the security, efficiency and stability standards required for human trial. This work should result in the creation of a suitable vector to pass on to a contract manufacturer for GMP production. To assess whether the newly created vaccine vector shows a sufficient efficacy and safety to justify progression into a phase I clinical trial, the vector should be tested *in vivo* by vaccinating WT mice as well as a mouse model for chronic HBV infection. Special emphasis should be put on the long-term effect of the vaccination and potential adverse events.

The second part of the thesis aimed at analyzing possible connections between the cccDNAs chromatin conformation and its vulnerability towards cytokine-mediated degradation. Therefore, different substances should be characterized regarding their impact on cccDNA conformation, viral transcription and non-cytolytic cccDNA degradation using *in vitro* cell culture systems.

The third and final part of thesis is focused on the enzyme ISG20, a crucial player in cytokine-mediated cccDNA degradation, and takes a closer look at potential ties between the intracellular localization of ISG20 and its anti-HBV activity. Intracellular distribution of HBV components and ISG20 as well as potential interactions between the two will be analyzed using different cell culture systems and varying conditions.

2. Results

2.1. A novel, MVA based viral vector for therapeutic vaccination

Previous studies on the treatment of chronic hepatitis B by therapeutic vaccination showed that this approach requires highly antigenic vaccines to overcome the immune tolerance caused by the virus [188]. This first part of the thesis was therefore focused on the development, creation and characterization of a novel vaccine vector, which fulfilled all criteria necessary for a phase I human trial.

2.1.1. Creation and purification of the vaccine vector MVA HBVac

To ensure global applicability of the therapeutic vaccination, the HBVac expression cassette was designed using consensus sequences including the five major HBV genotypes A, B, C, D and E, covering around 95 % of global hepatitis B cases. Five sequences covering five different HBV proteins (L, S, core, truncated core$_{1-149}$ and the reverse transcriptase domain of the viral polymerase (RT (Pol)) were used to ensure the creation of a broad neutralizing antibody and T cell response covering the HBV strains circulating world-wide in vaccinated patients (Figure 16). The different coding sequences were linked by T2A and P2A peptide genes to ensure equimolar translation of the encoded proteins from one single mRNA. The HBV sequences were partially optimized with regards to GC content and codon usage to support optimal expression in mammalian cells. To avert unwanted homologous recombination events during vector creation and amplification the HBVac sequence was only partially modified to avoid sequence homologies longer than 20bp. When the ribosome reaches the C terminus of any 2A sequence the created peptide causes ribosome skipping, leading to three possible outcomes: (1) Successful ribosome skipping and re-initiation of the translation leads to the production of two separate proteins. (2) Ribosome fall-off at the end of the 2A sequence causes a stop of translation and results in the production of only the first of the two linked proteins. (3) Failure to induce ribosome skipping leads to the production of so-called fusion proteins, consisting of two proteins linked by the 2A sequence (Figure 17) [189, 190]. Efficiency of the 2A sequences varies between constructs and is determined by several factors such as total length of the product, the specific 2A sequence which was used as well as the linked protein sequences [191, 192].
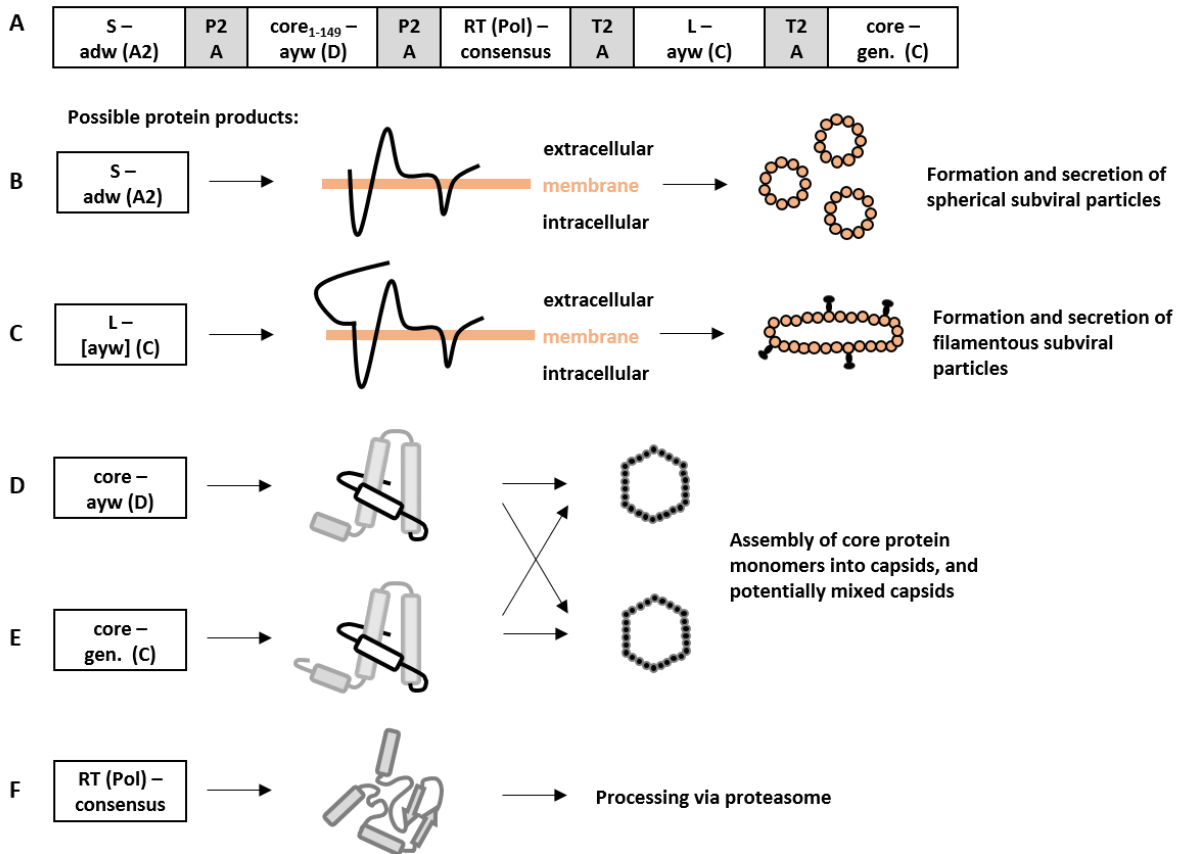
Figure 16: The HBVac insert and its protein products. (A) The HBVac insert encodes five different proteins (S - adw (A2), core$_{1-149}$ ayw (D), RT (Pol) consensus, L - ayw (C), core (C)) which are linked by P2A and T2A peptide genes. **(B, C)** The HBV surface proteins S and L both accumulate in the ER and can then be secreted in the form of spherical or filamentous subviral particles. **(D, E)** The proteins core$_{1-149}$ and core both accumulate in the cytoplasm of infected cells and self-assemble into capsids. Assembly of mixed capsids containing both proteins is also possible. **(F)** The RT (Pol) protein most likely accumulates in the cytoplasm and can get degraded via the proteasome.
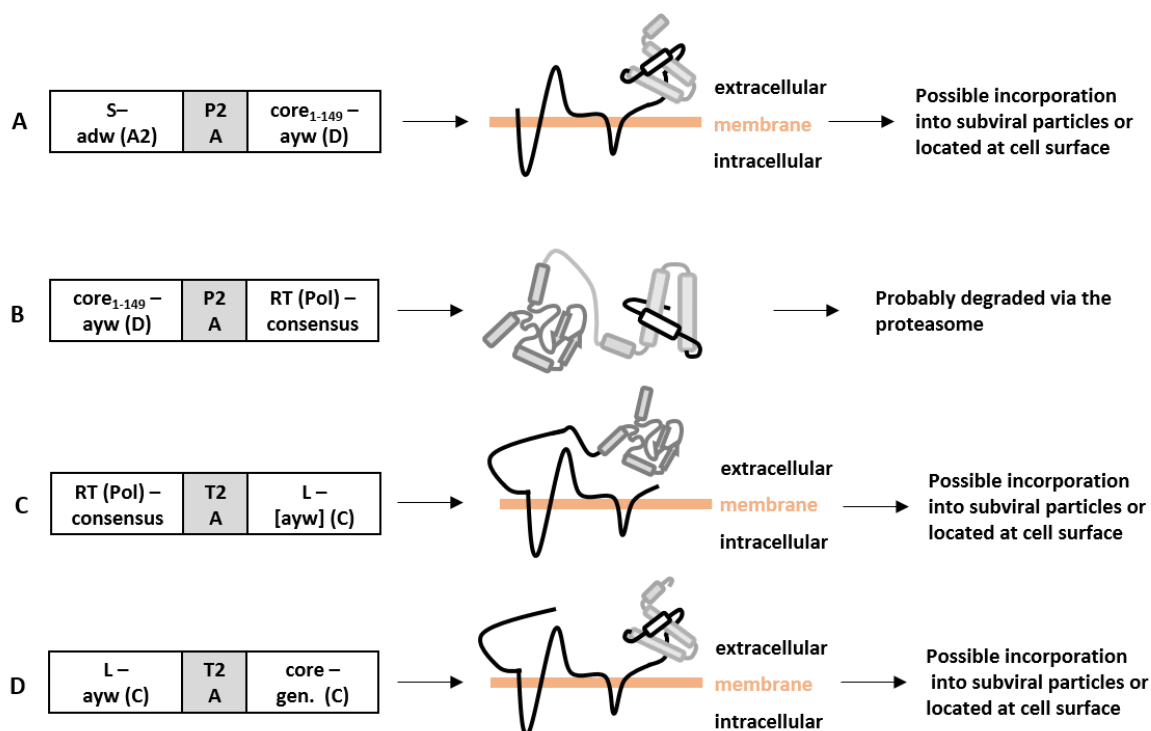
Figure 17: Possible fusion proteins formed by HBVac. (A, B, C, D) Failure to cleave at the P2A or T2A sites results in fusion proteins consisting out of S and core$_{1-149}$., core$_{1-149}$ and RT (Pol), RT (Pol) and L or L and core. The exact fate of these possible fusion proteins is not known. Integration of the S or L protein containing fusion proteins into the cellular membranes is possible and could lead to the extracellular localization of the fused protein. Alternatively, all fused proteins can be intracellularly degraded.

The recombinant MVA HBVac was created according to the protocol published in [193]. Briefly, the HBVac insert was cloned into a transfer plasmid containing two flanking regions for homologous recombination, the strong early/late promoter PmH5 as well as an mCherry expression cassette (Figure 18A). The DNA section located between the regions flank 1 and flank2 was then integrated into the genome of wildtype (WT) MVA F6 using homologous recombination, leading to the creation of MVA HBVac mCherrry (Figure 18B). This recombinant virus was passaged until loss of mCherry occurred by a random recombination event between the two del sequences (Figure 18C).
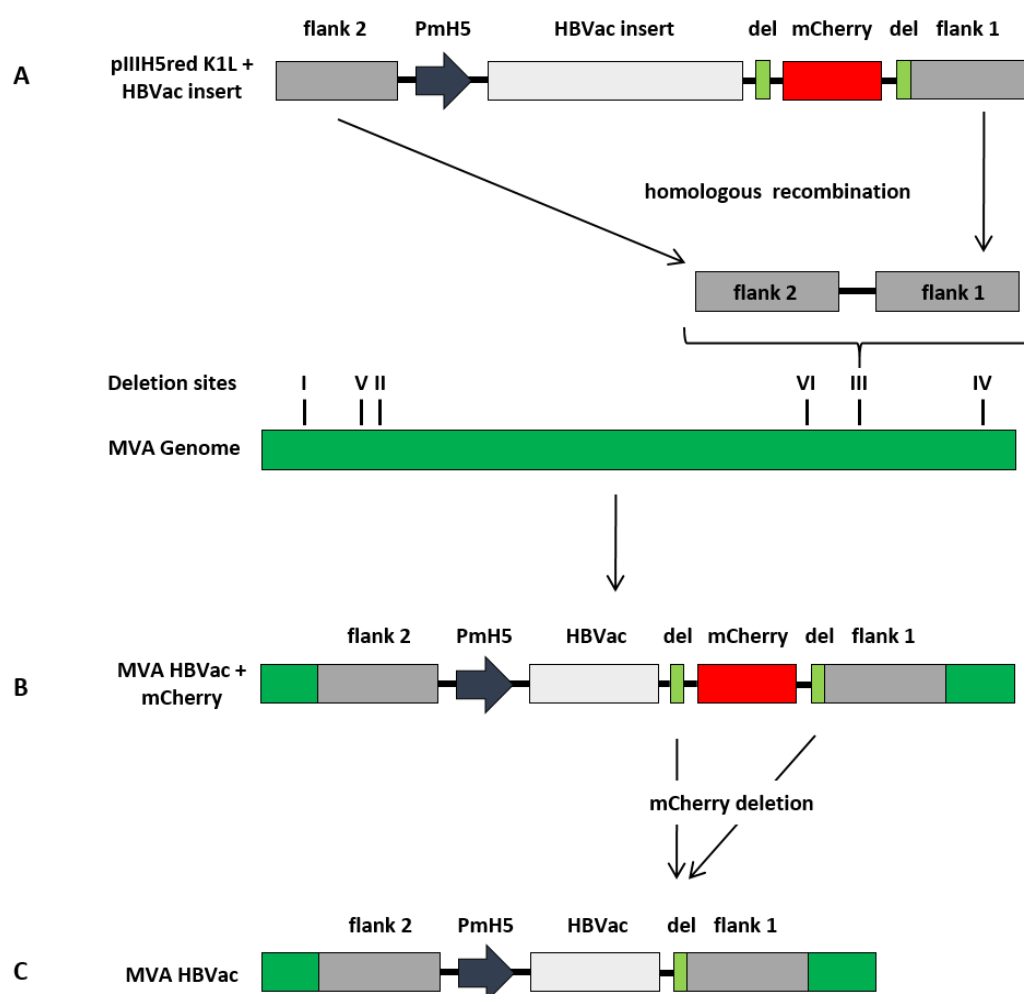
Figure 18: Creation of MVA HBVac. (A) The HBVac insert was cloned into the pIIIH5red K1L vector which contained the two flanking regions flank 1 and flank 2, the strong early/late promotor PmH5as well as an mCherry expression cassette flanked by two identical del regions. The pIIIH5 red K1L HBVac plasmid was then transfected into CEF cells, which had previously been infected with MVA F6. **(B)** Inside of infected cells, homologous recombination between the plasmid and the MVA F6 genome occurred leading to the integration of the HBVac cassette into deletion site III of the MVA F6 genome. The newly created recombinant MVA HBVac mCherry was isolated and purified using consecutive rounds of plaque purification to eliminate any remaining wildtype MVA F6. **(C)** After complete loss of MVA F6 was achieved, the recombinant virus was passaged until loss of mCherry via random homologous recombination.

Plaque purification of recombinant MVA HBVac was carried out by picking infected cells marked by red fluorescence. Continuous repetition of this step led to increasing purity of the MVA HBVac (Figure 19C). To ensure the purity of the newly created MVA HBVac, the virus was analyzed using PCR. Primers specific for deletion site III were used to ensure insert integrity and to check for remaining traces of MVA F6. The PCR results showed a solid band at the correct size of around 5kb for MVA HBVac without any remaining MVA F6 genomic material. The MVA F6 control showed only one band at the expected size of 800bp (Figure 19A). PCR was also used to check whether any unwanted integration occurred at the other deletion sites. Results showed equal bands for MVA HBVac and MVA F6 for deletion sites I, II, IV, V and VI indicating that no undesired, additional insertions took place (Figure 19B). After purified

MVA HBVac was obtained the HBVac insert and the surrounding region of the viral genome were analyzed using Sanger sequencing. Results showed correct integration of the insert into the genome as well as transfer of some small sequence parts of the pIIIH5 red K1l transfer plasmid (Figure 19D).
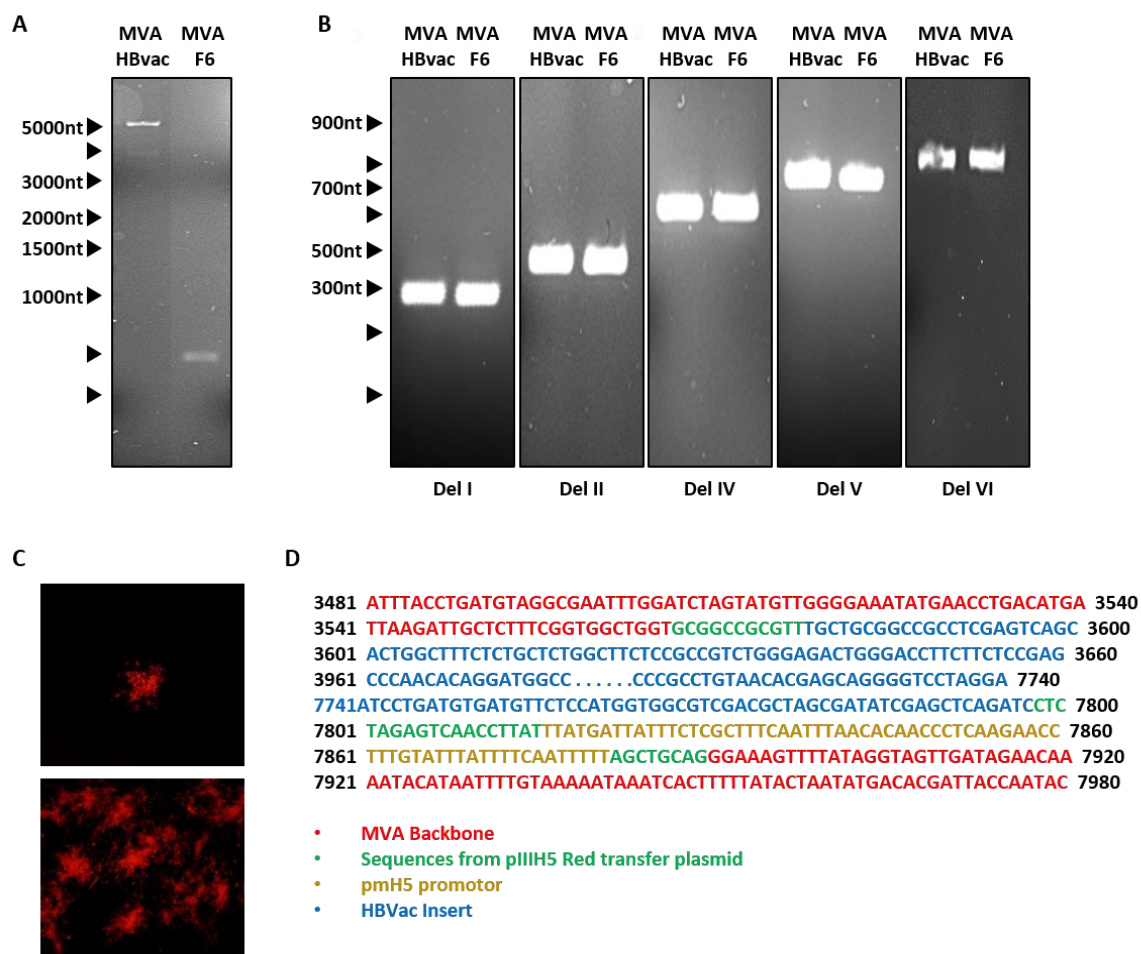
Figure 19: Genomic characterization of MVA HBVac. (A) The size of the sequence located in deletion site III was analyzed using primers that bind up-and downstream of Del III. **(B)** The five other available deletion sites inside the MVA genome were analyzed using PCR and primer pairs that bin up- or downstream of the respective deletion site (Del I, II, IV, V and VI) **(C)** Viral plaques containing recombinant MVA HBVac showed red fluorescence due to mCherry expression. Consecutive rounds of picking fluorescent plaques led to the purification of MVA HBVac. **(D)** The HBVac insert of the purified MVA HBVac was sequenced using a Sanger approach.

On the whole, the recombinant MVA HBVac was successfully created under GMP-like conditions using techniques appropriate for the creation of materials destined for use in small/medium scale GMP manufacturing. The virus did not show any additional insertions and the HBVac expression cassette was not mutated during virus creation or purification making the virus suitable for further experiments.

2.1.2. MVA HBVac expresses the desired proteins and allows for efficient replication *in vitro* and safe application *in vivo*

To test the *in vitro* functionality of MVA HBVac, DF-1 cells were infected with the virus (Multiplicity of infection (MOI) 0.1 incubated for 48 hours, lysed and analyzed using Western blot. In addition, the same setup was used to analyze the kinetics of protein expression in infected cells over the first 48 hours post infection.
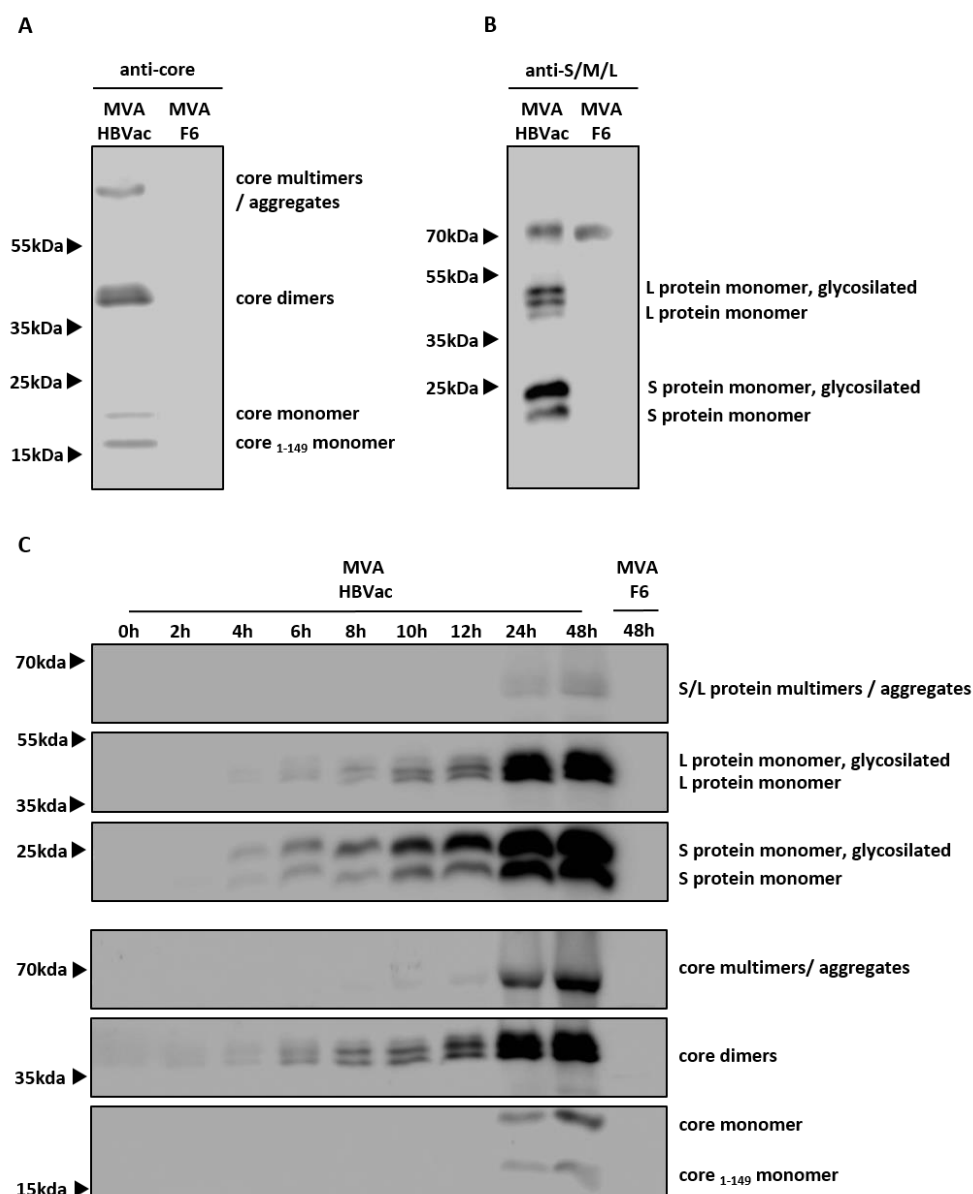
Figure 20: Protein expression in MVA HBVac infected DF-1 cells. DF-1 cells were infected with MVA HBVac (MOI 0.1)or MVA F6 (MOI 0.1)and lysed 48 hours post infection using RIPA buffer. **(A)** Expression of core and core$_{1-149}$ was verified using a monoclonal anti-core antibody. **(B)** Western blot using a monoclonal antibody directed against S, M and L protein. **(C)** Time course of the protein expression in MVA HBVac infected DF-1 cells for the first 48 hours post infection. Protein expression was detected from cell lysate using monoclonal anti-core or anti-S/M/L antibodies.

The anti-core blot shows bands at the expected sizes corresponding to monomers (21kDa and 19kDa) and dimers (42kDa) as well as one additional band at a higher molecular weight corresponding to core protein multimers or aggregates (Figure 20A). No unspecific bands in the MVA F6 control lane were detectable. Using an anti-S/M/L antibody for detection, the blot showed two bands around 25kDa which match with the naïve and glycosylated forms of S protein. The three additional bands around 40kDa correlate to the naïve and glycosylated forms of L protein as well as disulfide-linked S protein dimers [194]. The blot also shows an unspecific band around 70kDa which occurs in HBVac as well as in the MVA F6 WT control (Figure 20B). Expression kinetics for MVA HBVac were determined for the first 48 hours post infection. HBV proteins expressed in MVA HBVac infected cells started increasing four hours post infection and continually increased up to 48 hours. The core proteins were predominantly detected in the form of dimers while S and L proteins were detected mainly in the form of naïve/glycosylated monomers (Figure 20C).

To compare the newly created MVA HBVac with its predecessor vectors MVA-S and MVA-C, DF-1 cells were infected (MOI 0.1), and the supernatant was analyzed over the next 48 hours using a commercial BEP III HBeAg ELISA. In addition, the growth kinetics of MVA HBVac, MVA-S and MVA-C were compared in HeLa and DF-1 cells to ensure that the newly created MVA HBVac retained its excellent safety profile. MVAs incapability to efficiently grow in cells of human origin was an important safety feature and needed to be maintained since the product was intended for clinical use. To further characterize the virus, different cell lines were infected using MVA HBVac and analyzed using the same BEP III assay as mentioned above.
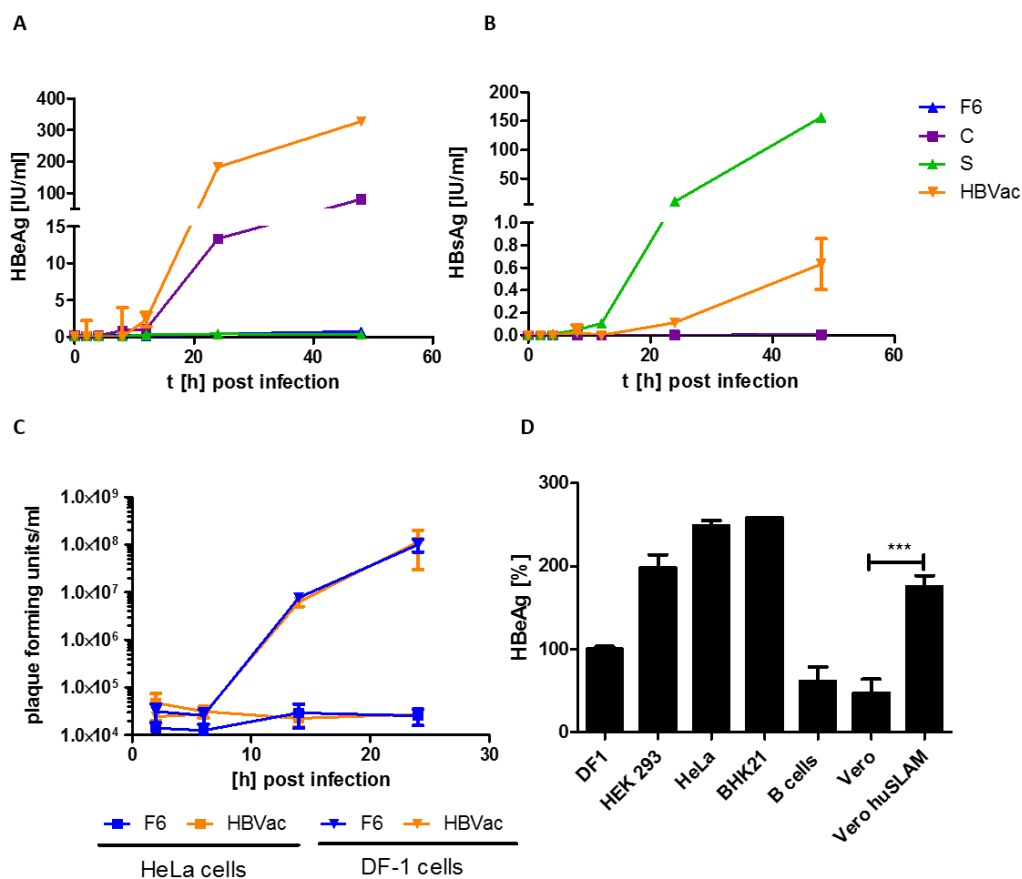
Figure 21: Comparison of MVA HBVac and its predecessors MVA-S and MVA-C. (A, B) DF-1 cells were infected using either MVA HBVac, MVA-S (expressing only the viral S protein), MVA-C (expressing only the viral core protein) or WT MVA F6 (MOI 0.1). HBeAg and HBsAg were determined by Architect for the first 48 hours post infection in the supernatant of the infected cells (n=2). **(C)** DF-1 and HeLa cells were simultaneously infected with MVA HBVac or MVA F6 (MOI 0.1). Viral growth was analyzed over the next 24 hours by determining the viral titer at different time points using plaque assay (n=2). **(D)** Seven different cell lines were infected with MVA HBVac (MOI 0.1) and 48 hours post infection, the amount of HBeAg in the supernatant of each cell line was analyzed using BEP III (n=6). Statistical analysis: Student's unpaired t-test with Welch's correction (ns: not significant; *p≤0.05; **p≤0.01; ***p≤0.001)

Infection of DF-1 cells with MVA HBVac and MVA-C led to increased HBeAg levels in the supernatant. However, cells infected with MVA HBVac showed much higher antigen titers when compared to MVA-C. MVA-F6 as well as MVA-S did not lead to any detectable increase of HBeAg (Figure 21A). HBsAg was detected in the supernatant of cells infected with either MVA-S or MVA HBVac. The amounts of secreted HBsAg were highest if MVA-S was used for infection, while infection with MVA-C and MVA F6 did not lead to any detectable HBsAg (Figure 21B). Both viruses, MVA HBVac as well as the MVA F6 wild type control, were able to efficiently grow in DF-1 cells but failed to establish a productive infection in HeLa cells (Figure 21C). Expression of HBsAg varied between different infected cell lines, the highest titers were detected in the supernatant of Hela and BHK21 cells (Figure 21D). Expression of the human SLAM receptor on Vero cells significantly increased the titers of HBeAg expressed.

Summarizing these results, the newly created MVA HBVac was able to efficiently express all desired proteins in infected cells. Expression of the transgenes was detectable as early as four hours post infection and protein amounts increased up to 48 hours. MVA HBVac maintained the replication deficiency in HeLa cells typical for MVA based vectors, but was able to grow in DF-1 cells with an efficiency similar to the MVA F6 wild type control.

2.1.3. The viral genome of MVA HBVac is stable over five low titer passages

To allow transfer of the MVA HBVac into clinical trials, the vector needed to meet the necessary requirements for production under GMP conditions.

Genome stability of MVA HBVac was tested by conducting five consecutive low titer passages in DF-1 cells. DNA was isolated from the viral stocks used for the first infection as well as from the infected cells in the fifth passage. PCR was used to analyze the size of the DNA sequences contained in each deletion site and the HBVac sequence in Del III was further characterized by Sanger sequencing.
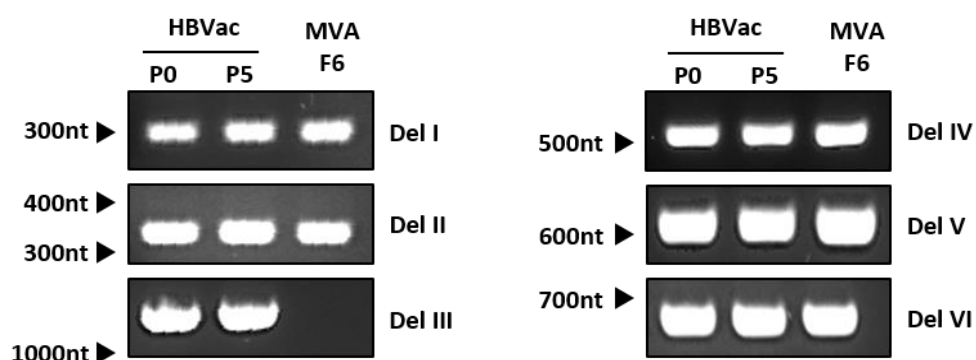
Figure 22: DNA inserts in deletion sites I, II, III, IV, V and VI before and after five low titer passages. The first passage was started by infecting DF-1 cells with MVA HBVac (MOI 0.01) using a viral stock solution. After infection was complete, the infected cells were harvested, the viral titer was determined and the next passage was infected using this crude stock (MOI 0.01). After the fifth passage, the DNA was isolated and the passages zero (P0) and five (P5) were compared using PCR and six different primer pairs.

Deletion sites I, II, IV, V and VI showed identical results for MVA HBVac passages zero (P0) and five (P5) as well as MVA F6, indicating no major changes in these regions. Deletion site III showed an identical signal for P0 and P5 but did not show anything in the MVA F6, meaning that the HBVac insert was stable over five low titer passages (Figure 22).

All in all, genomic stability of the MVA HBVac over five low titer passages was demonstrated, making the virus a suitable candidate for the production of clinical test material under GMP conditions. Genomic stability was further verified later on by using a deep sequencing approach on the virus

material produced under GMP conditions (data not shown). No mutants containing changed HBVac inserts were detected by this method, underlining the genetic stability of MVA HBVac.

2.1.4. MVA HBVac shows comparable *in vivo* antigenicity to its predecessors in C57Bl/6

Treatment of chronic hepatitis B by therapeutic vaccination requires highly antigenic vectors to overcome the virus-induced immune tolerance [188]. To compare the newly created MVA HBVac with its two precursors MVA-S and MVA-C, the new vector was integrated into an established vaccination scheme which was already shown to be effective [181]. All mouse experiments were performed in cooperation with Dr. Anna Kosinska.

C57Bl/6 mice were used as an immunocompetent model without any previous exposure to HBV. Animals either received an adjuvanted protein prime (20µgHBsAg + 20µg HBcAg + 30µg CpG) at day zero and an MVA boost at day 14 or did not receive any vaccination at all. At day 21, seven days after the boost vaccination, animals were sacrificed and their spleenocytes analyzed using intracellular cytokine staining (ICS) and flow cytometry (Figure 23A).

Animals that received a vaccination with either MVA HBVac or the MVA-S +MVA-C vector combination showed increased serum levels of anti-HBsAg and anti-HBcAg antibodies when compared to the untreated control. There were no significant discrepancies between the two different boosts vaccinations (Figure 23B). Analysis of the spleenocytes showed significantly increased numbers of HBsAg or HBcAg specific, IFNγ expressing CD4$^+$ and CD8$^+$ T cells in all vaccinated animals when compared to the unvaccinated controls. Vaccination with MVA HBVac seemed to induce slightly higher T-cell responses than the combination of MVA-S and MVA-C, however this difference was not significant (Figure 23C). Induction of IFNγ$^+$ CD8$^+$ T cells directed against RT (Pol) was also detectable in the vaccinated group, however the overall T-cell response against this antigen was comparatively weak (Figure 23D).

Overall, in a C57BL/6 model MVA HBVac showed a comparable *in vivo* performance as a mix of its predecessors MVA-S and MVA-C with regards to antibody and T-cell induction. Vaccination with MVA HBVac also led to the induction of RT (Pol) specific CD8$^+$ T cells albeit at a much lower level than the comparable S and core responses.
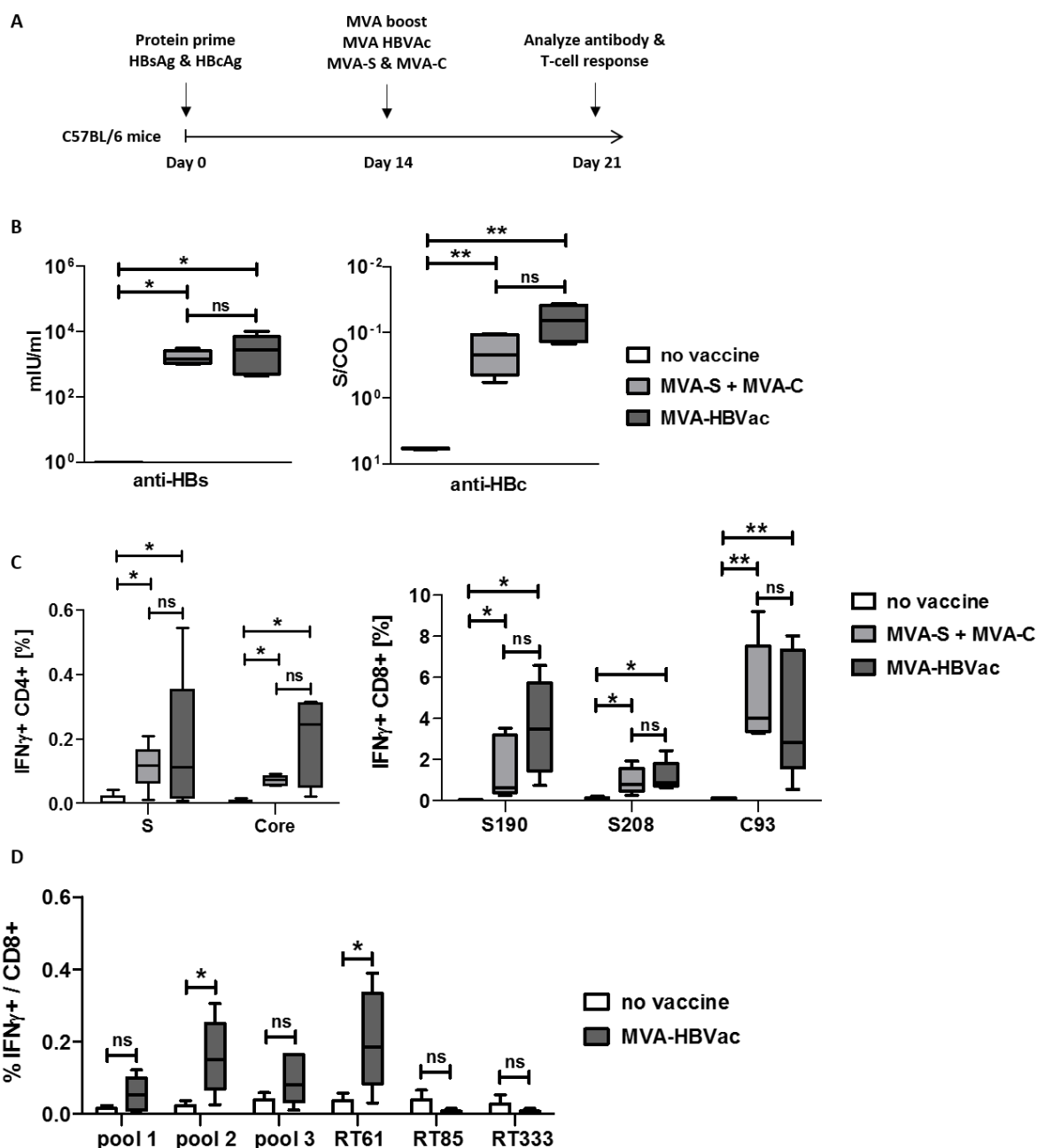
Figure 23: Efficacy of MVA HBVac in a naïve C57BL/6 mouse model. (A) The vaccinated mice all received one adjuvanted protein prime (20µg HBsAg + 20µg HBcAg + 30µg CpG) on day zero and one MVA boost on day 14. The MVA boost contained either MVA HBVac (6×10^7 infectious units (IFU)) or a mixture of MVA-S and MVA-C (3×10^7 IFU + 3×10^7 IFU). All animals, including one unvaccinated control group, were sacrificed at day 21. Spleenocytes were isolated, re-stimulated overnight using peptides or whole proteins and stained using intracellular cytokine staining. **(B)** Anti-HBsAg and anti-HBcAg antibody titers in the serum of all animals were determined by BEP III (n=5). **(C)** Flow cytometry was used to compare the amounts of HBsAg/HBcAg specific, IFNγ producing CD4$^+$ or CD8$^+$ T cells in the spleens of vaccinated and unvaccinated animals (n=5). **(D)** The number of RT(Pol) specific IFNγ$^+$ CD8$^+$ T cells in the spleens of animals which received HBVac or the unvaccinated control mice was determined (n=5). Statistical analysis: Mann-Whitney test (ns: not significant; *p≤0.05; **p≤0.01; ***p≤0.001)

Over all the results indicate a good immunogenicity of MVA HBVac, although the animals only received one protein prime. CD8$^+$ T-cell responses against all antigens encoded by MVA HBVac were detectable,

however the response was much weaker if the animal did not receive a prime with the corresponding protein.

2.1.5. Short term effects of MVA HBVac in a mouse-model of chronic HBV infection

Since mice are not naturally susceptible to HBV infection, different models have been developed to circumvent this problem [195, 196]. The mouse model used in this thesis is based on the delivery of the HBV genome via an adeno-associated virus vector (AAV-HBV) [197]. This liver-specific transduction leads to the expression of high levels of HBV proteins, the establishment of cccDNA molecules and does not induce an immune response [198]. The AAV-HBV model can be used to mimic chronic HBV infection in mice, it is however unable to replicate the full HBV infectious cycle. All mouse experiments were performed in cooperation with Dr. Anna Kosinska.

To test the short-term effects of the newly developed MVA HBVac in an *in vivo* model of chronic HBV infection, the AAV-HBV infected C57BL/6 mice received either two protein primes (10µg HBsAg + 10µg HBcAg + 30µg CpG) at day zero and day 14 as well as an MVA HBVac boost at day 28 or were not vaccinated at all. All animals were sacrificed at day 42. Analysis included HBsAg and HBcAg specific antibody titers, as well as determination of the amounts of HBV specific, CD4$^+$ or CD8$^+$ T cells in both liver and spleen via intracellular cytokine staining (Figure 24A).
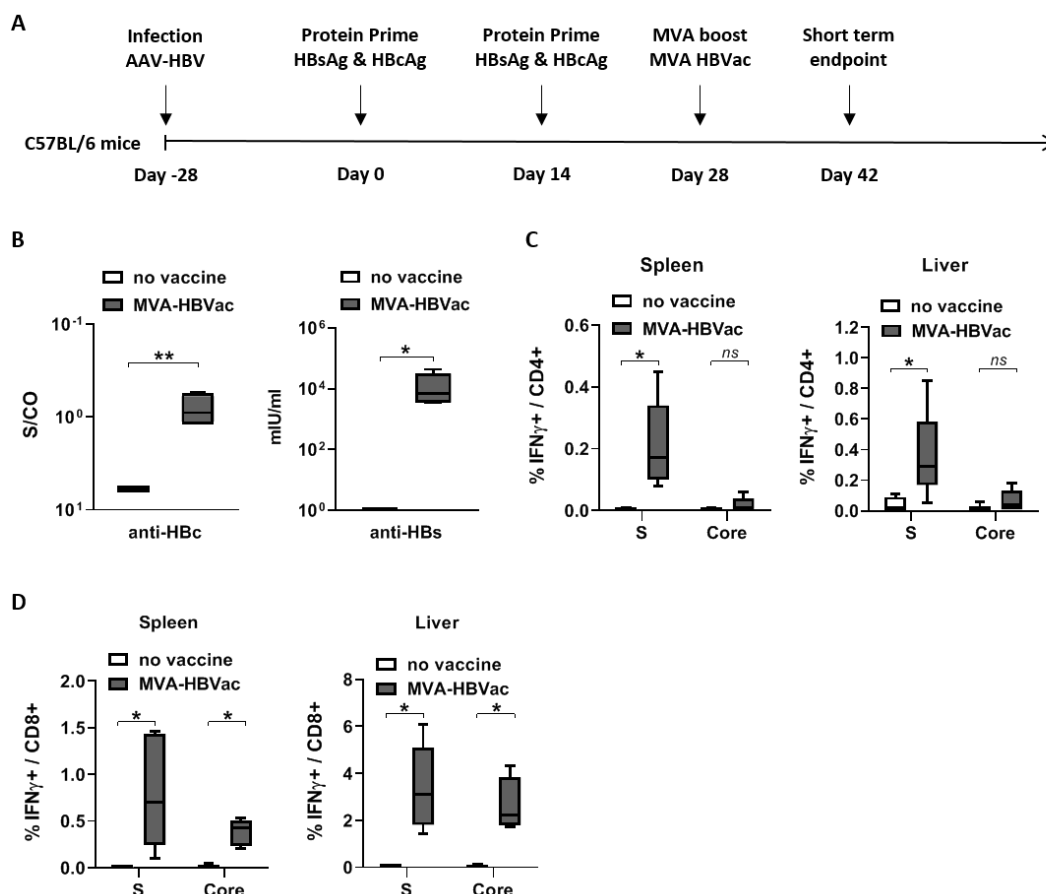
Figure 24:Short-term effects of MVA HBVac in an AAV-HBV mouse model. (A) All vaccinated mice received adjuvanted protein primes (10μg HBsAg + 10μg HBcAg + 30μg CpG) at day zero and day 14 as well an MVA HBVac boost (3x10^7 IFU) at day 28. The mice were sacrificed two weeks later at day 42. Lymphocytes were isolated from the livers and spleens of all animals, stimulated overnight using HBV proteins or peptides, stained using ICS and analyzed via flow cytometry. **(B)** Serum levels of HBsAg and HBcAg specific antibodies were determined (n=5). **(C, D)** The amounts of HBV specific CD4$^+$ and CD8$^+$ T cells in both, liver and spleen, was determined using ICS and flow cytometry (n=5). Statistical analysis: Mann-Whitney test (ns: not significant; *p≤0.05; **p≤0.01; ***p≤0.001)

The serum levels of anti-HBsAg and anti-HBcAg antibodies were significantly elevated in all vaccinated animals when compared to the unvaccinated control (Figure 24B). HBsAg specific CD4$^+$ T cells were significantly increased in the livers and spleens of all vaccinated animals. Induction of HBcAg specific, IFNγ$^+$ CD4$^+$ T cells was also observed. However, changes were marginal and not significant (Figure 24C). Heightened amounts of HBV specific IFNγ expressing CD8$^+$ T cells were detected in both liver and spleen, although the vast majority of cells resided inside the liver tissue (Figure 24D).

As a summary, the results showed a strong induction of antibody and T-cell responses in AAV-HBV C57Bl/6 mice 14 days after the animals received the MVA HBVac. CD4$^+$ as well as CD8$^+$ T cells were detected in liver and spleen, with the majority of effector cells residing inside of the liver.

2.1.6. Long term effects of MVA HBVac in an AAV-HBV mouse-model

In addition to the short-term effects, long term memory responses of MVA HBVac based therapeutic vaccination were evaluated in the AAV-HBV mouse model. All animals were infected using AAV-HBV 4 weeks prior to therapeutic vaccination. The vaccinated animals received protein primes at day zero and day 14 as well as a MVA HBVac boost at day 28. After vaccination, mice were kept for 14 weeks and sacrificed at day 126. The negative control group did not receive any vaccination. Serum levels of HBsAg, HBeAg and ALT were monitored over the course of the experiment in all mice (Figure 25A).
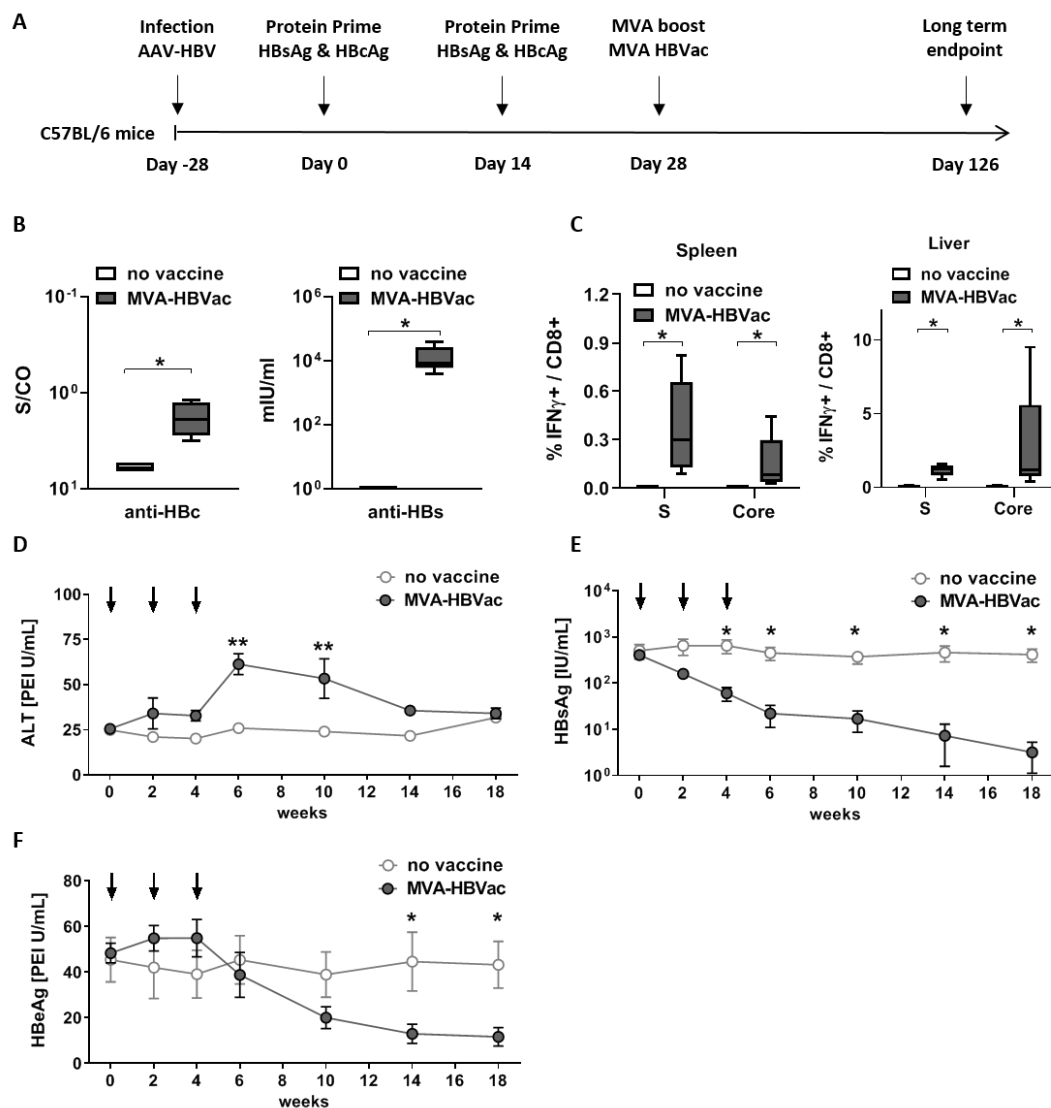
Figure 25: Long term effects of MVA HBVac in an AAV-HBV based mouse model. (A) Vaccinated animals received adjuvanted protein primes (10μg HBsAg + 10μg HBcAg + 30μg CpG) at day zero and day 14 as well as an MVA boost (3x10^7 IFU) at day 28. The control group did not receive any vaccination. All animals were sacrificed at day 126, the lymphocytes were isolated from liver and spleen and analyzed using flow cytometry. **(B)** HBsAg and HBcAg specific antibody titters were determined in the serum of all animals (n=5). **(C)** Lymphocytes were isolated

from both, liver and spleen, and analyzed using ICS and flow cytometry (n=5). **(D, E)** HBeAg and HBsAg levels in the blood of all animals were monitored over the course of the whole experiment (n=5). **(F)** Serum ALT was measured over the course of the whole experiment and serves as a marker for liver damage (n=5).Statistical analysis: Mann-Whitney test (ns: not significant; *p≤0.05; **p≤0.01; ***p≤0.001)

All vaccinated animals showed significantly increased levels of anti-HBsAg and anti-HBcAg antibodies in their serum up to 14 weeks after receiving the booster vaccination (Figure 25B). Significantly higher amounts of S and core protein specific IFNγ$^+$ CD8$^+$ T cells were detected in both liver and spleen of the vaccinated animals, with the majority of cells residing inside of the liver tissue (Figure 25C). HBsAg levels started to drop in all vaccinated animals after they received the first protein prime and continued to drop until the end of the experiment (Figure 25E). In contrast, HBeAg only started to decrease after the animals received the MVA HBVac boost. Similar to HBsAg, HBeAg levels continued to drop until the end of the experiment (Figure 25D). Vaccinated animals showed slightly increased ALT values after receiving the first protein prime, however this increase only became significant after the MVA HBVac boost vaccination. The ALT activity remained significantly increased for the next two weeks and then started to converge towards the ALT levels of the unvaccinated animals (Figure 25F).

To summarize, a therapeutic vaccination based on two protein primes and one MVA HBVac boost overcame the virus induced immune suppression and led to the induction of an efficient and long-lasting anti-HBV immune response. Immune induction resulted in a long-term increase of HBV specific antibodies and T cells, caused transient ALT increase and finally led to loss of HBeAg and HBsAg.

2.2. Influence of cccDNA conformation on interferon mediated cccDNA loss

As demonstrated in the previous part, induction of CD8$^+$ T cells by therapeutic vaccination led to clearance of HBeAg and was associated with loss of infected hepatocytes due to T-cell mediated cell death. However, cytokines produce by activated CD8$^+$ T cells have also been implicated in the non-cytolytic loss of cccDNA [199]. More precisely the cytokines IFNγ and TNFα, which are secreted by stimulated T cells and are elevated in the livers of patients suffering from acute hepatitis B, can lead to a strong reduction of intrahepatic HBV DNA *in vitro* without inducing hepatotoxicity [199, 200]. Since the non-cytolytic loss of cccDNA is an essential part of T-cell mediated HBV clearance, the second part of the thesis is focused on taking a closer look at this mechanism and possible ways to enhance its efficacy.

2.2.1. Interferon alpha treatment induces cccDNA loss in differentiated HepaRG cells.

To verify previously published results [86], differentiated (diff.) HepaRG cells were infected with HBV (MOI 100) and incubated for ten days to allow cccDNA establishment. Afterwards, cells were treated with nucleoside analog Entecavir (ETV) (1μM), IFNα (1000IU/ml) or the Lymphotoxin beta receptor agonist BS1 (1μg/ml) for seven consecutive days. Finally, the levels of the viral markers HBeAg, total intracellular viral DNA and cccDNA were determined (Figure 26A).
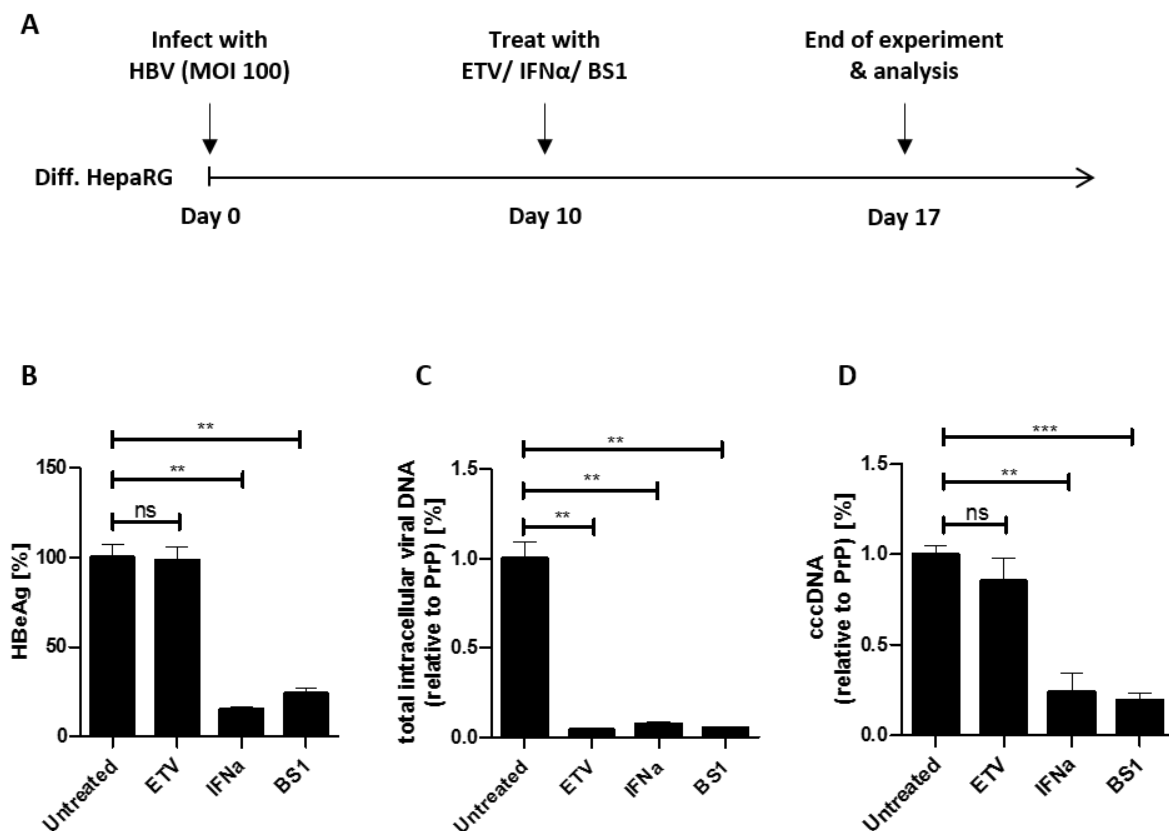
Figure 26: *In vitro* effect of interferon treatment on HBV infection in diff. HepaRG cells. (A) Differentiated cells were infected (MOI 100), incubated at 37°C, 5% CO_2 for ten days and subsequently treated with ETV (1μM), IFNα (1000IU/ml) or BS1 (1μg/ml) for seven days. At the end of the experiment different viral parameters were compared. **(B)** HBeAg levels in the supernatant were determined using BEP III (n=3). **(C, D)** Total intracellular viral DNA as well as cccDNA was determined using qPCR (n=3) and normalized against PRNP (prion protein gene). All results are given as % of untreated. Statistical analysis: Students unpaired t-test with Welch's correction (ns: not significant; *$p \leq 0.05$; **$p \leq 0.01$; ***$p \leq 0.001$)

Treatment with either IFNα or BS1 led to a significant reduction of HBeAg in the supernatant of the treated cells, while ETV did not show any effect (Figure 26B). Total intracellular viral DNA levels were strongly reduced by all three treatments (Figure 26C). cccDNA levels were decreased by roughly 60%

in cells which were treated with either IFNα or BS1. Treatment with ETV on the other hand did not show a significant effect on the levels of viral cccDNA (Figure 26D).

All in all, the previously published results could be successfully replicated and demonstrated a non-cytolytic loss of cccDNA via stimulation by interferon alpha or LTβR activation.

2.2.2. The viral X protein promotes interferon mediated cccDNA loss

To analyze the impact of HBx deletion on cccDNA establishment and transcriptional activity, diff. HepaRG cells were infected using either an HBx deficient HBV mutant (HBV X-) or a WT HBV. Cells were infected with different MOIs and ten days post infection the respective amounts of total intracellular viral DNA and cccDNA were compared (Figure 27A).
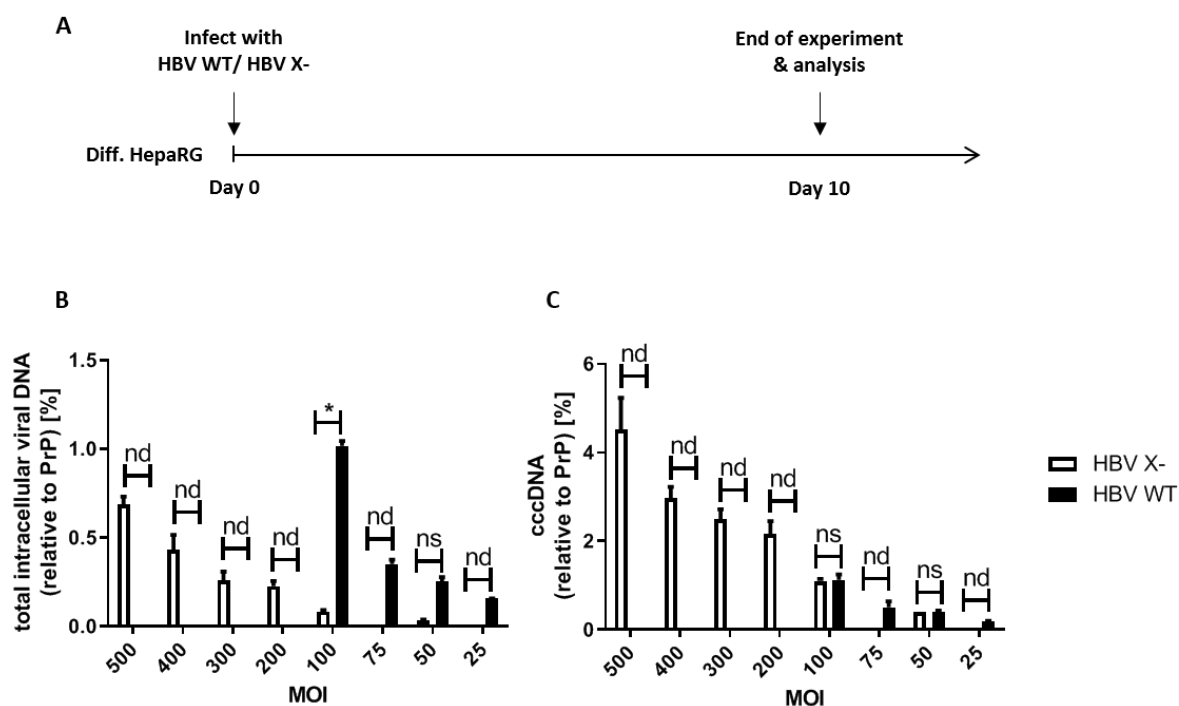
Figure 27: *In vitro* comparison of HBV WT and HBV X- in differentiated HepaRGs. (A) Differentiated cells were infected with different MOIs, incubated at 37°C, 5% CO_2 for ten days and analyzed using qPCR. **(B, C)** Total intracellular viral DNA as well as cccDNA levels were determined using qPCR (n=2) and normalized against PRNP (prion protein gene). All results are given as % of HBV WT MOI 100. Statistical analysis: Students unpaired t-test with Welch's correction (nd: not determined; ns: not significant; *$p \leq 0.05$; **$p \leq 0.01$; ***$p \leq 0.001$)

Infection with increasing MOIs of HBV WT or the HBx mutant led to increasing amounts of total intracellular viral DNA. However, when comparing the viral DNA amounts at identical MOIs, the detectable levels were significantly higher in cells infected with HBV WT than in HBV X- (Figure 27B).

cccDNA levels on the other hand were comparable for both viruses when matching identical MOIs (Figure 27C)

To check for a possible impact of HBx on non-cytolytic cccDNA degradation, diff. HepaRG cells were infected with HBV WT or HBV X-, incubated for ten days and treated for seven days. At the end of the experiment, HBeAg, total intracellular viral DNA and cccDNA levels were analyzed. Treatment with IFNα or BS1 led to significantly decreased amounts of HBeAg in the supernatant of cells infected with HBV WT (Figure 28A). Amounts of total intracellular viral DNA as well as cccDNA were also decreased in all treated samples (Figure 28B, C). Treatment of HBV X- infected cells with IFNα or BS1 significantly decreased HBeAg secretion into the supernatant (Figure 28D), which was comparable to the results observed in the treatment of HBV WT infected cells. Total intracellular viral DNA levels were also significantly affected by ETV, IFNα and BS1 in an HBV X- infection, however the effect was weaker than in HBV WT infected cells (Figure 28E). Lastly, cccDNA levels in HBV X- infected cells remained constant despite IFNα while treatment with BS1 still led to a reduction of cccDNA (Figure 28F).
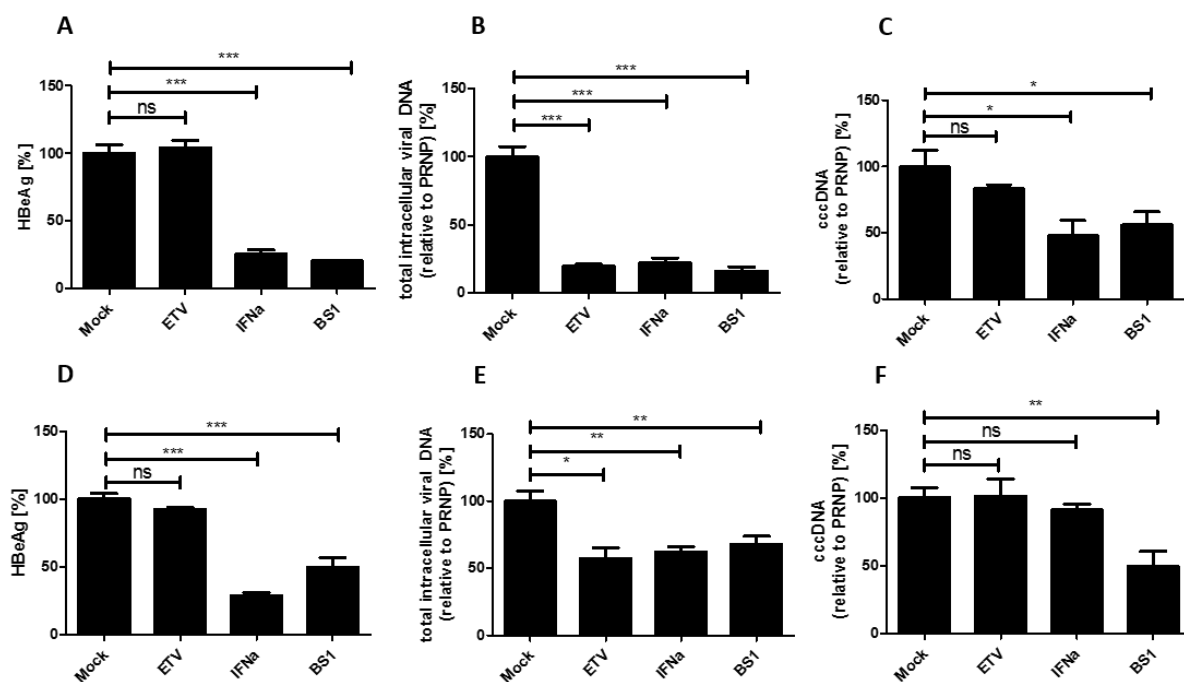
Figure 28: Effect of HBx deficiency on non-cytolytic cccDNA degradation. Diff. HepaRG cells were infected (MOI 100) with either HBV WT (**A**, **B**, **C**) or HBV X- (**D**, **E**, **F**), incubated for ten days at 37°C, 5% CO_2 and then treated for seven days using IFNα (1000IU/ml) or BS1 (1µg/ml). The samples were analyzed using BEP III (HBeAg) or qPCR (total intracellular viral DNA & cccDNA). **(A)** HBeAg levels after treatment in cells infected with HBV WT (n=6). **(B**; **C)** Levels of total intracellular viral DNA and cccDNA after treatment with IFNα or BS1 were determined using qPCR (n=6) and normalized against PRNP. **(D)** HBeAg levels after treatment in cells infected with HBV X- (n=6). (**E**, **F**) Levels of total intracellular viral DNA and cccDNA after treatment with IFNα or BS1 were determined

using qPCR (n=6) and normalized against PRNP. All results are given as % of untreated. Statistical analysis: Students unpaired t-test with Welch's correction (ns: not significant; *p≤0.05; **p≤0.01; ***p≤0.001)

In conclusion, the data showed that reduction of total intracellular viral DNA by either of the treatments was observed for HBV WT as well as HBV X-. However, IFNα mediated, non-cytotoxic cccDNA loss was dependent on the presence of HBx, while induction of cccDNA loss via the LTβR agonist BS1 did not appear to rely on the presence of HBx.

2.2.3. Inhibition of HBx activity by MLN4924 reduces cccDNA loss

As shown above, absence HBx expression reduced the susceptibility of the cccDNA towards interferon-mediated non-cytotoxic degradation. To check whether this effect was linked to HBx mediated Smc5/6 degradation or an alternative pathway, a small molecule inhibitor of the E3 ubiquitin ligase family called MLN4924 was used [70, 201]. To show an effect of the inhibitor on viral transcription, diff. HepaRG cells were infected with HBV WT, incubated for ten days and treated with different doses of MLN4924 for 7 days (Figure 29A).
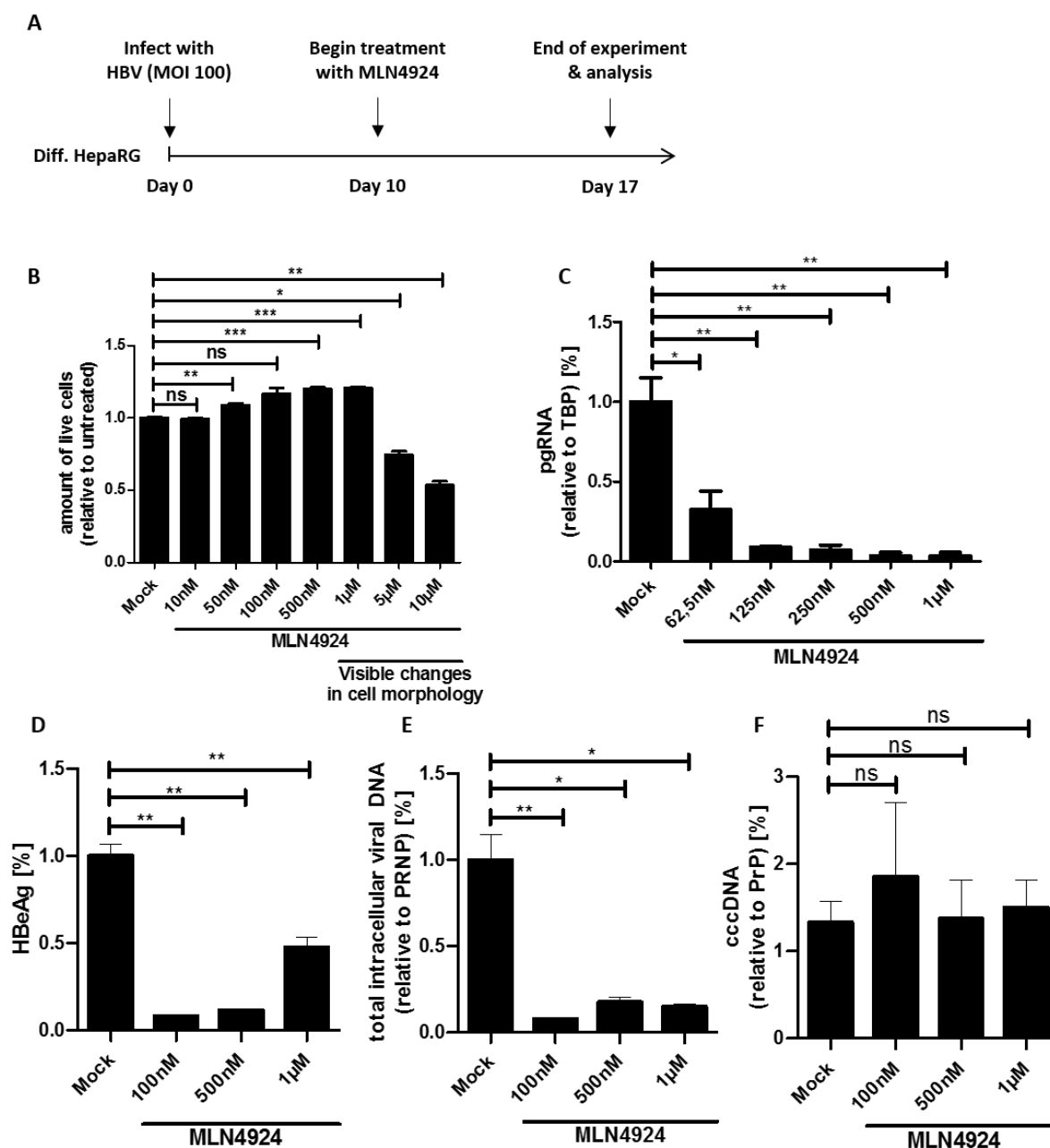
Figure 29: Effect of MLN4924 treatment on HBV infection. (A) Diff. HepaRG cell were infected with HBV WT (MOI 100), incubated for ten days at 37°C, 5% CO_2 and then treated with MLN4924 at varying concentrations. After seven days of treatment cells were analyzed. **(B)** Cell viability of treated and untreated cells was determined using CellTiter-Blue® assay (n=3). **(C)** pgRNA levels in treated and untreated cells were determined using qRT-PCR (n=4). (D) HBeAg in the supernatant of infected and treated cells was determined using the BEP III (n=3) **(E, F)** Levels of total intracellular viral DNA as well as cccDNA were determined using qPCR (n=3) and normalized against PRNP. All results are given as % of untreated. (Statistical analysis: Students unpaired t-test with Welch's correction (ns: not significant; *p≤0.05; **p≤0.01; ***p≤0.001)

Significant cellular toxicity of MLN4924 was only detectable at a concentration >1µM, however use of any concentration higher than 500nM led to changes in cell morphology and an increase of HBeAg

probably due to the irregular release of HBV capsids and was therefore avoided (Figure 29B). Treatment with MLN4924 led to dose dependent, significant decreases in pgRNA as well as HBeAg and total intracellular DNA (Figure 29C, D, E). Total intracellular viral DNA levels were also significantly reduced while the cccDNA remained unaffected indicating that the E3 ubiquitin ligase dependent activation of HBV transcription by HBx through Smc5/6 degradation was prevented (Figure 29E, F).

To determine whether HBx mediated Smc5/6 degradation is necessary for IFNα induced cccDNA loss, diff. HepaRG cells were infected with HBV, incubated for ten days, treated with MLN4924 and IFNα for seven days and analyzed using qPCR and BEP III (Figure 30A).
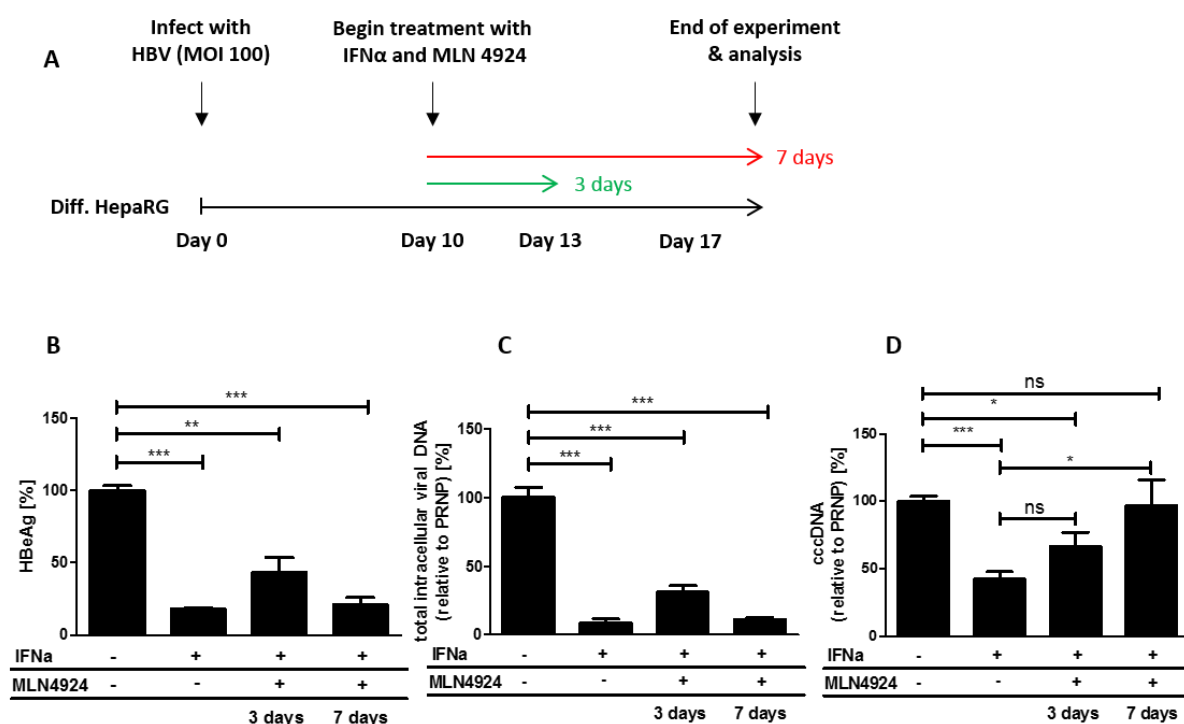
Figure 30: Effect of MLN4924 treatment on non-cytolytic cccDNA degradation. (A) Diff. HepaRG were infected with HBV WT (MOI 100), incubated for ten days at 37°C, 5% CO_2 and then treated with IFNα (1000 IU/ml) for seven days. MLN (500nM) was added simultaneously to IFNα, either for three or seven days. After the end of treatment, the samples were analyzed using qPCR and BEP III. **(B)** HBeAg amounts were determined from the supernatant of the infected cells (n=6). **(C, D)** Total intracellular viral DNA (n=6) and cccDNA (n=6) were determined using qPCR and normalized against PRNP. All results are given as % of untreated. Statistical analysis: Students unpaired t-test with Welch's correction (ns: not significant; *p≤0.05; **p≤0.01; ***p≤0.001)

The supernatant of IFNα or IFNα and MLN4924 treated cells contained significantly reduced amounts of HBeAg (Figure 30B). Total intracellular viral DNA was also decreased significantly by both treatments (Figure 30C). Similar to previous results, treatment with IFNα led to a significant reduction of cccDNA in the diff. HepaRG cells. If MLN4924 was additionally added for three days, cccDNA loss was still observable. However, if MLN was added during the whole IFNα treatment period, no reduction of

cccDNA was observed anymore, indicating that Smc5/6 degradation is essential to allow cccDNA decay (Figure 30D).

In summary, MLN4924 was well tolerated up to concentrations of 500nM and able to efficiently reduce HBV transcription by blocking HBx mediated Smc5/6 degradation. Combination of IFNα and MLN4924 interfered with the interferon-mediated cccDNA loss, indicating that an open cccDNA conformation and viral transcription was required for a non-cytolytic, IFN-induced cccDNA decay.

2.2.4. Reduction of viral transcription by the HAT inhibitor C646 does not influence IFN-mediated cccDNA loss

Previous results showed that interferon-mediated, non-cytotoxic cccDNA degradation is influenced by HBx-regulated viral transcription. Since the epigenetic state of a cccDNA molecule has a major impact on its transcriptional activity, the possible connection between this state and non-cytotoxic cccDNA loss was analyzed.

Here, HAT inhibitor C646 was applied to determine its potential effects on viral transcription and to analyze connections between hypoacetylation of cccDNA and non-cytolytic cccDNA loss [52]. To this end, diff. HepaRG cells were infected, incubated for ten days and treated with either IFNα, C646 or a combination of the two (Figure 31A).
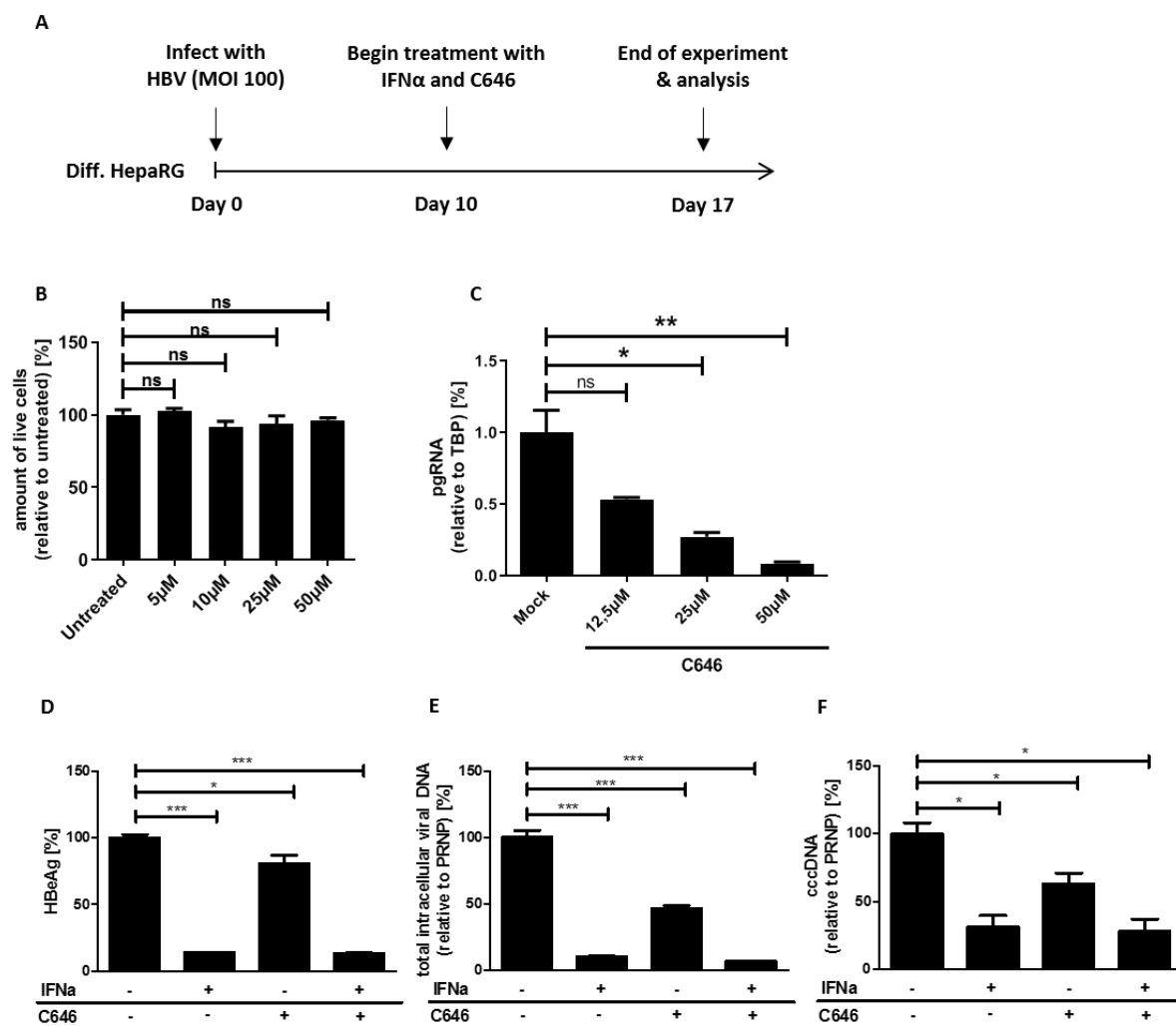
Figure 31: Effect of HAT inhibition on non-cytolytic cccDNA degradation. (A) Diff. HepaRG cells were infected with HBV WT (MOI 100), incubated at 37°C, 5% CO_2 for ten days and then received treatment with either IFNα (1000 IU/ml), C646 (25 μM) or a combination of both for seven days. **(B)** Cell viability of cells treated with different amounts of C646 was determined using the CellTiter-Blue® viability assay (n=3). **(C)** Amounts of viral pgRNA were determined by qRT-PCR and normalized against TBP (n=2). **(D)** HBeAg was determined in the supernatant of the cells using the BEP III system (n=3). **(E; F)** Total intracellular DNA (n=3) as well as cccDNA (n=3) was determined using qPCR and normalized against PRNP. All results are given as % of untreated. Statistical analysis: Students unpaired t-test with Welch's correction (ns: not significant; *$p \leq 0.05$; **$p \leq 0.01$; ***$p \leq 0.001$)

Treatment with C646 was well tolerated at all tested concentrations and resulted in a nearly complete loss of viral pgRNA (Figure 31B, C). C646 caused a significant reduction of HBeAg, but the effect was far weaker than the one observed when using IFNα treatment. Combination of both did not show any additive effects (Figure 31D). Similar results were observed for total intracellular viral DNA levels. Treatment with both, IFNα or C646 significantly reduced the amounts detected, while co-treatment did not show any additive effect (Figure 31E). cccDNA levels were slightly affected by C646 treatment, however the effect was less than that observed for interferon-mediated cccDNA degradation.

Simultaneous treatment with IFNα and C646 did not seem to influence the non-cytolytic loss of cccDNA (Figure 31F).

Taken together, the HAT inhibitor C646 was well tolerated and lead to efficient reduction of viral transcription by interfering with epigenetic regulation. However, unlike the effect observed in HBV X-virus infection, reduction of transcriptional activity did not show any effect on interferon-mediated non-cytolytic cccDNA degradation.

2.2.5. Increasing viral transcription by the HDAC inhibitor Trichostatin A does not influence cccDNA loss

Treatment of cells with the HDAC inhibitor Trichostatin A (TSA) results in the accumulation of acetylated histone H3/H4 and enhanced transcription [202]. A potential influence of an enhanced expression on non-cytotoxic cccDNA degradation was evaluated in the HepaRG model. Diff. HepaRGs were infected with HBV, incubated for ten days and treated using either IFNα, TSA or a combination of both (Figure 32A).
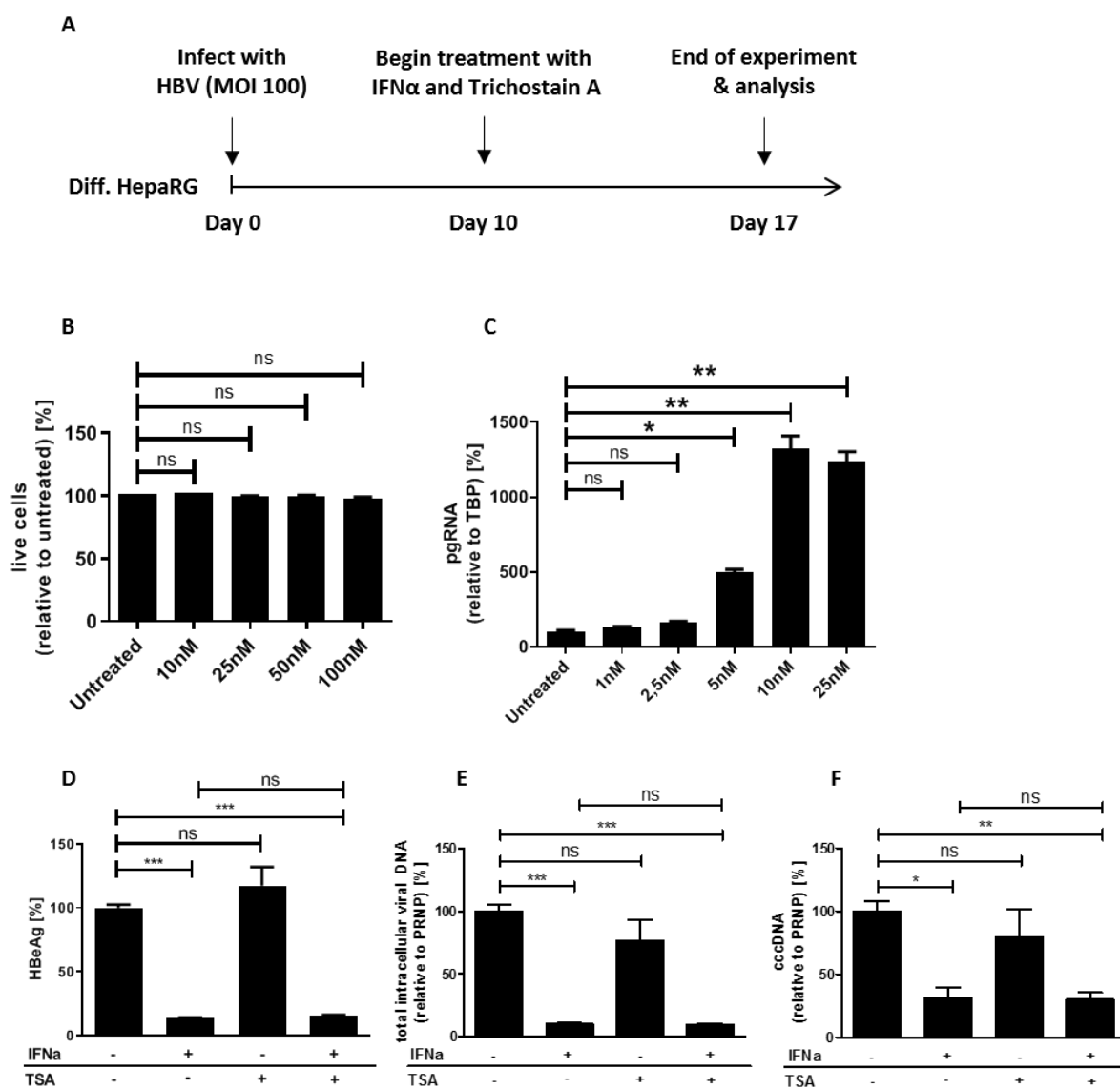
Figure 32: Effect of HDAC Inhibitor TSA on non-cytolytic cccDNA degradation. (A) Diff. HepaRG were infected with HBV (MOI 100), incubated at 37°C, 4% CO_2 for ten days and then treated with IFNα (1000 IU/ml), TSA (50nM) or a combination of both for seven days. **(B)** Cell viability of cells treated with different amounts of TSA was determined using the CellTiter-Blue® viability assay (n=3). **(C)** Amounts of viral pgRNA were determined by qPCR and normalized against TBP (n=2). **(D)** HBeAg titer was determined in the supernatant of the cells using a BEPIII measurement (n=3). **(E, F)** Total intracellular viral DNA (n=3) as well as cccDNA (n=3) levels were determined using qPCR and normalized against PRNP. All results are given as % of untreated. Statistical analysis: Students unpaired t-test with Welch's correction (ns: not significant; *p≤0.05; **p≤0.01; ***p≤0.001)

Treatment with TSA was well tolerated at all concentrations tested and led to a roughly tenfold increase of viral pgRNA (Figure 32B, C). Detected HBeAg levels showed a slight increase however, the effect was not significant and combinatorial treatment with IFNα and TSA did not show any difference to treatment with IFNα alone (Figure 32D). Total intracellular viral DNA as well as cccDNA levels were

not affected by TSA treatment showing no discernible effect of TSA treatment on the interferon-mediated non-cytotoxic cccDNA degradation (Figure 32E, F).

In summary, treatment with TSA resulted in a strong increase in viral transcription. However no effect on the interferon-mediated, non-cytotoxic cccDNA degradation was observed.

Altogether, we could show that the cytokine-induced, non-cytotoxic cccDNA degradation is strongly dependent on the presence and activity of the viral HBx protein. Loss of HBx-mediated Smc5/6 degradation, either due to knockout or MLN4924 treatment, significantly reduced the effect of IFNα on the cccDNA levels. Treatment of infected cells with substances which influence histone modification either reduced or increased viral transcription, however no effect on the interferon-mediated non-cytolytic degradation of cccDNA was detectable in either case.

2.3. Intracellular localization of ISG20 and its connection to cytokine-mediated cccDNA degradation

Our lab recently identified that a key player of the non-cytolytic cccDNA loss is a nuclease called interferon stimulated gene 20 protein (ISG20). ISG20 has been shown to localize in either cajal bodies, cytoplasmic processing bodies, promyelocytic leukiaemia (PML) nuclear bodies or the nucleolus, depending on the publication [203-206]. This information was used as the starting point to answer the question whether the process of cccDNA degradation is localized at specific areas of the cell and if yes which role does this location play for the process itself.

2.3.1. ISG20 localizes to the nucleoli in HepaRG and HepG2 NTCP cells

Diff. HepaRGs were stimulated using either IFNα or IFNγ and stained for PML proteins as well as ISG20 using immunofluorescence (IF). PML proteins showed the typical intra-nuclear distribution into several small structures. The formation of these structures was induced by both of the two interferon treatments. ISG20 seemed to localize mainly to large structures inside the nucleus, however there was a diffuse background stain over the whole cytoplasm. A co-localization between the PML bodies and the ISG20 enzyme could not be detected in this cell line (Figure 33).
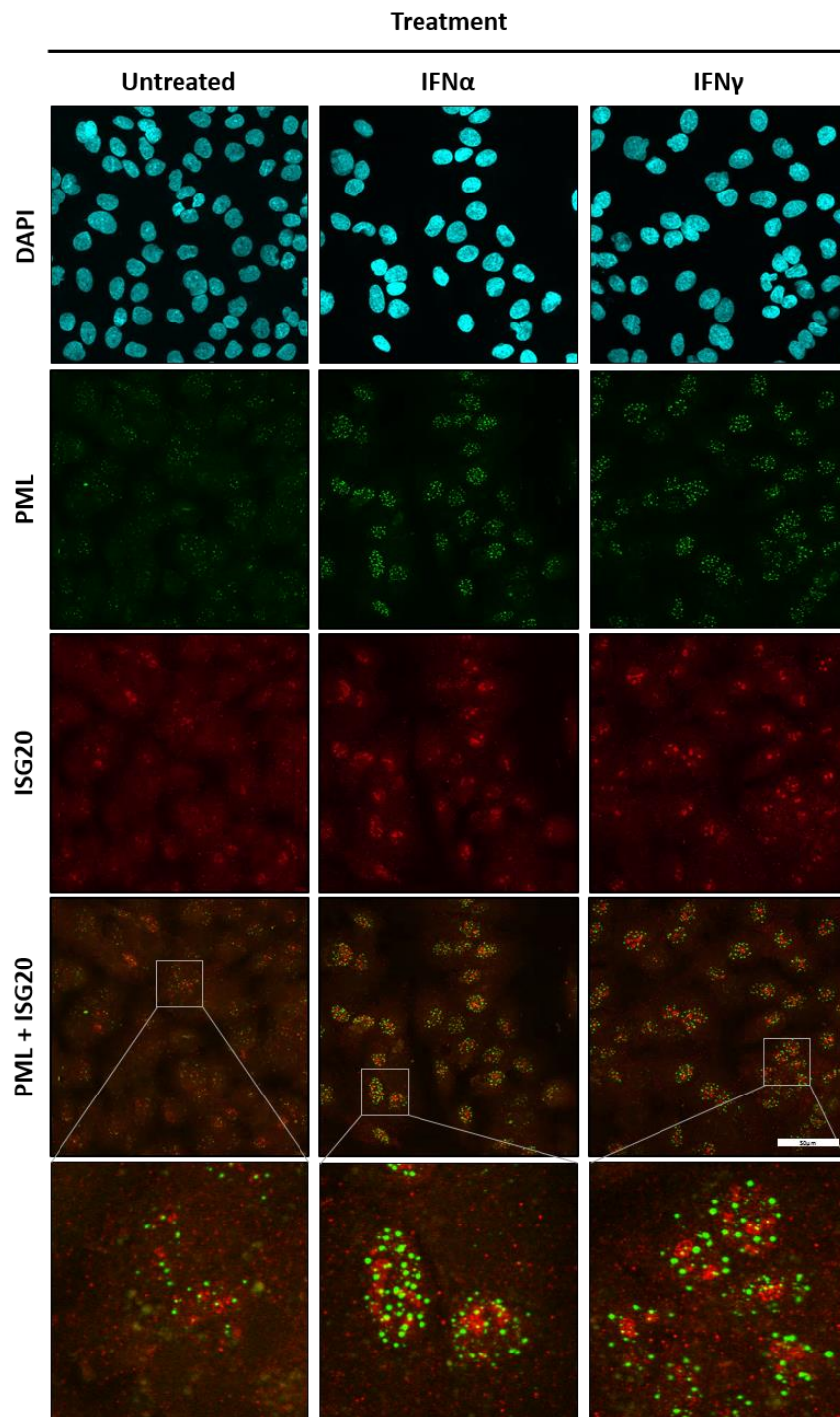
Figure 33: Intracellular localization of PML and ISG20 in HepaRG cells. Diff. HepaRG cells were stimulated using IFNα/γ (600/400 IU/ml) for 48 hours and after stimulation were fixed, permeabilized and stained using DAPI (nuclear stain) as well as antibodies directed against PML (all isoforms) or ISG20. Scale bar: 50μm.

Since Co-localization of the PML proteins and ISG20 could not be confirmed, we next investigated a possible nucleolar localization. Therefore, nucleoli were stained using a monoclonal antibody directed against the protein nucleophosmin, a component of cellular nucleoli.
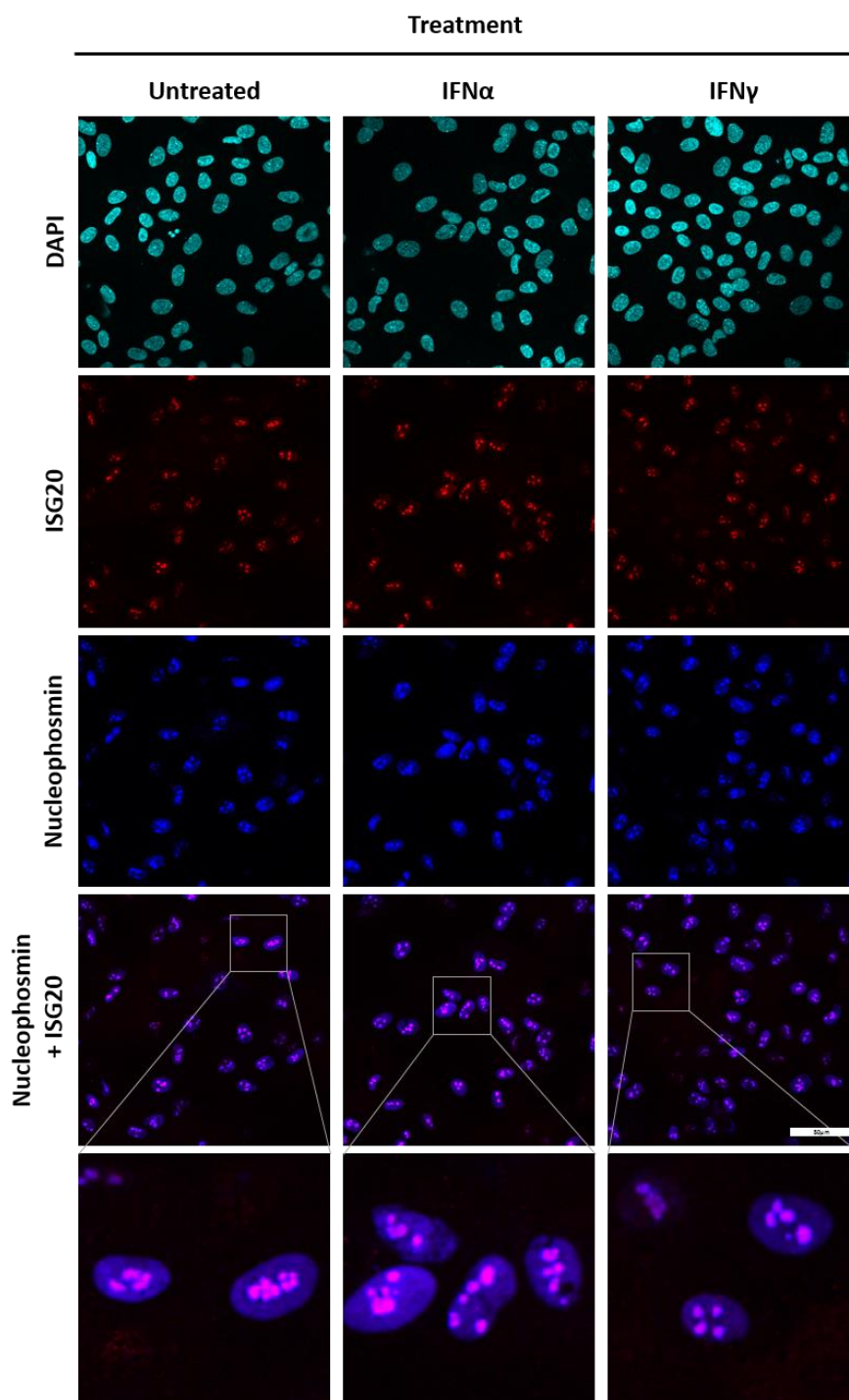
Figure 34: Intracellular localization of ISG20 and Nucleophosmin in diff. HepaRG cells. Diff. HepaRG cells were stimulated using IFNα/γ (600/400 IU/ml) for 48 hours and after stimulation were fixed, permeabilized and stained using DAPI (nuclear stain) as well as antibodies directed against nucleophosmin or ISG20. Scale bar: 50μm.

The intracellular distribution of nucleophosmin is mostly nucleolar and the majority of the protein is concentrated in distinct structures. Co-staining of nucleophosmin and ISG20 showed a clear co-localization between the two proteins (Figure 34).

Since protein localization can vary heavily between different cell lines an alternative hepatocyte cell line (HepG2-NTCPs) was used to verify the previous findings. The cells were differentiated, stimulated and stained using immunofluorescence (Figure 35).
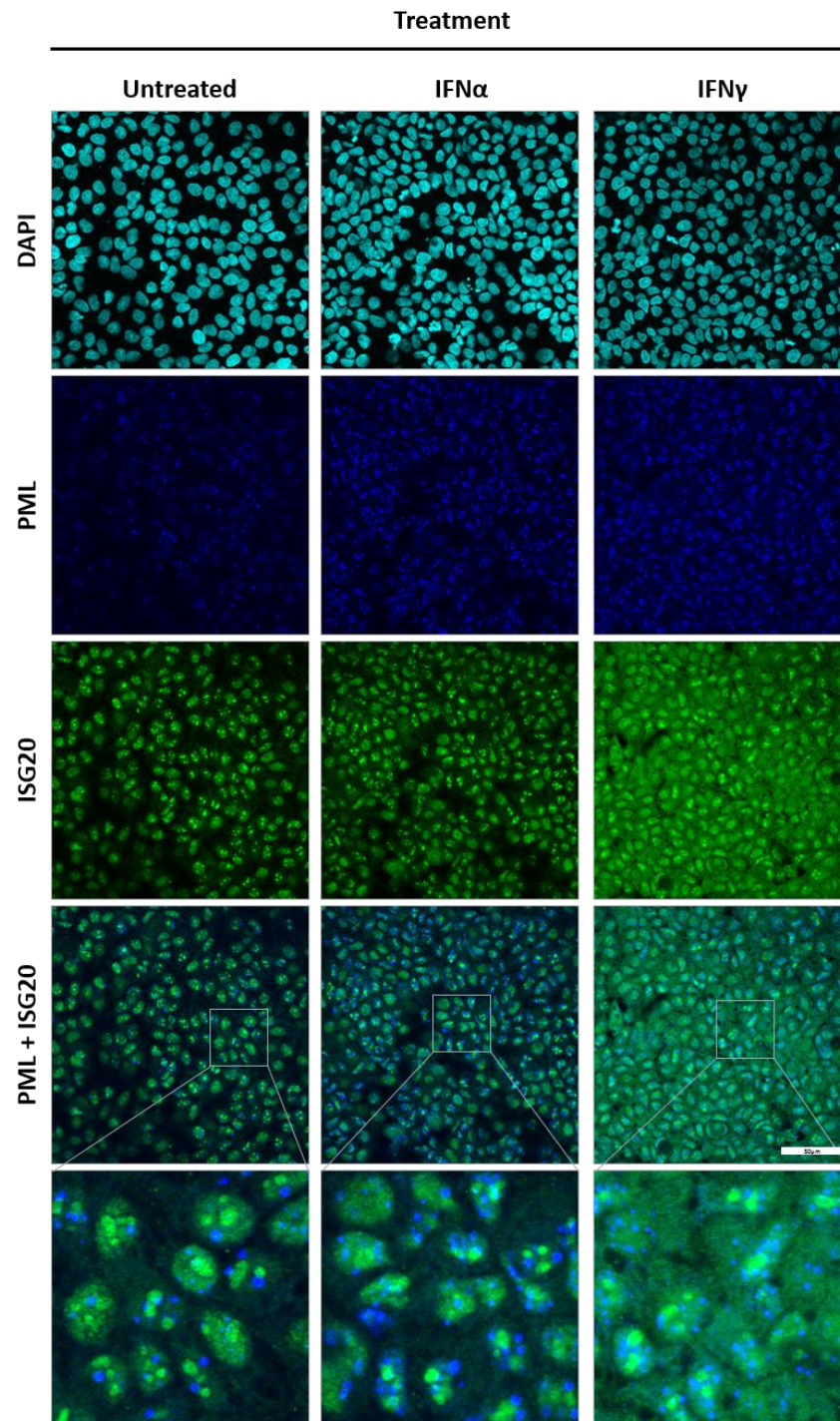
Figure 35: Intracellular localization of PML and ISG20 in HepG2-NTCP cells. Diff. HepG2-NTCP K7 cells were stimulated using IFNα/γ (500/200 IU/ml)for 48 hours and after stimulation were fixed, permeabilized and stained using DAPI (nuclear stain) as well as antibodies directed against PML (all isoforms) or ISG20. Scale bar: 50μm.

Similar to the results from the HepaRG cell line, the PML protein is distributed into several small, distinct, nuclear structures and treatment with IFNα/γ led to the upregulation of PML protein

expression. ISG20 was mainly localized in the nuclei, in the form of distinct structures and no co-localization with PML was observed (Figure 35). The baseline expression of ISG20 in HepG2-NTCP cells was comparatively high and treatment with either interferon led only to a slight increase. However, again there was no discernable co-localization between PML and ISG20.
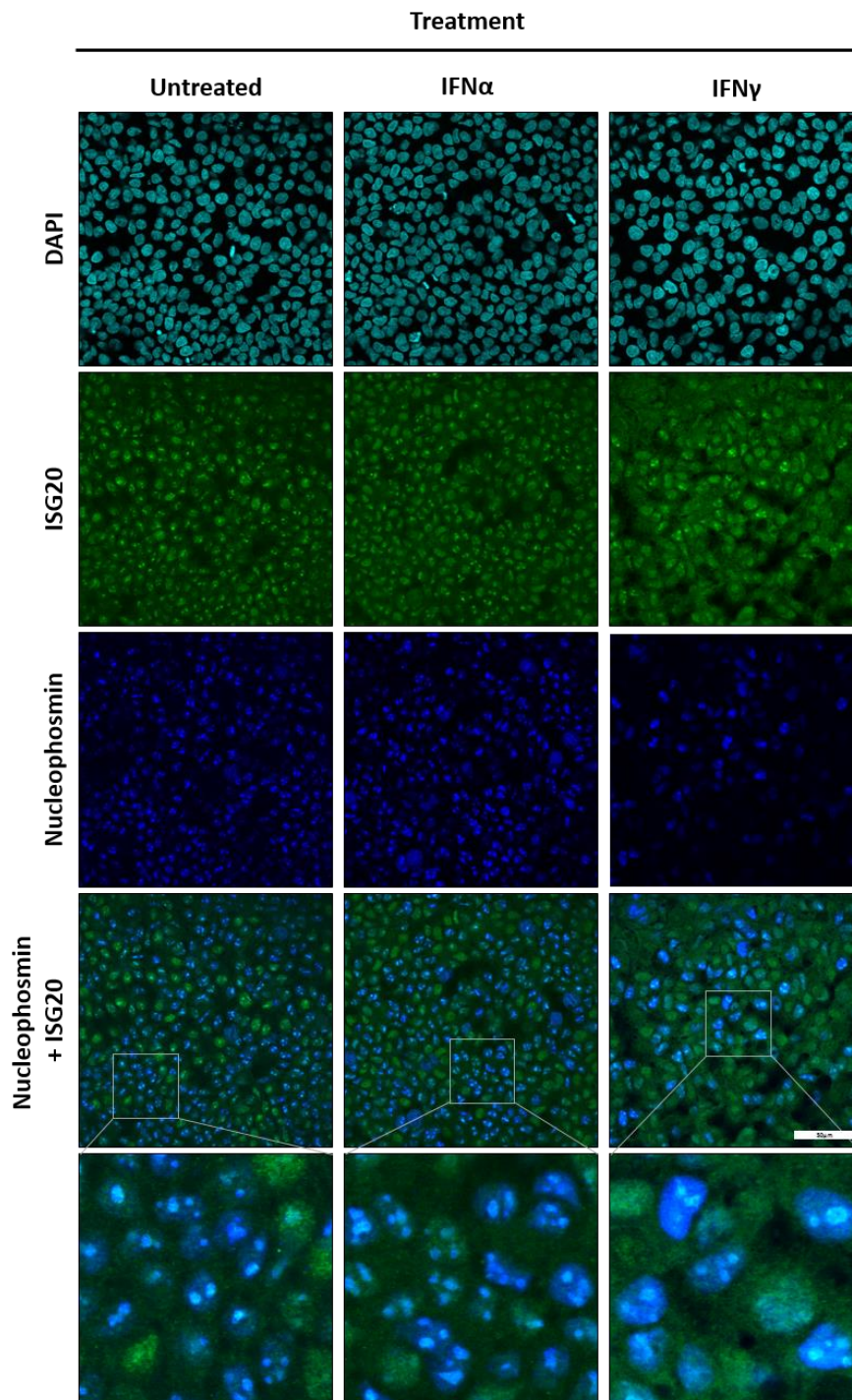
Figure 36: Intracellular localization of ISG20 and Nucleophosmin in HepG2 NTCP cells. Diff. HepG2-NTCP K7 cells were stimulated using IFNα/γ (500/200 IU/ml) for 48 hours and after stimulation were fixed, permeabilized and stained using DAPI (nuclear stain) as well as antibodies directed against Nucleophosmin or ISG20. Scale bar: 50µm.

As observed in the diff. HepaRG cells (Figure 34), ISG20 and nucleophosmin also co-localized in HepG2-NTCP cells (Figure 36). ISG20 staining in HepG2 NTCP cells produced a strong background signal in the whole cell. The brighter areas, however, were located exclusively in the nucleus of the cell and co-localized with the nucleophosmin signal.

To confirm these observations, diff. HepaRG cells were stimulated using IFNα (600IU/ml) for 24 or 48 hours and cells were separated into their cytoplasmic and nuclear fraction using the CelLytic™ NuCLEAR™ Extraction Kit.
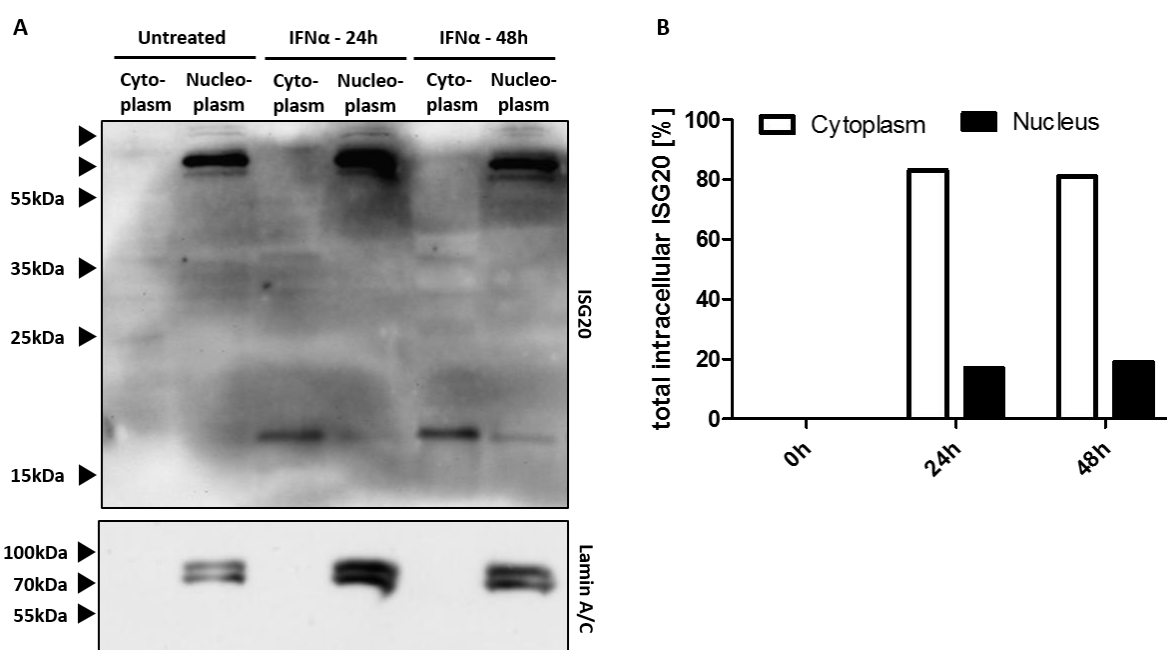
Figure 37: Western blot analysis of intracellular ISG20 distribution. Dif. HepaRG cell were stimulated using IFNα (600IU/ml) for up to 48h. After stimulation the cells were separated into their cytoplasmic and nuclear components using the NXTRACT kit and analyzed by Western blot. Lamin A/C is an exclusively nuclear protein and was used a marker for the purity of separation. **(A)** Analysis of the intracellular distribution of ISG20 and Lamin A/C. The correct ISG20 band appears in the upper blot at 20kDa. **(B)** Quantification of the intracellular distribution of ISG20 upon stimulation.

Detection of ISG20 by Western blot at the expected size of 20kDa was only possible after stimulation by IFNα. Most of ISG20 was localized in the cytoplasm of the cells, while only a small proportion was found in the nuclear fraction. The antibody also detects a large protein of unknown identity at around 70kDa which is exclusively localized to the cytoplasm (Figure 37A). Quantification of the ISG20 signal showed that only around 15% of ISG20 was detectable in the nuclear fraction (Figure 37B). The nuclear proteins Lamin A/C served as a control to confirm successful separation of cytoplasm and nucleus.

To ensure the functionality of the ISG20 antibody used in immunofluorescence and Western blots, cells were transfected with a plasmid encoding for ISG20 fused to an mKate fluorophore.
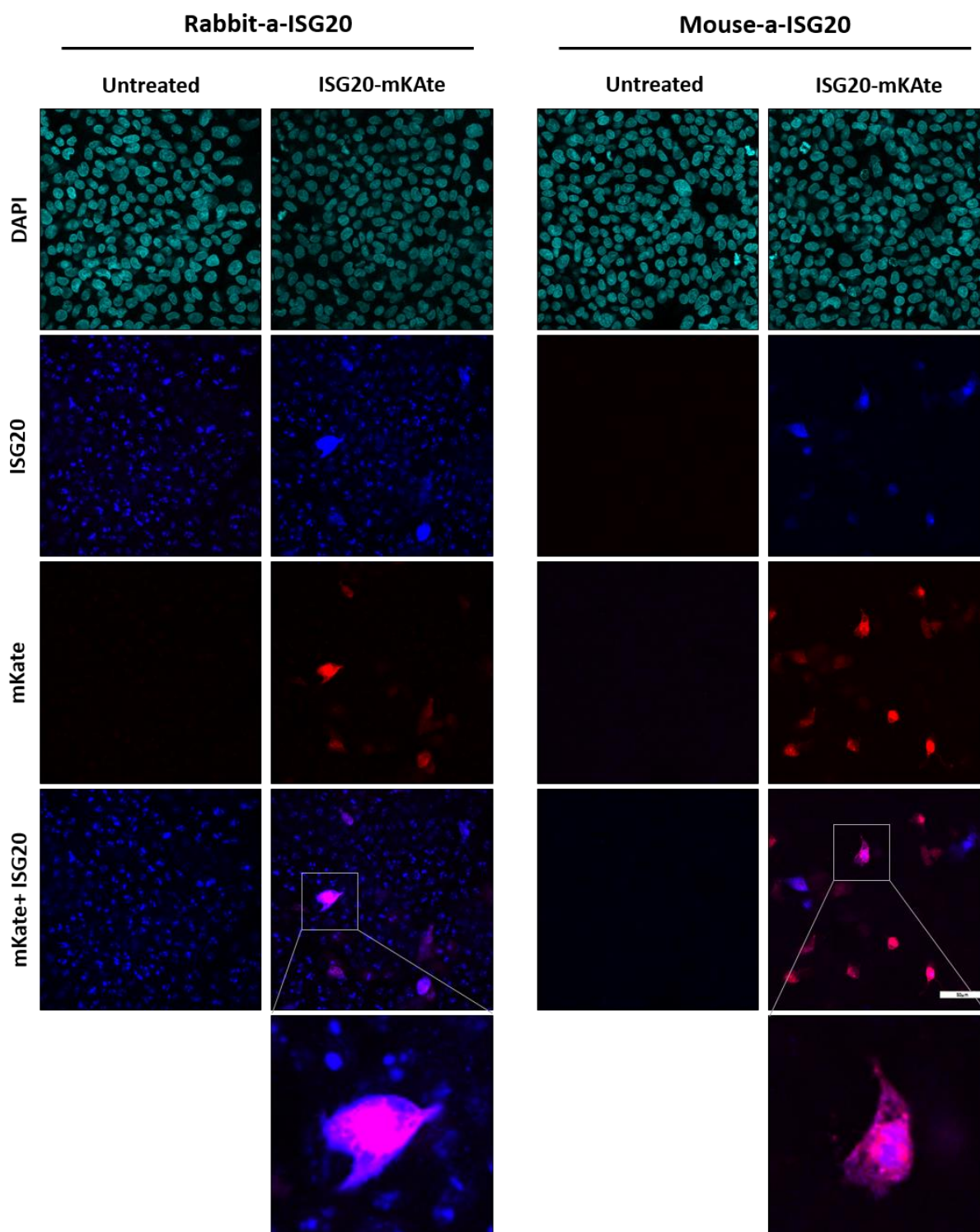
Figure 38: Specificity and sensitivity of anti-ISG20 antibodies. HepG2 NTCP cells were transfected using 5µg DNA/well, incubated for 72 hours at 37°C, 5% CO_2, stained using DAPI and two different anti-ISG20 antibodies and analyzed using immunofluorescence. Scale bar: 50µm.

Both of the tested antibodies were capable of recognizing the overexpressed ISG20 in the transfected cells, however only the Rabbit-a-ISG20 antibody showed the necessary sensitivity to detect the endogenous ISG20 (Figure 38). The overexpressed ISG20 was not specifically localized to any compartment of the transfected cells.

In addition, antibody specificity was verified using two different HepaRG derived cell lines (HepaRG NTsgRNA. HepaRG ISG20sgRNA) stably transduced with CRISPR/Cas9 system. These cells were transfected either with a nonsense or an ISG20 directed sgRNA to knock out of ISG20. Cell lines were treated with IFNα (600IU/ml) for 48 hours, stained and analyzed using IF.
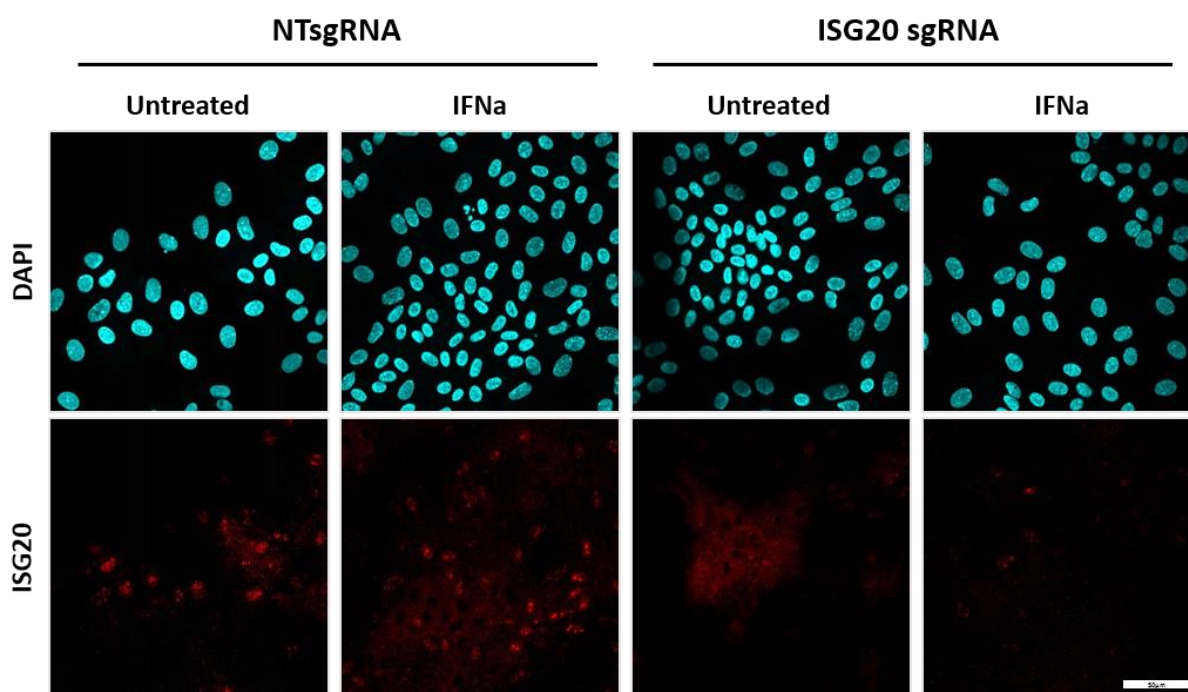
Figure 39: Specificity of Rabbit-a-ISG20. The knock-out cell line was created using CRISPR/Cas9 and an sgRNA specific for ISG20, a non-target sgRNA (NTsgRNA) was used as control. Diff. HepaRG cells were stimulated using IFNα (600 IU/ml) for 48 hours at 37°C, 5% CO_2. After stimulation the cells were stained using DAPI and antibodies against ISG20 and analyzed by immunofluorescence. Scale bar: 50μm.

Knockout of ISG20 led to loss of the bright, dot-like structures localized in the nucleus of the cells while upon IFNα treatment the background fluorescence in the cytoplasm of some cells remained detectable (Figure 39).

In summary, the data showed that ISG20 did not co-localize with the PML bodies and instead was detected in nucleoli. The majority of ISG20 inside of the cell was shown to be distributed throughout the cytoplasm, while around 15% of total ISG20 localized to the nucleus upon IFN treatment.

2.3.2. HBV infection does not influence the induction or localization of ISG20

Different viruses have been shown to influence ISG20 induction and co-localization between ISG20 and viral proteins has also been demonstrated for human alphainfluenzavirus [207]. To check whether HBV does affect the induction or localization of ISG20 in infected cells, diff. HepaRG cells were infected with HBV, incubated for ten days, treated for 48 hours using IFNα (600IU/ml) and then stained and analyzed using immunofluorescence.
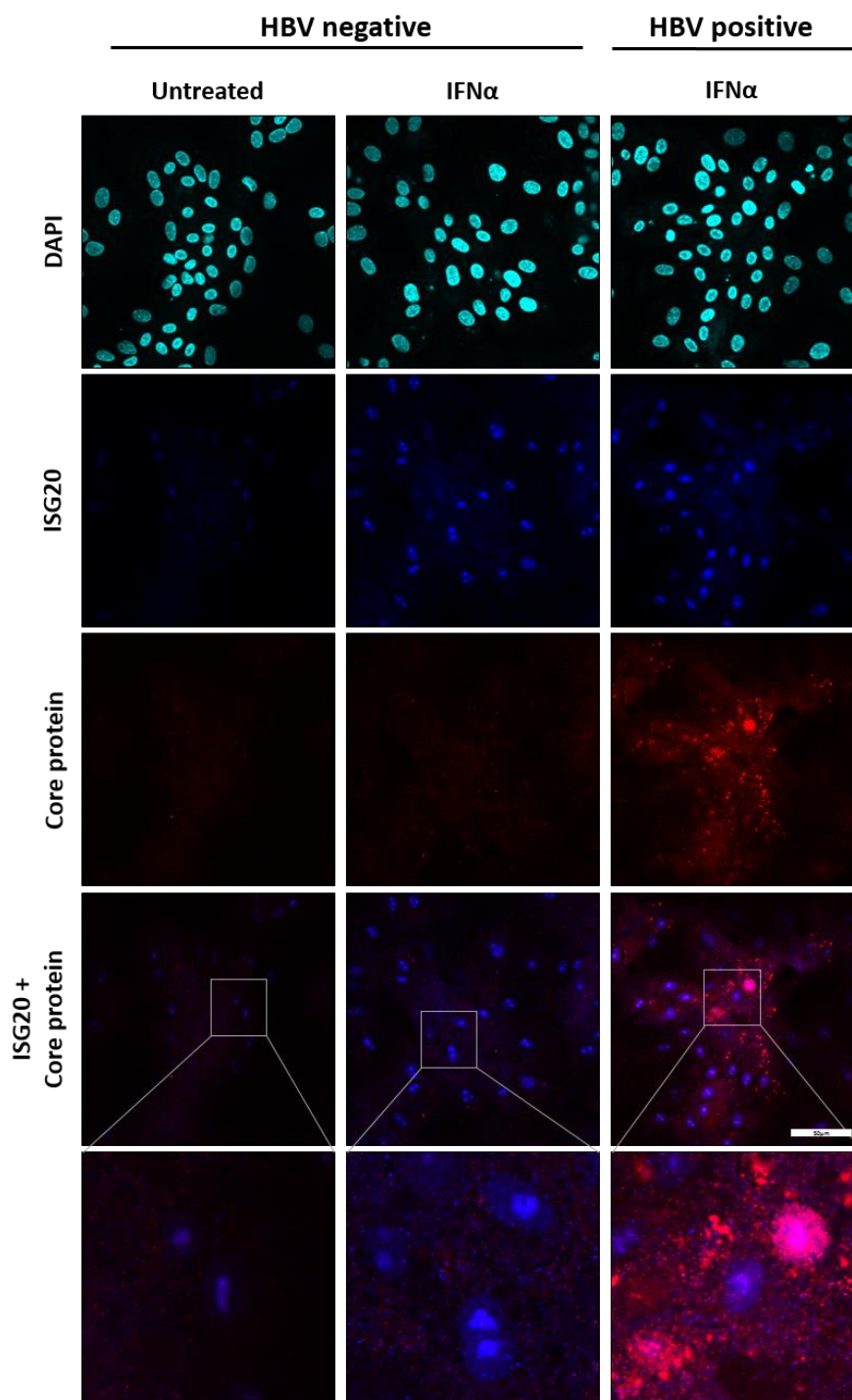
Figure 40: Effect of HBV infection on ISG20 induction and localization in diff. HepaRG cells. The diff. HepaRG cells were infected with HBV (MOI 100), incubated at 37°C, 5% CO_2 for ten days and then treated with IFNα (600 IU/ml) for 48 hours. After the treatment, cells were stained using antibodies against ISG20 and HBV core protein and analyzed using immunofluorescence. Scale bar: 50µm.

As shown previously, treatment with IFNα led to the induction of ISG20 in diff. HepaRG cells. Expression of ISG20 was detectable in infected as well as uninfected cells without a noticeable difference (Figure 40). The ISG20 signal showed brightly fluorescent dot-like structures in the nuclei of cells as well a background fluorescence throughout the nucleus. This distribution remained unchanged by HBV infection and there was no clear co-localization between ISG20 and the viral core protein.

This setup was repeated using primary human hepatocytes instead of the HepaRG cell line, to ensure that the observed effects were not dependent on the cell line used. PHH were infected with HBV and incubated for 72 hours before stimulation by IFNα. After 48 hours of treatment the cells were stained and analyzed by immunofluorescence.
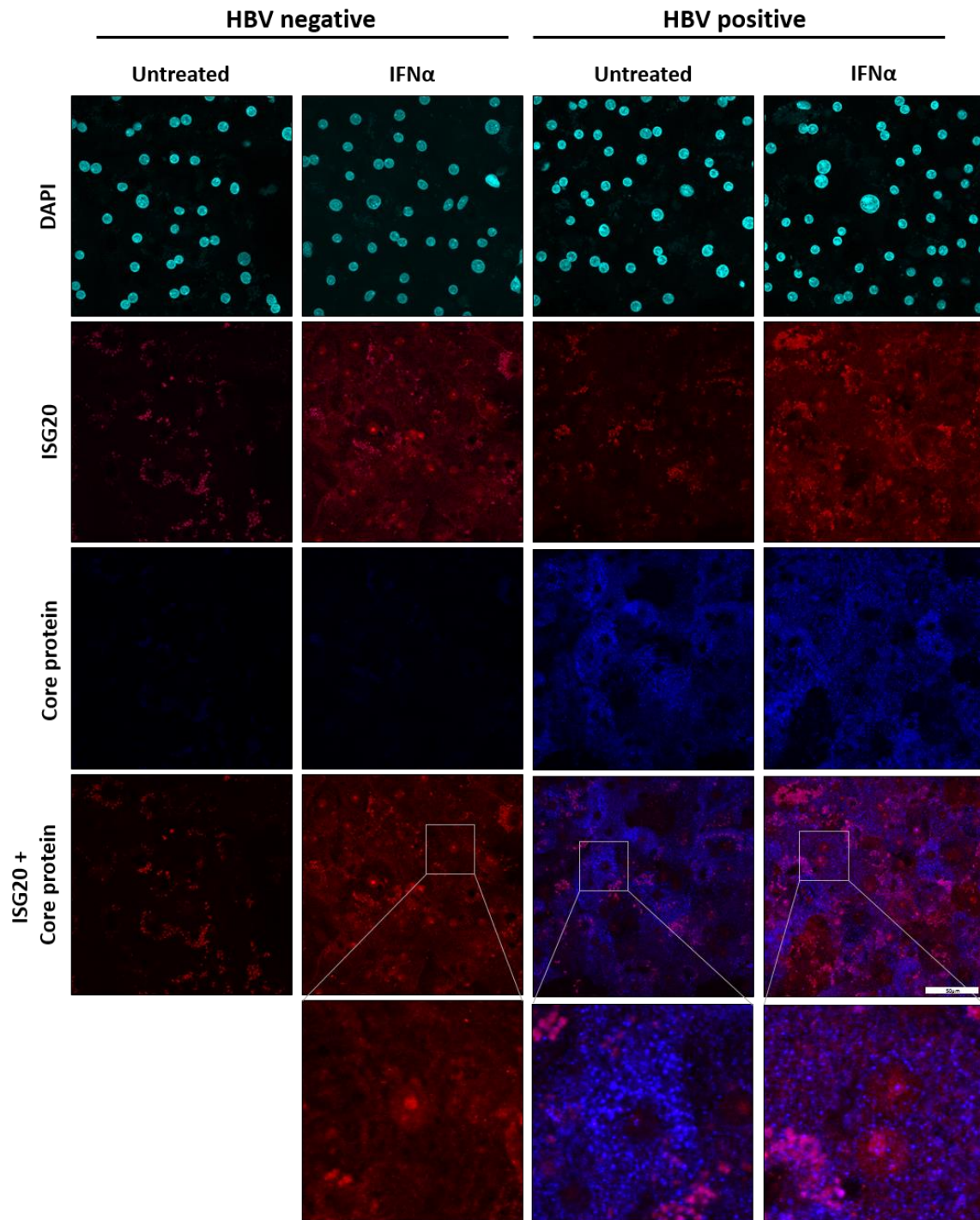
Figure 41: Effect of HBV infection on induction of ISG20 and distribution in infected primary human hepatocytes. PHH were infected with HBV (MOI 100), incubated for three days at 37°C, 5% CO_2 and then treated using IFNα (600 IU/ml)) for 48 hours. After treatment the cells were stained and analyzed using immunofluorescence. Scale bar: 50µm.

All PHH samples showed a strong background in the ISG20 staining which was increased by IFNα stimulation (Figure 41). The typical, bright, dot-like ISG20 structures could also be detected upon stimulation. However they were difficult to see due to the high background fluorescence. The core protein stain did not show any unspecific signal in uninfected cells. Upon infection with HBV, the core protein was equally distributed throughout the cytoplasm of infected cells, while the nuclei contained only very low amounts of the viral protein. HBV infection did neither influence ISG20 induction on a detectable level nor did it affect the intracellular distribution of the enzyme.

Since viral core protein was distributed throughout the cytoplasm and nucleus, detection of possible interactions between HBc and ISG20 via co-localization was difficult. Therefore, possible direct interactions between HBV core protein and ISG20 were analyzed using co-immunoprecipitation. Diff. HepG2-NTCP cells were infected with HBV, incubated for five days and stimulated with IFNα for 48 hours.
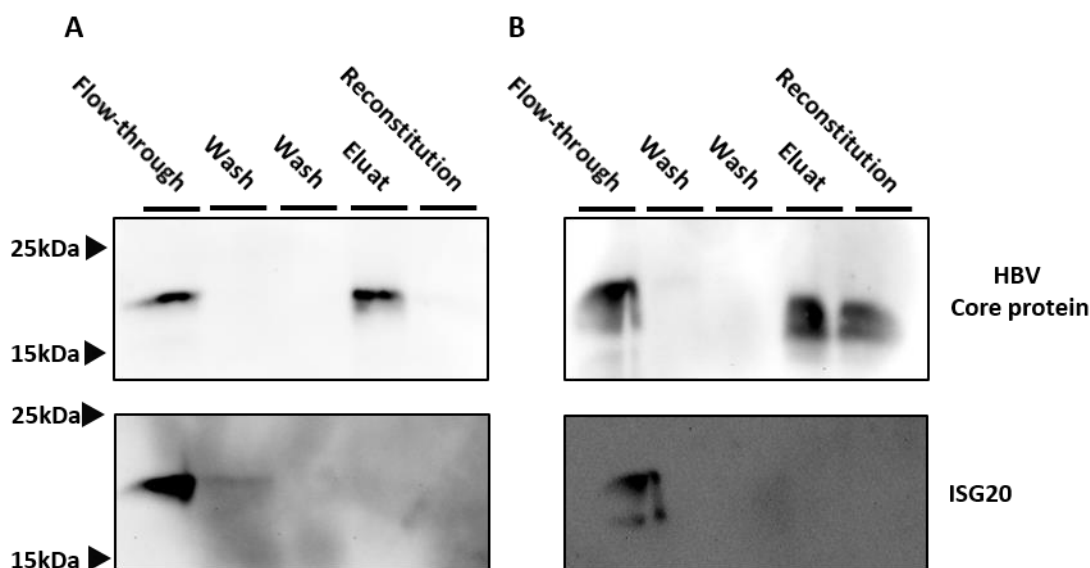
Figure 42: Co-immunoprecipitation of HBV core protein and ISG20. Diff. HepG2-NTCP cells were infected with HBV (MOI 100), incubated for ten days at 37°C, 5% CO_2 and then either **(A)** analyzed directly or **(B)** stimulated using IFNα (600 IU/ml) for 48 hours bevor analysis. Immunoprecipitation was done using monoclonal anti-core antibodies. The different fractions were analyzed using Western blot.

Immunoprecipitation with an anti-core antibody was successful and led to the detection of core protein in the eluate and reconstitution fractions. However, binding was incomplete and part of the core protein passed through the column. ISG20 was detected nearly exclusively in the flow-through in both the unstimulated (Figure 42A) as well as the stimulated setup (Figure 42B). There was no detectable direct interaction between the viral core protein and ISG20.

Summing up the previous results, infection with HBV did not seem to influence the induction or distribution of ISG20 in diff. HepaRG cells or PHH. There was also no detectable direct interaction between ISG20 and the viral core protein.

2.3.3. HBV infection as well as interferon treatment influence the nucleoli composition

Since there seemed to be a connection between ISG20 and the cellular nucleoli, possible effects of interferon stimulation or HBV infection on nucleolar components were evaluated. Nucleoli are composed of a high number of different proteins and vary in their composition, therefore we applied a panel containing five of the most prominent nucleolar proteins (Nucleolin, Nucleophosmin, Fibrillarin, NHP2-like protein 1, Nucleolar protein 56, Nucleolar protein 58). Diff. HepG2-NTCP were either treated with IFNα/IFNγ or infected with HBV. 48 hours after treatment or five days after infection RNA was isolated from the cells and gene expression was determined using qPCR.
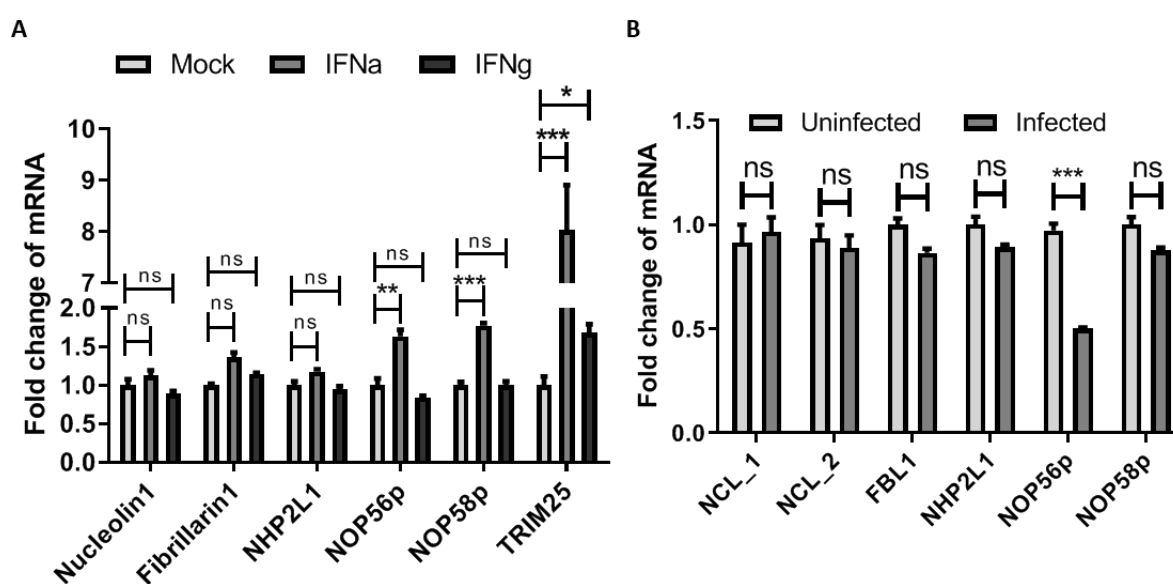
Figure 43: Gene expression of nucleolar components. Diff. HepG2 NTCP cells were either treated with **(A)** IFNα/γ (600/400 IU/ml) or **(B)** infected with HBV (MOI 100). 48 hours after treatment or five days after infection mRNA was isolated from the cells and analyzed using qPCR (n=3). All results are given as % of untreated. Statistical analysis: Students unpaired t-test with Welch's correction (ns: not significant; *p≤0.05; **p≤0.01; ***p≤0.001)

Treatment with IFNα upregulated two of the five analyzed mRNAs. NOP56p as well as NOP58p were significantly increased as well as TRIM25 which served as positive control (Figure 43A). HBV Infection on the other hand significantly decreased NOP56p mRNA levels without affecting any of the other factors (Figure 43B).

Summarily, the data indicate that interferon treatment as well as HBV infection can influence the expression levels of nucleolar proteins. IFNα treatment significantly upregulated NOP56p and NOP58p as opposed to HBV infection which led to a significant reduction of NOP56p expression.

2.3.4. The nucleoli of transgenic HepG2 H1.3 cells contain HBV DNA

Connections between the nucleolus and several viruses such as HIV, HCV and HSV-1 are well known, however there is no currently known link to HBV [208-211]. Due to the nucleolar localization of ISG20 the possible presence of HBV components inside of this compartment was analyzed. To this end a protocol for the isolation of nucleoli from transgenic HepG2 H1.3 cells, a cell line which has stably integrated the HBV genome, was established and the resulting cellular fractions were analyzed. Diff. HepG2-H1.3 were either treated with IFNα (600/IU/ml) or IFNγ (400IU/ml) for 48 hours, after treatment the nucleoli were isolated.
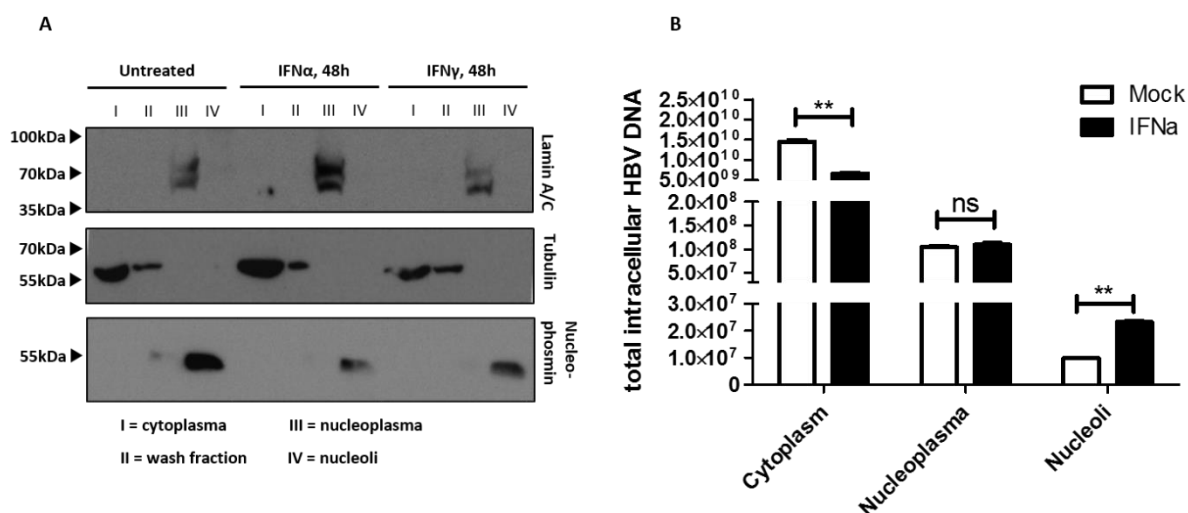
Figure 44. Distribution of viral DNA in different cellular fractions. (A) Diff. HepG2 H1.3 cells were treated for 48 hours with IFNα (600IU/ml) or IFNγ (400IU/ml) and separated into fractions using sucrose density gradient centrifugation. Each separation resulted in a total of four fractions per sample (cytoplasm (I), wash fraction (II), nucleoplasm (III) and nucleoli (IV)). Purity of these fraction was tested using Western blot for the detection of proteins specific to cytoplasm (tubulin), nucleoplasm (lamin A/C) or nucleolus (nucleophosmin). **(B)** Diff. HepG2 H1.3 cells were treated for 48 hours with IFNα (600IU/ml) and separated into fractions. Amounts of total viral DNA in each fraction was determined using qPCR (n=3). Statistical analysis: Students unpaired t-test with Welch's correction (ns: not significant; *p≤0.05; **p≤0.01; ***p≤0.001)

The established protocols allowed for purification of the different fractions with very little cross-contamination (Figure 44A). The isolated nucleolar fraction from untreated cells contained high amounts of viral DNA. Treatment with IFNα significantly decreased the amounts of viral DNA in the cytoplasm and at the same time significantly increasing the amounts in the nucleolar fraction (Figure 44B).

In summary, viral DNA was detected inside of the nucleolus of HBV transgenic cells. Treatment with IFNα decreased the detected amounts in the cytoplasm but increased them in the nucleoli.

3. Discussion

Therapeutic vaccination is a promising approach for the treatment of chronic viral infections, however previous attempts at targeting chronic hepatitis B were unsuccessful [172]. The first part of this thesis was focused on the development of a novel therapeutic vaccine vector suitable for clinical trials. The second part took a closer look at the mechanisms behind interferon-mediated, non-cytotoxic loss of cccDNA, which can be induced by vaccine-activated T cells.

3.1. Vector development for therapeutic vaccination against chronic hepatitis B

Clearance of chronic HBV infection is linked to the emergence of a rigorous, HBV specific T-cell response [160, 212]. This thesis demonstrates the design, development and characterization of an MVA based therapeutic vaccine vector, termed MVA HBVac, intended for use in a phase I clinical trial. The vector is shown to be stable and pure, attributes necessary for later GMP production. *In vitro* use of the vector results in the expression and correct folding of all desired proteins. Immunogenicity of the vector is proven using naïve C57BL/6 mice as well as the AAV-HBV mouse model. *In vivo* application of MVA HBVac induces persistent, HBV-specific antibodies along with strong and long-lasting T-cell responses. In the AAV-HBV model, MVA HBVac causes a transient ALT increase as well as HBeAg and HBsAg seroconversion, indicating a functional cure.

3.1.1. Modified vaccinia Ankara as a vaccine vector

The design of the HBVac insert as well as the choice of using MVA as vaccine vector were made with efficiency and clinical safety in mind. MVA itself offers an excellent safety record and was used as a smallpox vaccine in immunosuppressed populations without severe side effects [213]. This safety aspect is especially relevant since HIV/HBV co-infection is a frequent occurrence and these patients often suffer from defective immune responses [214]. When used as a vaccine vector, MVA shows efficient induction of TH_1/TH_2 balanced immune responses as well as induction of humoral immunity [162, 215]. Further enhancement of vector immunogenicity is possible and several deletions and mutations which arose by chance during its creation process can be reconstituted to provoke even stronger immune responses [216]. One major disadvantage of using an MVA vector can be found in pre-existing immunity, which occurs in persons who had previously received the smallpox vaccine, negatively affecting vaccine efficacy [217]. Fortunately, smallpox has been eradicated as of 1980 and the number of vaccinated individuals is steadily declining.

Creation of MVA HBVac via homologous recombination, as used during this project, results in a vector suitable for further development and production under GMP conditions, however it is technically challenging and very time and labor intensive [193, 218]. Alternative creation methods using bacterial artificial chromosomes (BACs) offer a higher throughput compared to the classical recombination approach, but are unfortunately limited by deletion site usage as well as regulatory restrictions [219, 220].

The intracellular tropism of MVA is fairly similar to other poxviruses, however the receptor responsible for viral uptake is still unknown. The viruses ability to infect a broad spectrum of cell types *in vitro* argues for the use of one or several ubiquitous cellular proteins [221]. *In vivo* MVA predominantly infects professional antigen presenting cells such as macrophages or dendritic cells, which might be one of the reasons for the high immunogenicity of the vector [222]. In our data, the CD150 (SLAM) receptor, which is normally expressed on a variety of immune cells including NK cells and DCs, enhances infection of Vero cells by MVA, indicating a hitherto unknown role of this receptor in the MVA infectious cycle [223]. Measles virus uses SLAM as one of the viral uptake receptors and a similar effect is possible in the case of MVA [224]. The use of SLAM as an uptake receptor or enhancer could explain the MVAs propensity to preferentially infect antigen presenting cells.

A broad array of viruses can be used as vectors, however direct comparison of these is difficult since their efficacies vary depending on the encoded antigen, the model used for testing and the target. In the case of HIV for example, MVA elicits polyfunctional $CD4^+$ and $CD8^+$ T-cell responses, however the strength of the immune response is slightly weaker than a comparable human adenovirus C serotype 5 (HAdV-5) based vector [225]. On the other hand, adenovirus based vaccines induce a more TH_1 based immune response when compared to MVA which induces a more balanced TH_1/TH_2 response [226]. In the case of chronic hepatitis B, HBV transgenic cytomegalovirus (CMV) vectors are being tested as potential candidates for development of a therapeutic vaccine. Initial results look promising, however the highly artificial nature of the used *in viv*o model makes the eventual efficiency in humans difficult to gauge [227].

In summary, MVA is a suitable vector for the development of a therapeutic vaccine due to its ability to induce strong, TH1/TH2 balanced immune responses while maintaining an excellent safety profile.

3.1.2. HBVac insert design and possible improvements

The HBVac insert was composed using consensus sequences covering the five major HBV genotypes to facilitate clinical application on a global scale [15]. Most patients suffering from acute hepatitis B mount strong and multispecific T-cell responses against the viral surface and core proteins as well as

the viral polymerase, therefore all of these proteins were included into the HBVac construct [228, 229]. All used HBV sequences are identical to naturally occurring HBV strains to ensure correct protein folding, which is necessary for efficient processing and presentation of the antigens [230]. Expression of the encoded, structural HBV proteins should lead to formation and secretion of capsids as well as subviral particles from infected cells, causing induction of humoral and cellular immunity [231]. The reverse transcriptase domain of the viral polymerase is the only non-structural protein that was included into the construct. The five proteins contained in the HBVac construct were linked by T2A and P2A sites. These were chosen since they offer the highest cleavage efficiency of all tested 2A peptides [189, 232]. This approach is superior to alternatives such as the use of internal ribosome entry sites (IRES) and should lead to equimolar expression of all proteins, it can however result in the creation of fusion proteins. The effects of these potential, unintended fusion proteins are difficult to gauge, although their number is expected to be very low [233]. Expression and assembly of fusion proteins into VLPs would lead to the creation of VLPs carrying additional HBV epitopes on their surface, an approach that was already shown to be safe and effective in inducing immune responses against difficult targets [234]. Potential detrimental effects on vaccine safety and efficacy therefore seem unlikely. New data from therapeutic HBV vaccines using AAVs expressing the viral X protein have been shown to induce strong CD4$^+$ and CD8$^+$ T cell responses and, in case of further vector development, inclusion of parts of this protein into the HBVac expression cassette might be considered [235]. Use of the full-length HBx is counter-indicated by its anti-apoptotic and potentially oncogenic properties [236, 237].

In conclusion, the HBVac insert encodes five different viral proteins and is designed to cover the epitopes of the majority of HBV genotypes. If necessary, the broadness of the induced T-cell response could be enhanced by including parts of HBx into the HBVac construct.

3.1.3. MVA HBVac *in vitro* characterization

The HBV surface and core proteins expressed in MVA HBVac infected cells show a behavior similar to proteins expressed from HBV. Dimerization of core proteins via disulfide bonds was observed, indicating correct folding of the proteins as well as formation of capsids [20]. This is especially important since *in vivo* models show that formation of capsids is needed to induce an effective immune response and viral clearance [238, 239]. Furthermore, HBV capsids are extremely efficient inducers of T-cell immunity and T cells primed by capsids enhance the development of antibodies directed against HBV surface proteins [240-242]. HBV Core protein also induces a strong B-cell response independent of T-cell help, an effect that only occurs if the core protein is present in its particulate form [20, 243].

The detected viral surface proteins show the expected glycosylation patterns. The viral S protein carries an N-linked glycosylation site at position 146 which in a normal *in vivo* HBV infection results in a roughly 50:50 distribution of glycosylated and non-glycosylated S protein [244]. S protein expressed in MVA HBVac infected cells shows a higher percentage of glycosylation. However, it is unclear whether this effect is due to the HBVac construct or created by the *in vitro* setting. Secretion of infectious HBV particles requires correct glycosylation, VLPs from S expressing cells however are not reliant on this mechanism [245]. Therefore, inhibition of VLP secretion by the observed changes in the glycosylated/non-glycosylated S protein ratio is unlikely. Similar to the S protein, the viral L protein carries one glycosylation site. The observed triple band most likely occurs due to the detection of remaining S protein dimers [246]. Formation and secretion of VLPs carrying S and L proteins from MVA HBVac infected cells is desired since these particles are highly immunogenic and can induce CD8 T cells via cross-presentation [247, 248].

Secretion levels of HBV core protein are significantly higher in HBVac infected cells when compared to its precursor MVA-C, on the other hand HBsAg secretion is significantly lower when compared to MVA-S. HBV capsids are not usually secreted from infected cells, however in the presence of S protein formation of empty virions is possible. This process is enhanced by the presence of L protein offering a potential explanation for the significantly elevated core protein levels in the supernatant when comparing MVA HBVac and MVA-C infected cells [25, 249]. Co-expression of core and S/L proteins might also reduce formation and secretion of HBsAg spheres or filaments when compared to purely S expressing cells.

Growth kinetics of MVA HBVac and MVA F6 in DF-1 and HeLa cells were similar, demonstrating one of the major safety features of MVA: replication deficiency in cell lines of human origin [246, 250]. Growth rate of MVA in susceptible DF-1 cells was not affected by insertion of the HBVac insert, indicating the suitability of the selected viral clone for large scale production of MVA HBVac.

In summary, MVA HBVac infected cells efficiently express all desired proteins and show secretion of VLPs as well as capsids. Despite its size, the HBVac insert does not influence virus growth in infected DF-1 cells and MVA HBVac is suitable for large scale production under GMP conditions.

3.1.4. Induction of humoral adaptive immunity in naïve or AAV-HBV infected C57/BL6 mice

Vaccination of naïve C57/BL6 mice using a single protein prime followed by an MVA boost induces strong antibody responses against HBsAg as well as HBcAg. Similar results are observed in the AAV-HBV mouse model, however these animals received two protein primes instead of one. This strong induction of humoral immunity is similar to the situation observed in patients suffering from acute

hepatitis B. They often show a strong increase in B-cell activity in the immune active (IA) phase of the infection which is crucial for viral suppression [251]. Conversely, depletion of B cells using rituximab can cause reactivation of HBV in previously cured patients [252, 253].

In AAV-HBV C57/BL6 mice, HBsAg levels drop after the animals receive their first protein prime indicating activation of B and possibly T_H cells as well as induction of anti-HBs antibodies [254, 255]. This effect is essential for vaccine efficacy, since circulating HBsAg has been implicated in the suppression of the hosts T-cell response and removal via neutralizing antibody was shown to restore cellular immunity in a transgenic mouse model [256]. Similarly, in HBV transgenic mice induction of efficient, HBV-specific CD8$^+$ T-cell responses by vaccination was only possible after knockdown of HBsAg expression via siRNA [257]. These results indicate a crucial role for HBsAg in the maintenance of virus induced immune tolerance. Removal of these viral proteins from the serum by vaccine induced antibodies should improve the induction of an HBV-specific T-cell response later on [162]. Consequently, any therapeutic approach based on HBV specific T-cell activation *in vivo* should aim to induce antibodies directed against the soluble viral proteins as observed in the data obtained from the AAV-HBV model. Alternatively, reduction of HBsAg titers is also possible by blocking viral transcription using siRNAs or small molecules. This approach does not only reduce serum HBsAg but also reduces the amount of HBs peptides bound to MHC I complexes. This might be advantageous since sustained, high-level antigen presentation of antigenic peptides can drive T cells towards exhaustion [258].

In addition to anti-HBs, all vaccinated animals also showed anti-HBc antibodies. In chronically infected patients detection of these antibodies is associated with increased ALT values and a favorable prognosis for therapy [259-261]. However, they also correlate with liver damage and inflammation [262]. It has been suggested that anti-HBc antibodies serve as the initial stage of the immune systems attack on the infected liver and can sometimes cause immunopathology, however this aspect is still under investigation [263]. The two protein primes used for vaccination in the AAV-HBV mice indeed induced a minor increase in ALT levels, which might indicate low levels of liver inflammation and hepatocyte death, however the changes were not significant. Furthermore, all animals showed a normalization of ALT values over the cause of the long-term experiment although anti-HBc antibody titers remained high. Data from occult hepatitis B virus infection (OBI) patients suggests a correlation between anti-HBc antibody titers and remaining cccDNA levels [264]. It is not known however, whether this correlation also exists in the AAV-HBV mouse model. Therefore, the quantities of remaining cccDNA in the livers of treated AAV-HBV mice should be analyzed when possible.

A non-particulate form of HBcAg, HBeAg has been described as an immunomodulatory protein inducing T-cell tolerance against HBcAg. Therefore elimination of this protein from the blood via antibodies might support reconstitution of the hosts anti-HBV immune response [265]. Further

reduction of HBeAg levels prior to therapeutic vaccination might improve its efficacy, however currently available treatment strategies are unfortunately unable to specifically target viral protein expression [188]. Since HBeAg and HBcAg share significant amino acid identity, cross-reactivity between antibodies directed against either of these antigens cannot be ruled out. However, HBeAg serum levels only started to decline after the animals received the MVA HBvac. This indicates that, at least in the AAV-HBV C57/BL6 model, loss of HBeAg is a result of T-cell activation and not mediated by antibodies.

In summary the MVA HBVac based therapeutic vaccine induces strong antibody responses against HBsAg as well as HBcAg. These antibodies should not only support the induction of CD8$^+$ T cells by clearing viral antigens from the serum but also are important for suppression of viral replication as well as a step in the direction of HBsAg seroconversion and a functional cure.

3.1.5. Induction of HBV specific T cell in naïve or AAV-HBV infected C57/BL6 mice

Integration of the newly developed MVA HBVac into an established heterologous protein prime/MVA boost vaccination leads to the induction of functional CD4$^+$ and CD8$^+$ T cells in HBV naïve as well as AAV-HBV infected C57/BL6 mice, indicating vaccine functionality. IFNγ expression is used as a marker for T-cell activity since increased frequencies of IFNγ producing CD4$^+$ and CD8$^+$ T cells are associated with liver damage and viral clearance [121, 266]. In the case of naïve mice, vaccination with MVA HBVac also leads to induction of HBs and HBc as well as HBV polymerase specific CD8$^+$ T cells [267]. However, the number of detected RT(Pol) specific T-cell is significantly lower than the ones directed against HBsAg or HBcAg. A possible explanation is the omission of RT(Pol) from the protein priming step. Without protein priming, RT(Pol) specific CD8$^+$ T-cells lack the support of the corresponding CD4$^+$ cells, which results in lower T cell activation and proliferation. In chronically infected patients presence of RT(Pol) specific CD8$^+$ T cells correlates with viral suppression after discontinuation of NUC treatment indicating their antiviral potential [268].

Similar to the effects in naïve mice, *in vivo* data from the AAV-HBV model indicate HBVac induced activation of HBV specific T-cell CD4$^+$ as well as CD8 T$^+$ cells. Unlike the data from the naïve mice however, CD4$^+$ levels were only marginally increased and not significant when compared to unvaccinated animals. It is possible that the CD4$^+$ T cell response was missed in the AAV-HBV animals since their T-cells were analyzed at a later time point post MVA boost, although this seems unlikely considering that the CD4$^+$ T cell response is usually known to persist until the infection is resolved [269]. It is also possible that this observation is an effect created by the AAV-HBV infection, albeit no such effect is described for either HBV or AAV infection. Significantly elevated levels of CD8$^+$ T cells can

be detected in both spleen and liver of vaccinated AAV-HBV mice, with the majority if cells residing in the latter. This migration of activated T cells from the lymph nodes toward their target site is mediated by inflammatory chemokines as well as changes in the expression of adhesion molecules on the lymphocytes surface and indicates successful T-cell priming and proliferation [270]. Levels of IFNγ$^+$ CD8$^+$ T cells remain elevated up to 14 weeks after the MVA boost indicating a sustained antiviral response. This maintenance of activity is especially important considering that both, the HBV infection as well as the tolerogenic liver environment, can shift active T cells towards exhaustion over time [271, 272]. However, it is important to note that IFNγ is the last cytokine to be lost in the case of T-cell exhaustion, it is therefore possible that some of the detected, IFNγ$^+$ T cells are partially exhausted [273].

In summary, the MVA HBVac based therapeutic vaccination induced a strong and long-lasting T-cell response in both, naïve as well as AAV-HBV infected mice. Improvements to the protein priming steps should be considered to enhance the T-cell response against RT(Pol).

3.1.6. Efficacy and safety of MVA HBVac in the C57/BL6 AAV-HBV mouse model

All vaccinated animals show a sustained loss of viral HBsAg and HBeAg in their sera, accompanied by a transient ALT increase.

Loss of HBsAg is detectable as early as two weeks after the first vaccination step and can be attributed to antibodies induced by the heterologous protein prime. Loss of HBeAg on the other hand only starts after the animals received the MVA boost, while ALT levels show a converse behavior and start to increase two weeks after MVA administration. Both effects are most likely caused by T-cell activation and killing of infected hepatocytes [121]. Towards the end of the experiment all treated animals show HBsAg and HBeAg levels converging towards their respective detection limits while ALT values normalized. It is important to note that normalization of ALT does not necessarily point towards loss of T-cell activity. Activated T cells can inhibit HBV replication and reduce of cccDNA levels without killing hepatocytes and these effects play a major role in clearing the virus during acute hepatitis B [274].

While the data show excellent efficacy, several points need to be considered: First, C57/BL6 mice were infected with AAV-HBV only 4 weeks prior to the start of the therapeutic vaccination. While these animals do not mount an immune response against HBV, an effect that closely resembles chronic infection, the timeframe over which their immune system is exposed to high loads of HBV proteins is rather low compared to the human setting. Therefore, the immunomodulatory effects which can be exerted by HBV proteins might not be as strong as in a chronically infected patient [275]. Second, many

cases of chronic hepatitis B are acquired during birth via mother to child transmission. It is known that the immune systems of neonates differ profoundly from adult humans and potential effects of extremely early HBV infection on immune system maturation cannot be emulated using the AAV-HBV model. Lastly, although infection of mouse hepatocytes with AAV-HBV leads to cccDNA formation via recombination of the AAV episome, this model is unable to mimic recycling of viral capsids and viral spreading. It is therefore possible, that the conformation as well as the number of cccDNA molecules per cell differ significantly when comparing the model to natural HBV infection and this could potentially influence vaccine efficacy.

Alternative approaches to the heterologous protein prime/MVA boost vaccination are also being evaluated and similar results can be obtained using a mixture of IFNα, granulocyte-macrophage colony-stimulating factor (GM-CSF) and a recombinant HBV vaccine [276]. However, IFNα as well as GM-CSF are known to induce medium to severe side effects in the patient and the combination might be difficult to use in a human setting [276, 277].

There were no observable adverse events in any of the animals receiving the MVA vector, which nicely fits to the MVAs well documented tolerability [278, 279]. The observed ALT increase hints towards hepatotoxicity, however it was only moderate and transient. Induction of a strong and potentially lethal hepatitis or cytokine release syndrome (CRS), as seen in CAR T-cell therapy, was not observed [280].

Summarily, the results obtained from testing the MVA HBVac in the AAV-HBV *in vivo* model demonstrate the excellent safety of this novel vector as well as its efficacy. Progression of the project into a phase I clinical study therefore was deemed reasonable and the proposal was submitted to and accepted by the regulatory authorities. The beginning of the phase I trial is set for the fourth quarter of the year 2021.

3.1.7. Possibilities to improve vaccine efficacy

As stated previously, overcoming the HBV induced immune tolerance is extremely challenging but crucial to developing an efficient therapeutic vaccine. It might therefore be necessary to further enhance the immunogenicity of HBVac. Since high HBsAg serum levels are linked to T-cell suppression, treatment of patients with anti-HBsAg antibodies prior to vaccination might increase vaccine efficacy [281]. Similarly, reduction of viral trasncription using siRNAs might be advantageous, especially in patients with high antigen loads, however this approach has only recently entered into clinical trials and additional research is required [282]. Alternatively, use of small molecules might also be possible. The substance MLN4924 which was used in this work and shown to effectively suppress HBV

transcription is well tolerated by humans and could lead to a reduction of viral antigen expression [283]. Lastly, pegIFNα therapy to reduce the antigen load followed by therapeutic vaccination might be interesting too, however not all patients respond well to interferon and the treatment can cause severe side effects [284].

Further optimization of the priming step by exchanging the protein prime for either RNA or DNA would allow for efficient priming against all targets contained in the HBVac insert and might further enhance vaccine efficacy [285]. Alternatively, one could also consider priming using adenovirus based viral vectors, an approach that has been demonstrated for hepatitis C virus [286]. Testing of different adjuvants for the protein prime might offer another possibility for further improvement, especially since these substances show major differences in their induction of TH1 and TH2 based immune responses [287].

Changing either the HBVac insert or the used viral vector could also be beneficial. For example, inclusion of sequences from the HBx protein, which are known to be immunogenic, into the HBVac construct might broaden the immune response [288]. It is also possible to improve the immunogenicity of the encoded HBV proteins by adding small modification sites. Myristylation of MVA expressed transgenes has been shown to change the intracellular distribution of these proteins and results in increased CD8$^+$ T–cell induction [289]. The use of alternative vectors such as adenovirus (AV), AAV, Sendai virus (SeV), cytomegalovirus (CMV) or even combinations offers further potential for improvement. However each of these vectors comes with certain pros and cons and additional research is required to better understand which vector is suited for which application [290].

In summary, further optimization of the MVA HBVac as well as the vaccination protocol by exchanging the priming components or the viral vector might be necessary. However, vaccine development is always an incremental process and waiting for the results from the phase I human study before implementing any changes would be advantageous.

3.2 Influence of cccDNA regulation on interferon mediated cccDNA loss

Due to its role as the viral persistence form, cccDNA is an appealing but challenging target for the development of therapeutics against chronic hepatitis B. This study demonstrates that non-cytolytic loss of cccDNA is dependent on the presence of active HBx protein. Inhibition of HBx mediated SMC5/6 degradation by mutation or the small molecule MLN4924 blocked IFNα mediated cccDNA degradation. Epigenetic modification of cccDNA leads to significant changes in its transcriptional activity, however, unlike the inhibition of HBx activity, these do not result in any significant impact on cccDNA loss.

Possible explanations for these observations as well as their potential for medical use are discussed in the following chapters.

3.2.1. Non-cytolytic reduction of cccDNA *in vitro*

Treatment of HBV infected HepaRGs using IFNα or the LTβR agonist BS1 results in a strong decrease of detectable cccDNA [86]. However, a certain number of cccDNA molecules seem to be resistant against non-cytolytic degradation and complete loss of cccDNA is not observed. This can be explained by the APOBECs preference for targeting single stranded over double stranded DNA, meaning that transcriptionally inactive cccDNA, which forms double stranded episomes, might be resistant against deamination and subsequent degradation [291, 292]. It is conceivable that hepatitis B virus has developed mechanisms to shift the chromatin conformation of a small part of its cccDNA pool from active to inactive in an attempt to outlast immune activation and restart viral replication at a later time point. Indeed, *in vivo* data from patients shows the existence of inactive cccDNA molecules which can be reactivated under certain circumstances such as immune suppression [291, 293, 294]. This is especially relevant since the antiviral properties of IFNα are partially based on its ability to modify the cccDNAs epigenetic state, driving it towards a closed conformation efficiently suppressing viral transcription. Meaning that IFNα, while necessary to induce the cccDNA degrading enzyme cascade, might simultaneously push cccDNA molecules towards APOBEC resistance by changing their chromatin conformation [53, 295].

3.2.2. APOBEC mediated cccDNA degradation requires HBx activity

Infection with HBV X- results in similar levels of cccDNA establishment as infections with WT HBV, however the amount of total intracellular HBV DNA is lower by around 95%. This demonstrates the dependency of viral transcription on the presence of HBx [60]. Interestingly, cccDNA establishment does not seem to be affected by the absence of HBx, probably because the process relies on cellular instead of viral proteins [296].

Treatment of cells infected with either HBV WT or the X- variant significantly reduces HBeAg in the supernatant as well as the amounts of total intracellular DNA. The reduced efficacy observed for treatment of HBV X- can be explained by the fact that the antiviral effect of IFNα at least partially relies on inhibition of viral transcription. In the case of HBV X- this transcriptional activity is already extremely low [60] and further reduction beyond a certain level does not seem to be possible. In addition to viral transcription, lack of HBx also blocks the IFNα mediated noncytolytic loss of cccDNA. The observed resistance of the HBV X- cccDNA argues for a transcriptional dependency of this mechanism. This is in

line with the observation that APOBEC3A preferentially targets single stranded DNA[292]. It is also possible that additional, yet unknown effects of HBx enhance the susceptibility of cccDNA towards A3A, however nothing has been described so far. Lymphotoxin beta receptor mediated cccDNA degradation seems to be less susceptible to the lack of transcriptional activity, possibly because it is based on APOBEC3B instead of APOBEC3A [86]. A3B has been shown to target DNA more efficiently than A3A, is distributed throughout the nucleus and is associated with the HBV antiviral response as well as cancer [297-300]. Furthermore, A3As binding to ssDNA is partially reliant on the structure of the DNA fragment and prefers binding to hairpin loops, a feature that has not been described for A3B so far [301].

In conclusion, IFNα mediated loss of cccDNA requires the presence of the viral HBx, possibly due to the A3As preference for single stranded DNA. No similar effect was observed if loss of cccDNA was mediated vie LTβR activation.

3.2.3. Effects of NEDD8-activating enzyme inhibition on viral transcription and cccDNA loss

MLN4924 is a potent inhibitor of the human NEDD8-activating enzyme. Inhibition of NAE activity prevents activation of the CUL4 complex and thereby blocks HBx mediated Smc5/6 degradation in HBV infected cells [201, 302]. The results indicate that treatment with MLN4924 efficiently suppresses viral transcription *in vitro*, without affecting cccDNA levels. In addition to its inhibitive effect on HBx-mediated Smc5/6 degradation, MLN4924 was also shown to reduce viral transcription by reducing the levels of several transcription factors required for efficient HBV replication [303].

If MLN4924 is administered simultaneously with IFNα, no or only limited loss of cccDNA is observed. Therefore, it seems that the presence of SMC5/6 inhibits non-cytolytic cccDNA degradation. A possible explanation could be that the restored SMC5/6 proteins strongly bind to cccDNA and represses its transcriptional activity, thereby creating a steric hindrance for the binding of APOBEC proteins. Alternative functions of the X protein such as recruitment of transcription factors are not affected by its ability to induce protein degradation via the Cul4-Ring complex and are therefore unlikely to play a role in this process [304, 305]. Furthermore, a direct interaction between HBx and NEDD8 has been shown, causing NEDDylation of HBx which increases its stability [306]. Targeting NAE might therefore cause two additive effects, simultaneously decreasing HBx mediated Smc5/6 degradation as well as the stability and the amount of available HBx itself.

In spite of promising *in vivo* data from an HBV mouse model [303], application of MLN4924 in the context of chronic hepatitis B needs to be considered carefully due to the hepatotoxicity observed in some of the human phase I trials [307]. Nevertheless, targeting the transcriptional activity of cccDNA

is an interesting approach which offers benefits over treatment with NAs [308, 309]. Efficient reduction of viral transcription by small molecules would decrease viral protein titers in the blood of infected patients, which current therapies fail to achieve. This is especially interesting since high antigen titers in blood of infected patients are linked to T-cell dysfunction and the development of chronic infection [310]. On the other hand, shifting cccDNA molecules towards an inactive state could negatively impact the antiviral effects mediated by cytokines and T cells and increase the risk to develop persistent latent or occult infections which could reactivate later on [293].

In summary, treatment of HBV infected cells using the NAE inhibitor MLN4924 efficiently reduces viral transcription and offers a novel treatment approach. However, in human application it needs to be carefully evaluated since the drug targets a cellular enzyme, causing potential side effects such as the observed hepatotoxicity.

3.2.4. Targeting the epigenetic state of cccDNA using small molecules

Transcriptional activity of cccDNA is regulated by the modification of its associated histones. However, in contrast to the human chromosomes, active PTMs are one of the main regulators of transcription from viral cccDNA while suppressive PTMs are usually barely detectable [50, 74]. Results showed that the small molecule C646, a specific inhibitor of the HAT p300/CBP, efficiently reduces transcription from viral DNA [74, 311-313]. This effect is mediated by changing the cccDNAs episomal structure, thereby reducing accessibility, similar to the effects observed when using MLN4924. In contrast to MLN4924 however, C646 treatment does not show any impact on interferon-mediated cccDNA degradation. An explanation would be that interferons themselves are potent inducers of epigenetic changes in the context of viral infections, causing interactions with HAT inhibitors which are difficult to evaluate [314, 315]. Furthermore, enzymes necessary for adding active or suppressive PTMs to cccDNA bound histones are recruited or respectively counteracted directly by HBx protein, meaning that while C646 would block acetylation of histones, HBx could still prevent development of suppressive PTMs [51].

Enhancement of non-cytolytic loss of cccDNA by drug substances would greatly benefit the development of novel, immune-based therapies [119, 120, 315]. The small molecule Trichostatin A (TSA) is a known HDAC inhibitor and treatment of HBV transfected HepG2.2.15 cells results in decreased HDAC activity and increased viral transcription [316]. Treatment with TSA is shown to induce hyperacetylation of cccDNA bound histones and results in increased transcription, however there is no detectable effect on interferon mediated cccDNA degradation [49, 315]. It is possible that the TSA mediated, epigenetic changes are overruled by the ones caused by IFNα treatment which would nullify

the effect of TSA on the cccDNA chromatin structure [53, 317]. Furthermore, since cccDNA associated histones are already heavily acetylated under normal conditions [49], it is conceivable that further acetylation does not significantly impact the minichromosomal structure.

Altogether it seems that, while non-cytolytic cccDNA degradation is linked to the chromatin structure of the cccDNA, targeted manipulation of this structure by inducing changes in its histone code is challenging due to its complicated regulation. Therapies based on epigenetic modifications represent a promising approach, especially in the field of chronic viral infections, however further knowledge about the mechanisms responsible for the epigenetic regulation of cccDNA are necessary to allow for a more targeted approach [318].

3.3. Viral infections and the nucleolus

Nucleoli are non-enveloped organelles that form around the chromosomal regions encoding for the ribosomal 18s, 28s and 5,8s rRNAs [319, 320]. While the composition of nucleoli can vary, a high percentage of the contained proteins are not associated with ribosomal biogenesis suggesting a far more multifunctional role than previously assumed [321, 322]. Originally described as the sites of ribosome biogenesis, recent results show the crucial role of nucleoli in the modification of different RNAs as well as a key player in DNA damage repair [323, 324]. A wide range of viruses, including human immunodeficiency virus (HIV), hepatitis C virus (HCV), dengue virus (DENV), Japanese encephalitis virus (JEV) as well as severe acute respiratory Syndrome coronavirus (SARS-CoV), are known to interact with nucleolar components [325]. The functions of these interactions vary between viruses and so far, effects on viral replication, cell cycle arrest, release of viral particles as well as RNA processing have been demonstrated.

3.3.1. Intracellular localization of ISG20

The results show that the majority of intracellular ISG20 resides in the cytoplasm, with only a minor fraction being localized to the nucleus. This distribution seems reasonable considering that, under physiological conditions, ISG20 acts as an antiviral protein targeting a broad spectrum of RNA viruses such as yellow fever virus (YFV) or vesicular stomatitis virus (VSV) that replicate in the cellular cytoplasm [326-328]. ISG20 usually functions by targeting viral RNAs or cellular factors required for efficient viral replication and, in the case of HBV, ISG20 has been shown to selectively target viral RNAs recognized by their N6-methyladenosin modification [329-331].

Induction of ISG20 upon interferon treatment as well as a clear co-localization of ISG20 with nucleolar protein is shown. Co-localization with proteins characteristic for PML bodies is not observed in any of the tested cell lines. In contrast to the data presented in this thesis, ISG20 was also shown to localize in either cajal bodies, PML nuclear bodies, cytoplasmic processing bodies or the general nucleoplasm, depending on interferon stimulation, cell cycle stage, model and the chosen method of detection [332-334]. A possible explanation for these discrepancies could be that most of the data was created using overexpression systems or ISG20 carrying a human influenza hemagglutinin (HA) tag. Both approaches can change the intracellular localization of the protein of interest [334-336]. Of course, it is also possible that the intracellular distribution of ISG20 varies depending on the cell line in question. To avoid such artefacts, primary cells should be used for localization studies where possible. Due to its function as a known RNase [337], the localization of ISG20 at one of the major RNA processing spots seems reasonable. Furthermore, some of the viruses known to be targeted by ISG20 were described to either directly interact with nucleoli or to require nucleolar factors for efficient RNA processing and replication [325, 338]. It has also been suggested that ISG20 may directly interact with ribosomal RNAs to modify transcription, however there has been no conclusive evidence so far [339].

There is no detectable influence of HBV infection on ISG20 induction or localization, although HBV interference with the interferon signaling pathways upstream of ISG20 induction has been demonstrated [148, 340]. There was also no discernible direct interaction between the viral core protein and ISG20. However, ISG20 detection by Western blot is challenging due to the relatively low abundance of the protein and the low sensitivity of the commercially available antibodies and more sensitive methods such as Co-IP followed by a mass spectrometry approach might be necessary [341].

In summary, ISG20 can efficiently be induced by interferon treatment and localizes to the nucleoli under all tested conditions. HBV infection does not seem to influence ISG20 induction or localization and a direct interaction between the viral capsid protein and ISG20 was not detectable.

3.3.2. Possible connections between hepatitis B virus and the nucleolus

Data shows significant upregulating in the expression of the two nucleolar components NOP56p and NOP58p upon IFNα treatment, while HBV infection significantly decreases NOP56p expression. Unfortunately, little is known about the intracellular function of these proteins in eukaryotic cells. Involvement in ribosome genesis and RNA modification has been proposed but is currently still under investigation [342]. Since only a very limited number of possible nucleolar interaction partners is analyzed, further validation must be performed, ideally using high-throughput methods like mass spectrometry or mRNA sequencing.

The data generated during this thesis also demonstrates the existence of substantial amounts of viral DNA in the nucleoli of infected cells, which fits to previous publications that show the presence of HBV capsids inside of the nucleolus [343]. It is currently unknown how the viral capsids inside of the nucleolus come into existence or if they play a significant role in the viral life cycle. Since HBV infected cells often show accumulation of core protein in the cytoplasm as well as the nucleoplasm this might lead to encapsidation of random RNA inside of the nucleolus, resulting in the accumulation of viral capsids. However, capsid assembly in infected cells is usually highly specific and requires an interaction between the capsid proteins and the ε packaging signal near the 5' end of the viral pgRNA, packaging of cellular RNA therefore seems unlikely. [344]. It is conceivable that HBV uses the cellular nucleoli as location for the encapsidation process and a similar mechanism has been demonstrated for AAV capsid assembly [345]. Considering that the capsids from both viruses are relatively similar were their size is concerned (AAV 22nm vs. HBV 36nm), the use of analogous mechanisms is a possibility. This theory is also supported by the fact that the I97D mutant of the HBc protein, which is unable to form capsids, accumulates inside of the nucleolus [346]. Alternatively to the formation of viral capsids inside of the nucleolus, mature rcDNA containing capsids could be imported into the nucleus, however the diameter of the viral capsid is too large for transport via nuclear pore complex (NPC) [347].

It is also possible, that the viral cccDNA localizes inside of the cellular nucleoli. Direct interactions between HBc and the nucleolar protein nucleophosmin have been shown and nucleophosmin has also been described as a histone chaperone, capable of transferring nucleosomes onto naked DNA causing chromatin assembly [348]. Since it is currently not known how cccDNA acquires its histones, the use of nucleophosmin is a definite possibility. Additionally, Smc5/6, a strong cccDNA binder and one of the major negative regulators of HBV transcription, has also been described to accumulate in the nucleolus under naïve conditions [349].

Succinctly, the results hint towards an undiscovered connection between HBV and the nucleolus. The observed accumulation of viral DNA together with previously published results suggests the nucleoli to be involved in HBV replication. One possibility could be the use of the nucleoli for efficient pgRNA packaging or alternatively, the presence of cccDNA inside of the nucleoli to directly profit from the highly effective mRNA production and processing capabilities.

3.4.   Conclusions

To summarize, this work demonstrates the successful development and testing of a novel vector suitable for therapeutic vaccination against chronic hepatitis B. Integration of the vector into a heterologous protein-prime/MVA-boost vaccination scheme led to induction of strong and sustained

antibody and T-cell responses in all vaccinated animals and resulted in a functional cure. The compelling safety and efficacy data generated during this work justify the progression into a phase I clinical trial. Closer investigation of the cytokine-mediated, non-cytolytic cccDNA loss revealed a strong connection between the cccDNA chromatin conformation and its susceptibility towards IFNα mediated degradation. It also demonstrated the effects of histone modification on the activity of cccDNA and established the NAE inhibitor MLN4924 as a potent inhibitor of viral transcription. Lastly, ISG20 was shown to localize to the nucleoli and the presence of significant amounts of viral DNA inside of the nucleolus was uncovered. While the exact role of these cell organelles in the viral infection cycle is still unclear, the collected data warrants further research in this direction.

4. Materials and Methods

4.1. Materials

4.1.1. Cell lines

Name	Description
BHK21	Immortalized aby hamster kidney cells, fibroblasts [350]
CEF	Primary chicken embryo fibroblasts [351]
DF-1	Immortalized chicken fibroblasts [352]
HEK293	Immortalized Human embryonic kidney cells [353]
HepG2	Human hepatoma cell line [354]
HepG2-NTCP K7	Transgenic HepG2 cells stably expressing human NTCP
HepaRG	Immortalized hepatic stem cells [355]
HepG2 H1.3	Transgenic HepG2 cells stably expressing all HBV RNAs and proteins[356]
PHH	Primary human hepatocytes

4.1.2. Antigens

Name	Supplier
HBcAg, genotype D	Dr. Dišlers, APP Latvijas Biomedicīnas, Riga, Latvia
HBsAg, genotype A	Biovac, South Africa

4.1.3. Viral vectors

Name	Supplier
AAV-HBV 1.2	Plateforme de Thérapie Génique in Nantes, France (INSERM U1089)
HBV, genotype D, serotype ayw	Institute of Virology TUM/HMGU
HBV X-, genotype D, serotype ayw	Institute of Virology TUM/HMGU
MVA-HBVac, genotype A (S), C (L and core); D (core$_{1-149}$)	Institute of Virology TUM/HMGU
MVA-WT (F6)	Prof. Sutter, LMU

4.1.4. Buffers

Name	Supplier
Lysogeny broth (LB medium, 1L)	10 g Tryptone
	5 g yeast extract
	10 g NaCl
	H_2O
Denat. SDS loading buffer	10 mL Glycerin
	12 mL 0.5 M Tris HCL pH 6.8 (NaOH)
	20 mL 10 % SDS
	0.1 g Bromophenol blue

	+ 70 µL β-Mercaptoethanol/mL
TAE-buffer (50x)	2 M Tris-HCl
	1 M Acetic acid
	50 mM EDTA
	pH 8.0, in H_2O
TBS-T (10x, 1L)	200 mM Tris base
	1.4 M NaCl
	10 mL Tween20
	pH 7.3 in H_2O
WB blocking buffer	5 % (w/v) milk powder solved in 1x TBS-T
WB running buffer (10x, 1L)	250 mM Tris base
	2 M Glycine
	1 % (w/v) SDS
	H_2O
WB transfer buffer (10x, 1L)	39.4 g Tris-HCl or 30.3 g Tris base
	144.1 g Glycine
	H_2O
Immunofluorescence blocking buffer	10% (v/v) goat serum
	0,1% Saponin
	PBS
Immunofluorescence permeabilization buffer	0,5% Saponin
	PBS

4.1.5. Cell culture media

Components	DMEM Full	DMEM Differentiation
Dulbecco's Modified Eagle's Medium	500ml	500ml
Heat-inactivated fetal calf serum (FCS)	10%	10%
Penicilin/Streptomycin	100 U/ml	100 U/ml
L-glutamine	2mM	2mM
Non-essential amino acids (NEAA)	1%	1%
Sodium pyruvate	1mM	1mM
DMSO		2.5%

Components	William's E Full	William's E Differentiation
Dulbecco's Modified Eagle's Medium	500ml	500ml
Heat-inactivated fetal calf serum (FCS)	10%	10%
Penicilin/Streptomycin	100 U/ml	100 U/ml
L-glutamine	2mM	2mM
Human insulin	0.023 U/ml	0.023 U/ml
Hydrocortisone	4.7µg/ml	4.7µg/ml
Gentamicin	80µg/ml	80µg/ml
DMSO		1.8%

Components	VP-SFM Full
VP-SFM	1000ml
Penicilin/Streptomycin	100 U/ml
L-glutamine	2mM
Non-essential amino acids (NEAA)	1%

4.1.6. Mouse strains

All *in vivo* experiments, were conducted in male wild-type C57BL/6J mice (haplotype H-2$^{b/b}$) purchased from JANVIER LABS.

4.1.7. Peptides

RT pool 1 (18mers, overlapping by 11aa)		
	1	EDWGPCAEHGEHHIRIPR
	2	EHGEHHIRIPRTPARVTG
	3	RIPRTPARVTGGVFLVDK
	4	RVTGGVFLVDKNPHNTAE
	5	LVDKNPHNTAESRLVVDF
	6	NTAESRLVVDFSQFSRGK
	7	VVDFSQFSRGKTRVSWPK
	8	SRGKTRVSWPKFAVPNLQ
	9	SWPKFAVPNLQSLTNLLS
	10	PNLQSLTNLLSSNLSWLS
	11	NLLSSNLSWLSLDVSAAF
	12	SWLSLDVSAAFYHIPLHP
	13	SAAFYHIPLHPAAMPHLL
	14	PLHPAAMPHLLVGSSGLS
	15	PHLLVGSSGLSRYVARLS
	16	SGLSRYVARLSSNSRIFN

RT pool 2 (18mers, overlapping by 11aa)		
	17	ARLSSNSRIFNHQHGNLQ
	18	RIFNHQHGNLQNLHDSCS
	19	GNLQNLHDSCSRNLYVSL
	20	DSCSRNLYVSLLLLYKTF
	21	YVSLLLLYKTFGRKLHLY
	22	YKTFGRKLHLYSHPIILG
	23	LHLYSHPIILGFRKIPMG
	24	IILGFRKIPMGVGLSPFL
	25	IPMGVGLSPFLLAQFTSA
	26	SPFLLAQFTSAICSVVRR
	27	FTSAICSVVRRAFPHCLA
	28	VVRRAFPHCLAFSYMDDV
	29	HCLAFSYMDDVVLGAKSV
	30	MDDVVLGAKSVQHLESLF

	31	AKSVQHLESLFTAVTNFL
	32	ESLFTAVTNFLLSLGIHL

RT pool 3 (18mers, overlapping by 11aa)	33	TNFLLSLGIHLNPNKTKR
	34	GIHLNPNKTKRWGYSLNF
	35	KTKRWGYSLNFMGYVIGS
	36	SLNFMGYVIGSWGTLPQE
	37	VIGSWGTLPQEHIVQKIK
	38	LPQEHIVQKIKQCFRKLP
	39	QKIKQCFRKLPVNRPIDW
	40	RKLPVNRPIDWKVCQRIV
	41	PIDWKVCQRIVGLLGFAA
	42	QRIVGLLGFAAPFTQCGY
	43	GFAAPFTQCGYPALMPLY
	44	QCGYPALMPLYACIQSKQ
	45	MPLYACIQSKQAFTFSPT
	46	QSKQAFTFSPTYKAFLCK
	47	FSPTYKAFLCKQYLNLYP
	48	FLCKQYLNLYPVARQ

S pool (15mers, overlapping by 10aa)	37	GNCTCIPIPSSWAFA
	38	CIPIPSSWAFAKYLW
	39	PSSWAFAKYLWEWAS
	40	AFAKYLWEWASARFS
	41	YLWEWASARFSWLSL
	42	WASARFSWLSLLVPF
	43	RFSWLSLLVPFVQWF
	44	LSLLVPFVQWFVGLS
	45	VPFVQWFVGLSPTVW
	46	QWFVGLSPTVWLSAI
	47	GLSPTVWLSAIWMMW
	48	TVWLSAIWMMWYWGP
	49	SAIWMMWYWGPSLYS
	50	MMWYWGPSLYSIVSP
	51	WGPSLYSIVSPFIPL
	52	LYSIVSPFIPLLPIF
	53	VSPFIPLLPIFFCLW
	54	IPLLPIFFCLWVYI

C pool (18mers, overlapping by 11aa)	188	TWVGGNLEDPISRDLVVS
	189	EDPISRDLVVSYVNTNMG
	190	LVVSYVNTNMGLKFRQLL
	191	TNMGLKFRQLLWFHISCL

	192	RQLLWFHISCLTFGRETV
	193	ISCLTFGRETVIEYLVSF
	194	RETVIEYLVSFGVWIRTP
	195	LVSFGVWIRTPPAYRPPN
	196	IRTPPAYRPPNAPILSTL
	197	RPPNAPILSTLPETTVVR
	198	LSTLPETTVVRRRGRSPR
Single Peptides		
S190adw		VWLSAIWM
S208adw		IVSPFIPL
C93		MGLKFRQL
RT333		KQYLNLYPV
RT61		FAVPNLQSL
RT85		SAAFYHIPL

4.1.8. Antibodies

Name	Specificity	Supplier
HB1 (mouse, monoclonal)	HBsAg (S, M, L)	Prof. Glebe (Gießen)
Anti-PML (mouse, monoclonal)	PML	Santa Cruz Biotechnology
Anti-ISG20 (rabbit, polyclonal)	ISG20	Abcam
Anti-ISG20 (mouse, monoclonal)	ISG20	Santa Cruz
Anti-Lamin-A/C (mouse, monoclonal)	Lamin A/C	Santa Cruz Biotechnology
Anti-Nucleophosmin (mouse, monoclonal)	Nucleophosmin Tubulin	Abcam
Anti-Vaccinia Lister strain (rabbit, monoclonal)	Vaccinia Lister strain	Acris Antibodies GmbH
AffiniPure anti-human IgG (H+L) (goat, monoclonal, HRP)	Human IgG	Jackson Immuno Research
Anti-rabbit IgG (goat, monoclonal, Alexa647)	Rabbit IgG	Thermo Fisher Scientific
Anti-mouse IgG (goat, monoclonal, Alexa647)	Mouse IgG	Thermo Fisher Scientific
Anti-rabbit IgG (goat, monoclonal, Alexa549)	Rabbit IgG	Thermo Fisher Scientific
Anti-mouse IgG (goat, monoclonal, Alexa594)	Mouse IgG	Thermo Fisher Scientific
Anti-rabbit IgG (goat, monoclonal, Alexa488)	Rabbit IgG	Thermo Fisher Scientific
Anti-mouse IgG (goat, monoclonal, Alexa488)	Mouse IgG	Thermo Fisher Scientific
Anti-rabbit IgG (goat, monoclonal, HRP)	Rabbit IgG	
Anti-mouse IgG (goat, monoclonal, HRP)	Mouse IgG	Serva Electrophoresis
BS1	Hu-LTβR	

4.1.9. Plasmids

Name	Insert	Supplier
pMX-HBV-vac	HBcAg	Invitrogen
pIII H5 Red K1L	HBsAg (S, M, L)	Prof. Sutter (Munich)

4.1.10. Primers

Name	Sequence
Del I Fw	CTTTCGCAGCATAAGTAGTATGTC
Del I Rev	CATTACCGCTTCATTCTTATATTC
Del II Fw	GGGTAAAATTGTAGCATCATATACC
Del II Rev	AAAGCTTTCTCTCTAGCAAAGATG
Del III Fw	GATGAGTGTAGATGCTGTTATTTTG
Del III Rev	GCAGCTAAAAGAATAATGGAATTG
Del IV Fw	AGATAGTGGAAGATACAACTGTTACG
Del IV Rev	TCTCTATCGGTGAGATACAAATACC
Del V Fw	CGTGTATAACATCTTTGATAGAATCAG
Del V Rev	AACATAGCGGTGTACTAATTGATTT
Del VI Fw	CGTCATCGATAACTGTAGTCTTG
Del VI Rev	TACCCTTCGAATAAATAAAGACG
63	ATAAAACGCCGCAGACACATCCA
64	GATGTGTCTGTGGCGTTTTATCA
194	CTTGCCGAGTGCAGTATGG
422	ACGTGGCCCGGCTGAGCAGC
423	AGGTCTTGTACAGCAGCAGC
425	GCTCTGTCTATTGGTGCTGG
426	TGTGGCTGAGCGGCGTGATCTGG
434	TGGGTCCAGGGTTCTCTTCC
464	CATGGAGAACATCACATCAGG
465	TCAGCACTGGTCTTTCTCTGC

Name	Sequence
cccDNA 2251	AGCTGAGGCGGTATCTA
cccDNA 98	GCCTATTGATTGGAAAGTATGT
Fibrillarin1 Fw	GCTGAGGCTGTGGAGTCAAT
Fibrillarin1 Rev	CCTGCGTAATGGAGGACACT
HBV DNA 1745	GGAGGGATACATAGAGGTTCCTTGA
HBVDNA 1844	GTTGCCCGTTTGTCCTCTAATTC
NHP2L1 Fw	GCTACTGGACCTCGTTCAGC
NHP2L1 Rev	ACTCAGAGATGCCCCTGTTG
NOP56 Fw	GTAGGCTCTGGCGGTATTCA
NOP56 Rev	AGGCTATTCTGGATGCCTCA
NOP58 Fw	CGGTTCATGGGCTTCTTTTA
NOP58 Rev	TGATGGAGGGCAAAATCAAT
Nucleolin1 Fw	GTCAGCAAGGATGGGAAAAG
Nucleolin1 Rev	TAGATCGCCCATCGATCTCT
PRNP Fw	TGCTGGGAAGTGCCATGAG
PRNP Rev	CGGTGCATGTTTTCACGATAGTA
TBP_1 Fw	TATAATCCCAAGCGGTTTGC

TBP_1Rev	CTGTTCTTCACTCTTGGCTCCT
TRIM25 Fw	AAAGCCACCAGCTCACATCCGA
TRIM25 Rev	GCGGTGTTGTAGTCCAGGATGA

4.1.11. Kits

Name	Supplier
Architect anti-HBsAg Reagent Kit	Abott Laboratories, Chicago, USA
Architect HBeAg Reagent Kit	Abott Laboratories, Chicago, USA
Architect HBsAg Reagent Kit	Abott Laboratories, Chicago, USA
CellTiter-Blue Viability assay	Promega Corporation, Madison, USA
CelLytic NucCLEAR extraction kit	Promega Corporation, Madison, USA
Cytofix/Cytoperm Kit	BD Biosciences, New Jersey, USA
CytoTox-ONE Homogeneous Membrane	Sigma Aldrich, St. Louis, USA
Integrity Assay	Promega Corporation, Madison, USA
LightCycler 480 SYBR Green I Master mix	Roche, Mannheim, German
NucleoSpin RNA isolation Kit	Macherey-Nagel, Düren, Germany
NucleoSpin Tissue Kit	Macherey-Nagel, Düren, Germany
SuperScript III First-Strand Synthesis	Invitrogen, Carlsbad, CA, USA
SuperMix for qRT-PCR	

4.1.12. Chemicals and reagents

Name	Supplier
Agar-agar	Roth, Karlsruhe, Germany
Amersham ECL Prime Western Blotting	GE Healthcare Life Sciences, Freiburg, Germany
Detection Reagent	Roth, Karlsruhe, Germany
Ampicillin	Serva Electrophoresis, Heidelberg, Germany
APS	Serva Electrophoresis, Heidelberg, Germany
Collagen R	Sigma-Aldrich, Steinheim, Germany
DMSO	Roth, Karlsruhe, Germany
Ethanol	Roth, Karlsruhe, Germany
Formaldehyde	Thermo Fisher Scientific, Scotland, UK
Geneticin (G418)	Roche, Vienna, Austria
IFN-α (interferon alpha-2a/Roferon-A)	Boehringer Ingelheim, Vienna, Austria
IFN-β (interferon gamma-1b/ Imukin)	Roth, Karlsruhe, Germany
Isopropanol	Roth, Karlsruhe, Germany
Methanol	Roth, Karlsruhe, Germany
Milk powder	Roth, Karlsruhe, Germany
NaCl	Roth, Karlsruhe, Germany
NaOH	Roth, Karlsruhe, Germany
Page Ruler Plus Prestained protein ladder	Thermo Scientific, Waltham, USA
PBS	Gibco/Invitrogen, Carlsbad, USA
Pierce RIPA buffer	Thermo Scientific, Rockford, USA
Polyacrylamide	Roth, Karlsruhe, Germany

Protease inhibitor (Complete)	Roche, Mannheim, Germany
RotiSafe	Roth, Karlsruhe, Germany
SDS	Roth, Karlsruhe, Germany
T5 exonuclease	New England Biolabs, Ipswich, USA
TEMED	Roth, Karlsruhe, Germany
Tris HCl	Roth, Karlsruhe, Germany
Trypan blue	Gibco/Invitrogen, Carlsbad, USA
Trypsin	Gibco/Invitrogen, Carlsbad, USA
Tween 20	Roth, Karlsruhe, Germany

4.1.13. Laboratory Equipment and consumables

Name	Supplier
Amersham Hybond PVDF membrane	GE Healthcare Life Sciences, Freiburg, Germany
BEP (HBeAg measurement)	Siemens Molecular Diagnostics, Marburg, Germany
Plastics (cell culture flasks, plates, e.g.)	TPP, Trasadingen, Switzerland
Cell culture incubator HERAcell 150i	Thermo Scientific, Rockford, USA
Centrifuge 5417C / 5417R	Eppendorf, Hamburg, Germany
Cryo vials	Greiner Bio One, Kremsmünster, Austria
Falcon tubes	Greiner Bio One, Kremsmünster, Austria
Fluorescence microscope CKX41	Olympus, Hamburg, Germany
Freezing container	Thermo Fisher Scientific, Waltham, USA
Fusion Fx7	Peqlab, Erlangen, Germany
Gel chambers (agarose gel electrophoresis)	Peqlab, Erlangen, Germany
Gel chambers (SDS-PAGE)	Bio-Rad, Hercules, USA
Heating block	Eppendorf, Hamburg, Germany
Light Cycler 480 II	Roche, Mannheim, Germany
Nanodrop Photometer	Implen, Munich, Germany
Pipette "Accu-jet pro"	Brand, Wertheim, Germany
Pipette filter tips	Starlab, Ahrensburg, Germany
Serum pipettes	Greiner Bio One, Kremsmünster, Austria
qPCR 96-well plates	4titude, Berlin, Germany
Reaction tubes	Eppendorf, Hamburg, Germany
Reflotron ALT stripes	Roche, Mannheim, Germany
Reflotron Reflovet Plus	Roche, Mannheim, Germany
Sterile hood	Heraeus, Hanau, Germany
Tecan plate reader Infinite F200	Tecan, Männedorf, Switzerland
Western Blotting Chamber (Wet Blot)	Bio-Rad, Hercules, USA
Whatman paper	Bio-Rad, Hercules, USA

4.1.14. Software

Name	Supplier
Graph Pad Prism 5.01	Graph Pad, La Jolla, USA
Graph Pad Prism 9	Graph Pad, La Jolla, USA
ImageJ	NIH, Bethesda, USA
LightCycler 480 Software 1.5.1.62	Roche, Mannheim, Germany
Windows10	Microsoft, Redmond, USA
MS Office	Microsoft, Redmond, USA

4.2. Methods

4.2.1. Cloning of the HBVac insert into the shuttle vector pIIIH5 Red K1L

The HBVac insert was synthesized by Invitrogen and delivered in a shuttle-plasmid termed pMX-HBV-vac. The shuttle-plasmid was digested using the Restriction enzymes BglII and AfeI for 2h at 37°C and the HBVac insert was purified using gel extraction. The target vector pIIIH5 Red K1L was digested using the enzymes BamHI and PmeI for 2h at 37°C. Fragments were loaded onto a 1% agarose gel containing Roti-Safe® stain together with a 10kb ladder and separated at 120V. DNA bands were then purified using a gel extraction kit (GeneJET Gel Extraction Kit) according to the manufacturer's instructions. HBVac insert was ligated into pIIIH5 red K1L at 22°C for 2h using a T4 ligase and a 1:3 (vector/insert) ratio. Successful integration of the insert was verified using digestion with XbaI.

4.2.2. Preparation of chicken embryo fibroblasts

CEFs were isolated from 11 day old chicken embryos. First, eggs were candled to check for viable embryos, non-fertilized eggs were discarded. Eggs were then placed under the laminar flow with the air bubble facing up and disinfected using 70% EtOH. Part of the egg shell was removed by using scissors without damaging the membrane. Finally the membrane was removed and the embryo was lifted from the eggs using forceps and transferred into a DPBS containing petri dish. Head, legs and wings of the embryo were removed using scissors and the torso was transferred into a second petri dish containing DPBS. After a second washing step in DPBS the torsos were shred using scissors until a homogenous pulp was created. This pulp was transferred into an Erlenmeyer flask and mixed with 1x trypsin (5ml of 1x trypsin per embryo). After adding a magnetic stir bar, the flasks were heated to 37°C and incubated for 20min while stirring. After incubation the mixture was poured through a gauze sieve, transferred into 50ml falcons and mixed with culture medium. The diluted cells were then centrifuged

(1500rpm, 7min). After centrifugation the supernatant was discarded and the soft pellets were reuspended in medium and seeded in T175 flasks with $3.5*10^7$ cells/flask.

4.2.3. Creation of MVA HBVac using MVA F6 WT and pIIIH5 Red K1L HBVac plasmid

CEFs were seeded into 6-well plates at roughly $1*10^6$ cells/well. At the next day, medium was replaced with 2ml of fresh medium. Six hours after medium exchange, cells were infected with MVA F6 with an MOI of 0.05. After adding the virus, cells were incubated at 37°C, 5% CO_2. During this incubation period a transfection mix containing 100µl media, 1µg of pIIIH5 Red K1l HBVac plasmid and 3µl XtremeGene was prepared. 45 minutes after the infection, the transfection mix was added slowly, drop by drop to the wells. 24 hours after transfection the plates were frozen at -40°C. The thusly obtained crude lysate contained MVA F6, MVA-HBVac as well as remaining pIIIH5 Red K1l HBVac plasmid.

4.2.4. Purification of MVA HBVac using a plaque purification approach

Purification was done according to protocols previously published in [193]. On day one, CEFs were seeded into 6 well plates, at roughly $1*10^6$ cells/well. The plates from the previous infection/transfection cycle were thawed and refrozen three times. After the third cycle the lysate was transferred into 1,5ml tubes and stored at -40°C. Two days after seeding the medium of the cells was exchanged in the morning. In the afternoon, the cell lysates of the previous infection/transfection cycle were thawed and transferred into an ultrasound bath on ice. The ultrasound treatment was repeated three times with max settings for 1 min. Between each of the ultrasound steps the tubes were vortexed vigorously. Next, dilution series were created based on the available virus suspensions. Usually dilutions with the factors 10^{-1} - 10^{-6} from each of the available samples were used. After removing the media from the CEF plates, 2ml of virus dilution per well were added. Two days after infection, fluoresced plaques were detected and marked using the microscope. Ideally the selected plaques were rather big and as far away from any non-fluorescent plaques as possible. Plaques from wells which were infected with highly diluted viral suspensions were preferred. The plaques were picked using a 20µl pipette. The pipette was set to a volume of 5µl and the tip was placed directly on the previously marked plaque. The plaque containing the recombinant MVA was then aspirated and transferred into one of the previously prepared, 500µl of media containing, Eppendorf tubes. These were stored at -40°C until further usage. This process was repeated until three consecutive rounds of purification without any detectable traces of MVA F6.

The following program was used to selectively amplify MVA F6 DNA

	T [°C]	t [sec]	Cycles
Denaturation	95	120	1
Amplification	95	30	
	55	5	30
	72	120	
Final Elongation	72	600	1
Cooling	4		1

4.2.5. Selection of a non-fluorescent MVA HBVac clone

The process was identical to the purification of MVA-HBVac from MVA F6. Only this time, non-fluorescent plaques were picked. To avoid loss of virus, roughly 10 plaques were picked per dilution series. The process of 3x freezing/thawing, dilution, infection and selection (see also 1.4) of non-fluorescent plaques was repeated until no fluorescent MVA was left in the viral suspension. During this whole process the loss of MVA F6 and the integrity of the insert were checked using separate PCRs [193]. A PCR using the primer pair DelIII Fw and DelIII Rev was used to check for MVA F6 while the primer pairs DelIII Rev + 194 and DelIII Fw + 426 were used to verify the integrity of the insert.

The following program was used for the primer pairs DelIII Rev and DelIII Fw

	T [°C]	t [sec]	Cycles
Denaturation	95	120	1
Amplification	95	30	
	55	5	30
	72	30	
Final Elongation	72	600	1
Cooling	4		1

The following program was used for the primer pairs DelIII Rev + 194 and DelIII Fw + 426

	T [°C]	t [sec]	Cycles
Denaturation	95	120	1
Amplification	95	30	
	60	30	30
	72	120	
Final Elongation	72	600	1
Cooling	4		1

4.2.6. MVA amplification and production

After obtaining the recombinant non-fluorescent virus, MVA HBVac was amplified. This was achieved by gradually increasing the amount of cells used for infection. First the viral suspension was used to infect CEF containing 6-well plates. After nearly all cells showed a cytopathic effect, the virus was harvested as before (3x freezing/thawing). This process was repeated until the amount of viral particles obtained was high enough to completely infect a 6-Well plate well within 2 days. This suspension was then used to infect a T25 flask. Here the same steps as in the 6-well plate setting were repeated. After obtaining a solution capable of completely infecting a T25 within 2 days, the next step was infection of a T75 and finally a T175. The viral solution obtained from one T175 could now be used to produce a first crude virus stock by infecting several T175 flasks. The final viral titers which could be obtained by this method differed greatly depending on the insert and varied between $1*10^6$ and $1*10^9$ PFU/ml.

4.2.7. Quantification of MVA viral titers

The virus stock of interest was thawed, sonicated and a tenfold dilution series in medium was prepared (Dilution steps: 10^{-1}: 30µl stock+ 270µl medium; 10^{-2}: 100µl 10^{-1} + 900µl medium; Dilution 10^{-3} to 10^{-9}: 500µl + 4.5ml medium). Dilutions 10^{-4} to 10^{-9} were then used to infect confluent CEFs in a 6-well format using 1ml of diluted virus/well, for each dilution step two wells were infected. After incubation at 37°C, 5% CO_2 for two hours, infection medium was removed and the cells were washed once using PBS. After washing 2ml of medium was added and the cells were incubated at 37°C, 5% CO_2 for two days. Cells were then fixed by replacing the medium with a 1:1 mixture of ice-cold (-20°C) acetone: methanol for 5min at RT. The fixative was then removed and the plates were dried before adding 2ml of blocking solution (PBS + 3%FCS). Plates were blocked either for 1h at room temperature or at 4°C overnight. For staining, primary antibody (rabbit anti-VACV) was diluted 1:2000 in blocking buffer and added to the wells. Plates were then incubated for 1h at RT while rocking gently. After staining, plates were

washed tree times using blocking buffer and then stained using the secondary antibody (anti-rabbit HRP) in a 1:5000 dilution in blocking buffer. Plates were again incubated for 1h at RT while rocking gently. After the secondary staining step, plates were washed three times using blocking buffer and 1ml of True-Blue substrate was added to each well. After 10 minutes of incubation at RT and gentle rocking, substrate was removed and 2ml of H_2O was added to each well. The stained plaques were counted by eye and the viral titre was calculated.

4.2.8. Isolation and analysis of MVA genomes

DNA was isolated from virus stock using the Nucleo Spin Blood QuickPure Kit according to the manufacturer's instructions and established protocols [193].

Purity and insert integrity of MVA HBVac was tested by PCR using the following parameters:

	T [°C]	t [sec]	Cycles
Denaturation	95	120	1
Amplification	95	30	
	60	30	30
	72	Varied between primer pairs	
Final Elongation	72	600	1
Cooling	4		1

Primer pair	Elongation time [sec]
Del I Fw + DelI Rev	30
Del II Fw + DelII Rev	30
Del III Fw + DelIII Rev	300
Del IV Fw + DelIV Rev	45
Del V Fw + DelV Rev	60
Del VI Fw + DelVI Rev	60

After the PCR, products and a 10kb marker were loaded onto a 1% agarose gel containing Roti-safe®. The gel was run in 1x TAE buffer and 120V until a nice separation of the marker was observed. The gel was analyzed using a Fusion FX7 imaging system.

4.2.9. Sanger sequencing

For sequencing samples and primers were send to the GATC services offered by Eurofins Genomics. Samples were labeled using barcodes and a LightRun Tube approach was used for Sanger sequencing. To cover the whole HBVac insert, the following primers were used: Del III Fw, Del III Rev, 63, 64, 194, 422, 423, 425, 426, 434, 464 and 465.

4.2.10. Protein detection and quantification by Western Blotting

For Western blotting, cells were lysed using Pierce RIPA buffer containing cOmplete™ protease inhibitor. After lysis the lysate was transferred into an Eppendorf tube, incubated on ice for 10 min and vortexed vigorously at regular intervals. The lysate was then centrifuged (20.000g, 20min, 4°C) and the supernatant transferred into a new Eppendorf tube while the pellet was discarded. For subcellular localization assays, cells were lysed using the CelLytic™ NuCLEAR™ Extraction Kit according to instructions. Proteins were separated using a denaturing SDS page. The amount of polyacrylamide used for casting of the gel was varied according to the size of the proteins of interest (12% for S,M,L, core and ISG20; 10% for Lamin A/C).

Separation gel	10%	12%
Acrylamide (40%)	2.5	3 ml
Tris (1.5M, pH 8,8)	2.6	2.6 ml
H_2O	4.7	4.2 ml
SDS (10%)		100µl
TEMED	8µl	8µl
APS (10%)	100µl	100µl
Total volume	10ml	10ml
Collection gel	5%	
Acrylamide (40%)	0,5 ml	
Tris (1.5M, pH 8,8)	0,5ml	
H_2O	2,96ml	
SDS (10%)	40µl	
TEMED	8µl	
APS (10%)	40µl	
Total volume	4ml	

Gels were run in 1x Running buffer at 120V for around 1,5 hours. After running the gel, proteins were transferred onto a 0,2µM PVDF membrane using 1x transfer buffer at 300mA, during transfer the setup was cooled using ice. After protein transfer membranes were blocked for 1 hour using 5% Milk powder in TBST at room temperature. For detection of proteins by antibody, the blocked membranes were incubated with the primary antibody over night at 4°C on a roller. After staining membranes were washed thrice with PBS and stained using an HRP labeled secondary antibody. Staining was done for 2h at room temperature on a roller. After incubation membranes were again washed thrice with PBS and staining was detected using GE Healthcare Amersham™ ECL Prime Western-Blot solution and the INTAS ECL Imager machine.

4.2.11. Infection assays using MVA HBVAc, MVA-S and MVA-C

Cells were seeded in 12 well plates 24h pre infection, with a total amount of $6*10^5$ cells per well. At time point zero, cells were infected with the defined MOI by directly adding virus to the medium. HBeAg and HBsAg in the supernatant of infected cells were determined by commercial ELISA using the Abbott ARCHITECT system according to the manufacturer's instructions. For quantification of viral replication cells were washed twice using PBS and 200µl of medium was added per well. The cells were then transferred to -80°C until frozen.

4.2.12. Assessment of MVA genome stability

Cells were seeded in 12 well plates 24h pre infection, with a total amount of $6*10^5$ cells per well. At time point zero, cells were infected with MOI 0.01 by directly adding virus to the medium. Cells were monitored for the cytopathic effects of MVA infection over the next 96 hours. Once the majority of cells were infected, plates were frozen at -80°C and the viral titers in each of the wells was determined. The thusly obtained crude stocks were then used for the next round of infection. After five passages MVA DNA was isolated using the NucleoSpin Blood QuickPure by Macherey Nagel following the manufacturer's protocol and analyzed via PCR, using the primer pairs described in 1.8 [193]. Additionally, isolated DNA samples were sent for Next Generation Sequencing (NGS).

4.2.13. The AAV-HBV model

C57BL/6 mice were intravenously injected with $4*10^9$ genome equivalents (geq) of an AAV-HBV1.2 overlength vector. Four weeks after injection of the vector into the tail vein, mice showed stable levels of HBV serum proteins and were used for experiments [197]. To ensure comparability of the different

groups during the experiments, mice were bled one day prior to vaccination and grouped according to their respective HBV antigen titres.

4.2.14. Protein-prime MVA-boost vaccination

C57BL/6 mice were vaccinated according to a modified protocol from [181]. The animals received one intramuscular protein prime at day 0, containing 20µg of particulate HBsAg as well as 20µg particulate HBcAg and 10µg of c-di-AMP. The vaccine dose was injected into both hind legs (quadriceps) of the animals. Fourteen days after the protein prime, the MVA-HBVac boost was injected. Each animal received one intramuscular dose of $6x10^7$ infectious units (IFU) of MVA-HBVac or a mixture of MVA-S and MVA-C ($3x10^7$ IFU + $3x10^7$ IFU). All animals were sacrificed one week after receiving the MVA boost and analyzed.

4.2.15. Blood withdrawal from mice

Blood was taken from the submandibular vein and collected in Z-Gel Micro tubes. After centrifugation at 10.000g for 5min sera were transferred into new Eppendorf tubes and stored at -20°C until further use.

4.2.16. Isolation of organs and spleenocytes

Mice were sacrificed by cervical dislocation and the chest cavity was opened. The animal's livers and spleens were removed and the livers were perfused using 1x PBS to remove any non-liver associated lymphocytes. Both organs were stored in 10% RPMI medium on ice until further use. To isolate lymphocytes from spleens, the organs were mashed trough a 100µM cell strainer using the plunger of a syringe. Cell strainers were then washed with 5ml of 10% RPMI medium. Cells were then centrifuged (450g, 5min, 4°C) and the supernatant was discarded. Any erythrocytes in the cell pellet were removed by resuspending in ammonium-potassium chloride (ACK) lysis buffer for 1.5 min at 4°C. After incubation 5ml of 10% RPMI was added and the cells were again centrifuged (450g, 5min, 4°C) to remove the supernatant. The new pellet was resuspended in 5ml of 10% RPMI and filtered through a 100µM cell strainer to remove any remaining clumps. Cell number and viability were determined using a Neubauer counting chamber and trypan blue staining. The counted cells were stored in 10% RPMI on ice until further processing. For isolation of liver-associated lymphocytes (LALs) a modified protocol from [357] was used. After perfusion with 1x PBS, livers were mashed through a 100µM cell strainer, washed once with 10% RPMI (450g, 5min, 4°C) and then resuspended in 8ml of collagenase type IV solution (25µg/ml in 10 % RPMI medium). The resuspended cells were incubated for 25min at 37°C, mixed with 10% RPMI and centrifuged (450g, 5min, 4°C). The supernatant was discarded to remove

any remaining collagenase. LALs were isolated from the cell suspension via density gradient centrifugation. Therefore cell pellets were resuspended in 3ml of 40% Percoll™ supplemented with 100IU/ml heparin and layered over 3ml of 80% Percoll™ solution. The gradient was centrifuged at 1200g for 20min at RT and without breaks. The lymphocytes were visible as a greyish band and collected with a serum pipette. After collection, LALs were washed using 10% RPMI (450g, 5min, 4°C) and resuspended in a small volume of the same medium. Cell number and viability were determined using a Neubauer counting chamber and trypan blue staining. Similar to the lymphocytes isolated from the spleens, the counted cells were stored in 10% RPMI on ice until further processing.

4.2.17. Intracellular cytokine staining

Isolated spleenocytes and LALs were stimulated *ex vivo* in a U-bottom 96 well plate. $2*10^6$ were seeded per well in 200µl of 10% RPMI. Cells were the stimulated at 37°C using single peptides or pools at a final concentration of 0,2µg/ml. For a list of peptide sequences see 4.1.7. One hour after the peptides Brefeldin A was added at a final concentration of 75ng/ml and cells were incubated for 14h at 37°C until ICS. After stimulation, lymphocytes were transferred into a V-bottom 96 well plate and washed using 10%RPMI (450g, 2.5 min, 4°C). All following incubation and staining steps were performed in the dark at 4°C. CD4 and CD8 were stained using pacific blue antibodies in a final dilution of 1:100 in FACs buffer for 20min. Simultaneously, cells were stained using Fixable Viability Dye eFluor™ 780 at a final dilution of 1:3000. After staining cells were washed once using FACS buffer followed by fixation and permeabilization using the Cytofix/Cytoperm Kit. For ICS, permeabilized and fixed cells were stained at a final dilution of 1:300 diluted in 1x Perm/Wash buffer for 25 min. After staining cells were washed twice (first with Perm/Wash buffer then witch FACS buffer) and stored in 200µl/ well of FACS buffer until analysis. Samples were measured using a CytoFLEX S cytometer and the FlowJo software was used for data analysis.

4.2.18. Analysis of animal sera

ALT levels were determined in serum using a Reflotron® GPT/ALT assays. Samples were diluted 1:4 with PBS before measurement. HBeAg, HBsAg and anti-HBs titers were determined on the Architect™ platform according to the manufacturer's instructions. Anti-HBc levels were determined using an Enzygnost® Anti-HBc monoclonal test according to the manufacturer's instructions. Samples were diluted with 1x PBS prior to measurement (1:20 for HBsAg/HBeAg; 1:50-1:100 for anti-HBc and anti-HBs).

4.2.19. Statistics and data analysis

Data were analysed using GraphPad Prism software, version 5.01. Average data are shown as mean values with standard deviation (SD) for *in vitro* data or standard error of mean (SEM) in the case of *in vivo* data. Statistical differences were calculated using the Mann-Whitney test (*in vivo*) and the Students unpaired t-test with Welch correction (*in vitro*). *P*-values <0.05 were considered as significant.

4.2.20. Ethical statement

Mouse experiments were performed according to the European Health Law of the Federation of Laboratory Animal Science Associations (FELASA), the regulations of the Society of Laboratory Animal Science (GV-SOLAS), and the 3Rs. The local Animal Care and Use Committee of Upper Bavaria (permission number: ROB-55.2-2532. Vet_02-18-24) approved the experiments and the study protocols according to the institution's guidelines. Animals were kept in a specific pathogen free animal facility at TUM and all experiments were performed during the light phase of the day.

4.2.21. Cell culture

All cells were tested for mycoplasma and cultured under standard conditions of 37°C, 5% CO_2 and 95% humidity. All work steps involving live cells were carried out under sterile conditions using a laminar flow hood. For passaging, cells were washed once, using sterile PBS and incubated with trypsin under standard conditions until the cells detached from the flask. Detached cells were diluted using cell culture medium and then used for re-seeding. Frequencies and dilution factors used for passaging varied between the different cell lines used in this work. HepaRG cells and related cells lines were passaged once a week using a 1:10 dilution factor while HepG2 and HepG2 related cell lines were passaged twice a week using a dilution factor of 1:5. DF-1, HEK293, HeLa, BHK21, Vero and Vero SLAM cells were passaged twice a week using a 1:10 dilution factor. HepG2 and HepG2 related cell lines were kept in culture flaks with collagen coated surfaces. Primary human hepatocytes were received from the Department of General, Visceral, and Transplant Surgery at Hannover Medical School and cultured under standard cell culture conditions using HepaRG differentiation medium. To conserve cells for extended timeframes, trypsinated and diluted cells were centrifuged (300g, 5min), the supernatant was discarded and the remaining cell pellet was resuspended in freezing medium (FCS with 10% DMSO). Resuspended cells were transferred into cryovials, put into a freezing device and stored at -80°C. After 24h frozen cells were transferred to long-term storage in liquid nitrogen. For thawing, cells were taken from liquid nitrogen and put in a 37°C water bath. After thawing, cells were diluted in 50ml of cell culture medium, centrifuged (300g, 5min) and the supernatant was discarded. The cell pellet was resuspended in cell culture media and transferred into a cell culture flask. After seeding HepaRG

cells were grown in Williams E standard media for 10 days and then differentiated for 14 days, using differentiation medium as described previously [358]. Only fully differentiated HepaRG cells were used for infection experiments.

4.2.22. HBV infection protocol

Infection was performed using highly concentrated HBV stocks provided by Jochen Wettengel. Cells were infected at a Multiplicity of infection (MOI) of 100 infectious viral particles/cell unless indicated otherwise. For infection, cells were incubated in infection solution (differentiation medium supplemented with 5% PEG6000 and appropriate amounts of virus) for 24h. After infection cells were washed with 1x PBS and the infection medium was replaced with differentiation medium. For HepG2-NTCP and HepG2 based cell lines experiments were started 7 days post infection (p.i.) while experiments in HepaRG and HepaRG based cell lines were started 10 days p.i. unless indicated otherwise.

4.2.23. Extraction of DNA from infected cells

DNA was isolated using the Nucleo Spin Tissue Kit according to the manufacturer's instructions for cultured cells with light modifications. The protocol was modified to include an additional 1 hour 56°C pre-lysis incubation step.

4.2.24. Measurement of HBV nucleic acids and proteins from cell culture

Total intraccellur viral DNA (rcDNA +cccDNA) as well as cccDNA were quantified by qPCR on a LightCycler 480 Real-Time PCR machine using their respective primer pair (primers 1745 and 1844 for rcDNA and primer 92- and 2251- for cccDNA) [359]. Amounts of DNA were calculated using the advanced relative quantification program and normalized to a reference gene (PRNP for DNA and TBP for cDNA). Each PCR reaction contained 4µl of DNA, 5µl of Sybergreen I Master Mix and 0,5µl per primer. For cccDNA quantification, samples were subjected to a T5 digestion prior to PCR to remove any nicked or linear DNA fragments. This serves to enhance cccDNA specificity by digesting rcDNA, nicked cccDNA as well as linear HBV genomes. For each sample, one digestion containing 8,5µl DNA, 1µl digestion buffer and 0,5µl of T5 exonuclease was used. The samples were incubated at 37°C for 30 min to facilitate digestion and then heated to 95°C for 5 min to inactivate the T5 exonuclease. After digestion samples were diluted with water (30µl water + 10µl of sample) [359]. HBeAg and HBsAg were measured by ELISA.

Total intracellular HBV DNA and PRNP were determined using the following program:

	T [°C]	t [sec]	Ramp [°C/sec]	Acquisition mode	Cycles
Denaturation	95	300	4.4		1
Amplification	95	25	4.4		
	60	10	2.2		40
	72	30	4.4	single	
Melting	95	1	4.4		
	65	60	2.2		1
	95		0.11	Continuous: 5/°C	
Cooling	40	30	2.2		1

cccDNA was determined using the following program:

	T [°C]	t [sec]	Ramp [°C/sec]	Acquisition mode	Cycles
Denaturation	95	600	4.4		1
Amplification	95	15	4.4		
	60	5	2.2		
	72	45	4.4		50
	88	2	4.4	single	
Melting	95	1	4.4		
	65	60	2.2		1
	95		0.11	Continuous: 5/°C	
Cooling	40	30	2.2		1

4.2.25. Cell vitality assay: CellTiter-Blue®.

CellTiter-Blue® Cell Viability Assay was used to determine cell viability during and after treatment. The Kit is based on the conversion of resazurin into resorufin in living cells and was used according to the manufacturer's instructions. Fluorescence was detected using a Tecan plate reader.

4.2.26. RNA extraction and reveres transcription into cDNA

RNA was isolated using the NucleoSpin RNA isolation Kit according to the manufacturer's instruction. In the case of HBV infection, DNA digestion time was increased to 40min and all samples were eluted in 50µl. SuperScript III First-Strand Synthesis SuperMix was used for reverse transcription into cDNA.

The protocol used was modified from the manufacturers: each sample contained 5µl Reaction Mix, 4µl of RNA and 1µl of RT Enzyme mix. After reverse transcription 0,5µl of RNAse were added to remove any remaining RNA and the samples were analyzed by qPCR. Amounts of cDNA were calculated using the advanced relative quantification program and normalized to a reference gene (TBP for cDNA). Each PCR reaction contained 4µl of DNA, 5µl of Sybergreen I Master Mix and 0,5µl per primer.

Factors from cDNA were quantified using the program GE_C3:

	T [°C]	t [sec]	Ramp [°C/sec]	Acquisition mode	Cycles
Denaturation	95	300	4.4		1
Amplification	95	15	4.4		
	60	10	2.2		
	72	25	4.4		45
Melting	95	1	4.4		
	65	60	2.2		1
	95		0.11	Continuous: 5/°C	
Cooling	40	30	2.2		1

4.2.27. Immunofluorescence staining

For immunofluorescence staining cells were seeded on coverslips in a 48-well plate. After infection and/or treatment cells were washed once with 1x PBS and then fixed using 4% paraformaldehyde at RT for 10min. After fixation, cells were washed once using 1x PBS and the permeabilized using 0,5% saponin in PBS for 10min at RT. Next, cells were blocked using a PBS-based blocking buffer containing 0,1% saponin and 10% goat serum. Cells were incubated in blocking buffer over night at 4°C. After blocking, cells were stained using blocking solution containing the primary antibodies at their respective dilution (PML (1:200), ISG20 (1:100), Nucleophosmin (1:100), HBV core protein (1:400)). Cells were incubated in the staining solution over night at 4°C. After staining, cells were washed thrice for 10min with 1x PBS containing 0,1% saponin and then incubated with the secondary staining solution containing 1x PBS, 0,1% saponin, 2% goat serum as well as the respective, fluorophor coupled secondary antibodies. All secondary antibodies were used in a 1:1000 dilution. The cells were covered with aluminum foil and incubated for 2 hours at RT on a shaker. After incubation, the staining solution was removed and the cells were washed thrice for 10min with 1x PBS containing 0,1% saponin. Finally, cells were briefly washed in 1x PBS. After the final washing step, coverslips were removed from the wells and flipped onto an object slide covered with DAPI mounting solution. The mounted coverslips were dried at 4°C overnight. After drying, coverslips were fixed on the object slide by circling them

with transparent nail polish. All coverslips were observed and photographed using the Olympus Fluoview FV10i confocal microscope.

4.2.28. Co-immunoprecipitation assay

Co-immunoprecipitation (Co-IP) from lysate of infected HepG2-NTCP cells was performed using the Pierce™ Co-Immunoprecipation Kit according to the manufacturer's instructions. 75µg of anti-HBc antibody were coupled to the aminolink resin to create the binding columns. 200µl of purified cell lysate were used for each precipitation approach. Antibody binding took place over night at 4°C and the tubes containing the samples were stored on a rotator to ensure constant agitation. Bound protein was eluted from the columns in a volume of 50µl. All fractions obtained after protein binding were analyzed by western blot.

4.2.29. Subcellular fractionation of infected HepG2-NTCP

Cells were cultured in 15cm dishes to acquire sufficient material and for each sample cells from five 15cm dishes were pooled. After trypsinization, cells were pooled and resuspended in pre-warmed DMEM medium containing 10% FCS. Next, cells were washed once in ice-cold 1x PBS, centrifuged (218g, 4°C, 5min) and then resuspended in ice-cold detergent buffer (20mM Tris pH 7.4, 1mM KCl, 3mM $MgCl_2$, 0.1% NP40, 10% glycerol) for 12 minutes. After lysis of the cytoplasmic membrane, the solution was centrifuged at 1350g for 10 min at 4°C. The supernantant was removed and contained the cytoplasmic fraction. The pellet containing the nuclei was resuspended in 3ml of buffer S1 (0,25M sucrose, 10mM $MgCl_2$) and passed through a 100µM cell strainer to remove any remaining clumps. The resuspended nuclei were layered over 3ml of buffer S2 (0.35m sucrose, 0.5mM $MgCl_2$) in a 15ml falcon and then centrifuged at 1430g for 5min at 4°C. The supernatant was discarded as wash fraction. The pellet was then resuspended in 3ml of S2 buffer and sonicated thrice using a sonication needle (76D/E, 10sec, continuous) with one minute cooling intervals between each 10sec pulse. The sonicated solution was then layered over a 3ml cushion of buffer S3 (0.88M sucrose, 0.5mM $MgCl_2$) and centrifuged for 10min at 2800g, 4°C. The supernatant contained the nucleoplasmic fraction, while the pellet contained the nucleoli. The pellet was washed once by resuspending in 0.5ml S2 buffer followed by a centrifugation step (1430g, 5min, 4°C). The resulting pellet contained the highly pure nuclei and was resuspended in western blot analysis or DNA lysis buffer for analysis by qPCR or western blot.

5.   Figures

6. References

1. WHO, *Global Hepatitis Report 2017.* 2017.
2. Kwon, H. and A.S. Lok, *Hepatitis B therapy.* Nat Rev Gastroenterol Hepatol, 2011. **8**(5): p. 275-84.
3. Lars Magnius, W.S.M., John Taylor, Michael Kann, Dieter Glebe, Paul Dény, Camille Sureau, Helene Norder, and ICTV Report Consortium, *CTV Virus Taxonomy Profile: Hepadnaviridae.* ournal of General Virology, 2020. **101**: p. 571-572.
4. Koonin, E.V., et al., *Global Organization and Proposed Megataxonomy of the Virus World.* Microbiology and Molecular Biology Reviews, 2020. **84**(2).
5. Kramvis, A., et al., *Relationship of serological subtype, basic core promoter and precore mutations to genotypes/subgenotypes of hepatitis B virus.* Journal of Medical Virology, 2008. **80**(1): p. 27-46.
6. Norder, H., et al., *Genetic Diversity of Hepatitis B Virus Strains Derived Worldwide: Genotypes, Subgenotypes, and HB_sAg Subtypes.* 2004. **47**(6): p. 289-309.
7. Norder, H., A.M. Courouce, and L.O. Magnius, *Molecular basis of hepatitis B virus serotype variations within the four major subtypes.* Journal of General Virology, 1992. **73**(12): p. 3141-3145.
8. Sunbul, M., *Hepatitis B virus genotypes: global distribution and clinical importance.* World J Gastroenterol, 2014. **20**(18): p. 5427-34.
9. Zhang, H.W., et al., *Risk factors for acute hepatitis B and its progression to chronic hepatitis in Shanghai, China.* 2008. **57**(12): p. 1713-1720.
10. Marcellin, P., et al., *Sustained Response of Hepatitis B e Antigen-Negative Patients 3 Years After Treatment with Peginterferon Alfa-2a.* 2009. **136**(7): p. 2169-2179.e4.
11. Buster, E.H., et al., *Sustained HBeAg and HBsAg loss after long-term follow-up of HBeAg-positive patients treated with peginterferon alpha-2b.* Gastroenterology, 2008. **135**(2): p. 459-67.
12. Schweitzer, A., et al., *Estimations of worldwide prevalence of chronic hepatitis B virus infection: a systematic review of data published between 1965 and 2013.* Lancet, 2015. **386**(10003): p. 1546-55.
13. Lauber, C., et al., *Deciphering the Origin and Evolution of Hepatitis B Viruses by Means of a Family of Non-enveloped Fish Viruses.* Cell Host & Microbe, 2017. **22**(3): p. 387-399.e6.
14. Paraskevis, D., et al., *Dating the origin and dispersal of hepatitis B virus infection in humans and primates.* Hepatology, 2013. **57**(3): p. 908-916.
15. Velkov, S., et al., *The Global Hepatitis B Virus Genotype Distribution Approximated from Available Genotyping Data.* Genes, 2018. **9**(10): p. 495.
16. Ghasemi, F., et al., *Current progress in the development of therapeutic vaccines for chronic hepatitis B virus infection.* Iran J Basic Med Sci, 2016. **19**(7): p. 692-704.
17. Dane, D.S., C.H. Cameron, and M. Briggs, *Virus-like particles in serum of patients with Australia-antigen-associated hepatitis.* Lancet, 1970. **1**(7649): p. 695-8.
18. Heermann, K.H., et al., *Large surface proteins of hepatitis B virus containing the pre-s sequence.* J Virol, 1984. **52**(2): p. 396-402.
19. Nassal, M., A. Rieger, and O. Steinau, *Topological analysis of the hepatitis B virus core particle by cysteine-cysteine cross-linking.* J Mol Biol, 1992. **225**(4): p. 1013-25.
20. Zhou, S. and D.N. Standring, *Hepatitis B virus capsid particles are assembled from core-protein dimer precursors.* Proceedings of the National Academy of Sciences, 1992. **89**(21): p. 10046-10050.
21. Crowther, R.A., et al., *Three-dimensional structure of hepatitis B virus core particles determined by electron cryomicroscopy.* Cell, 1994. **77**(6): p. 943-50.
22. Roseman, A.M., et al., *A structural model for maturation of the hepatitis B virus core.* Proceedings of the National Academy of Sciences, 2005. **102**(44): p. 15821-15826.

23. Gerlich, W.H. and W.S. Robinson, *Hepatitis B virus contains protein attached to the 5' terminus of its complete DNA strand.* Cell, 1980. **21**(3): p. 801-9.

24. Blumberg, B., *Australia antigen and the biology of hepatitis B.* Science, 1977. **197**(4298): p. 17-25.

25. Ning, X., et al., *Secretion of Genome-Free Hepatitis B Virus – Single Strand Blocking Model for Virion Morphogenesis of Para-retrovirus.* PLoS Pathogens, 2011. **7**(9): p. e1002255.

26. Yan, H., et al., *Sodium taurocholate cotransporting polypeptide is a functional receptor for human hepatitis B and D virus.* eLife, 2012. **1**.

27. Ni, Y., et al., *Hepatitis B and D viruses exploit sodium taurocholate co-transporting polypeptide for species-specific entry into hepatocytes.* Gastroenterology, 2014. **146**(4): p. 1070-83.

28. Engelke, M., et al., *Characterization of a hepatitis B and hepatitis delta virus receptor binding site.* 2006. **43**(4): p. 750-760.

29. Rabe, B., et al., *Nuclear import of hepatitis B virus capsids and release of the viral genome.* Proceedings of the National Academy of Sciences, 2003. **100**(17): p. 9849-9854.

30. Schmitz, A., et al., *Nucleoporin 153 Arrests the Nuclear Import of Hepatitis B Virus Capsids in the Nuclear Basket.* PLoS Pathogens, 2010. **6**(1): p. e1000741.

31. Bock, C.T., et al., *Structural organization of the hepatitis B virus minichromosome.* J Mol Biol, 2001. **307**(1): p. 183-96.

32. Protzer, U. and H. Schaller, Virus Genes, 2000. **21**(1/2): p. 27-37.

33. Addison, W.R., et al., *Half-Life of the Duck Hepatitis B Virus Covalently Closed Circular DNA Pool In Vivo following Inhibition of Viral Replication.* 2002. **76**(12): p. 6356-6363.

34. Zhu, Y., et al., *Kinetics of Hepadnavirus Loss from the Liver during Inhibition of Viral DNA Synthesis.* 2001. **75**(1): p. 311-322.

35. Ko, C., et al., *Hepatitis B virus genome recycling and de novo secondary infection events maintain stable cccDNA levels.* J Hepatol, 2018. **69**(6): p. 1231-1241.

36. Bartenschlager, R. and H. Schaller, *Hepadnaviral assembly is initiated by polymerase binding to the encapsidation signal in the viral RNA genome.* The EMBO Journal, 1992. **11**(9): p. 3413-3420.

37. Perlman, D. and J. Hu, *Duck Hepatitis B Virus Virion Secretion Requires a Double-Stranded DNA Genome.* 2003. **77**(3): p. 2287-2294.

38. Perlman, D.H., et al., *Reverse transcription-associated dephosphorylation of hepadnavirus nucleocapsids.* Proceedings of the National Academy of Sciences, 2005. **102**(25): p. 9020-9025.

39. Bruss, V., *Hepatitis B virus morphogenesis.* World Journal of Gastroenterology, 2007. **13**(1): p. 65.

40. Piper, R.C. and D.J. Katzmann, *Biogenesis and Function of Multivesicular Bodies.* Annual Review of Cell and Developmental Biology, 2007. **23**(1): p. 519-547.

41. Watanabe, T., et al., *Involvement of host cellular multivesicular body functions in hepatitis B virus budding.* Proceedings of the National Academy of Sciences, 2007. **104**(24): p. 10205-10210.

42. Ko, C., T. Michler, and U. Protzer, *Novel viral and host targets to cure hepatitis B.* Current Opinion in Virology, 2017. **24**: p. 38-45.

43. Allis, C.D. and T. Jenuwein, *The molecular hallmarks of epigenetic control.* Nature Reviews Genetics, 2016. **17**(8): p. 487-500.

44. Kouzarides, T., *Chromatin Modifications and Their Function.* Cell, 2007. **128**(4): p. 693-705.

45. Rodríguez-Paredes, M. and M. Esteller, *Cancer epigenetics reaches mainstream oncology.* Nature Medicine, 2011. **17**(3): p. 330-339.

46. Bock, C.-T., et al., *Hepatitis B virus genome is organized into nucleosomes in the nucleus of the infected cell.* 1994. **8**(2): p. 215-229.

47. Bock, C.T., et al., *Structural organization of the hepatitis B virus minichromosome.* Journal of Molecular Biology, 2001. **307**(1): p. 183-196.

48. Shi, L., et al., *Characterization of Nucleosome Positioning in Hepadnaviral Covalently Closed Circular DNA Minichromosomes.* Journal of Virology, 2012. **86**(18): p. 10059-10069.

49. Pollicino, T., et al., *Hepatitis B Virus Replication Is Regulated by the Acetylation Status of Hepatitis B Virus cccDNA-Bound H3 and H4 Histones.* Gastroenterology, 2006. **130**(3): p. 823-837.

50. Hong, X., E.S. Kim, and H. Guo, *Epigenetic regulation of hepatitis B virus covalently closed circular DNA: Implications for epigenetic therapy against chronic hepatitis B.* Hepatology, 2017. **66**(6): p. 2066-2077.

51. Belloni, L., et al., *Nuclear HBx binds the HBV minichromosome and modifies the epigenetic regulation of cccDNA function.* Proceedings of the National Academy of Sciences, 2009. **106**(47): p. 19975-19979.

52. Tropberger, P., et al., *Mapping of histone modifications in episomal HBV cccDNA uncovers an unusual chromatin organization amenable to epigenetic manipulation.* Proc Natl Acad Sci U S A, 2015. **112**(42): p. E5715-24.

53. Belloni, L., et al., *IFN-α inhibits HBV transcription and replication in cell culture and in humanized mice by targeting the epigenetic regulation of the nuclear cccDNA minichromosome.* Journal of Clinical Investigation, 2012. **122**(2): p. 529-537.

54. Allweiss, L., et al., *Immune cell responses are not required to induce substantial hepatitis B virus antigen decline during pegylated interferon-alpha administration.* J Hepatol, 2014. **60**(3): p. 500-7.

55. Rongrui, L., et al., *Epigenetic mechanism involved in the HBV/HCV-related hepatocellular carcinoma tumorigenesis.* Curr Pharm Des, 2014. **20**(11): p. 1715-25.

56. Cheng, Y., et al., *Targeting epigenetic regulators for cancer therapy: mechanisms and advances in clinical trials.* Signal Transduct Target Ther, 2019. **4**: p. 62.

57. Zheng, Y., J. Li, and J.H. Ou, *Regulation of Hepatitis B Virus Core Promoter by Transcription Factors HNF1 and HNF4 and the Viral X Protein.* Journal of Virology, 2004. **78**(13): p. 6908-6914.

58. Lin, W.J., *Suppression of Hepatitis B Virus Core Promoter by the Nuclear Orphan Receptor TR4.* 2003. **278**(11): p. 9353-9360.

59. Raney, A.K., et al., *Members of the nuclear receptor superfamily regulate transcription from the hepatitis B virus nucleocapsid promoter.* J Virol, 1997. **71**(2): p. 1058-71.

60. Lucifora, J., et al., *Hepatitis B virus X protein is essential to initiate and maintain virus replication after infection.* J Hepatol, 2011. **55**(5): p. 996-1003.

61. Keasler, V.V., et al., *Enhancement of Hepatitis B Virus Replication by the Regulatory X Protein In Vitro and In Vivo.* 2007. **81**(6): p. 2656-2662.

62. Tsuge, M., et al., *HBx protein is indispensable for development of viraemia in human hepatocyte chimeric mice.* 2010. **91**(7): p. 1854-1864.

63. Park, S.G., et al., *Up-regulation of Cyclin D1 by HBx Is Mediated by NF- B2/BCL3 Complex through B Site of Cyclin D1 Promoter.* 2006. **281**(42): p. 31770-31777.

64. Avantaggiati, M.L., et al., *The hepatitis B virus (HBV) pX transactivates the c-fos promoter through multiple cis-acting elements.* Oncogene, 1993. **8**(6): p. 1567-74.

65. Bouchard, M.J., et al., *Activation and Inhibition of Cellular Calcium and Tyrosine Kinase Signaling Pathways Identify Targets of the HBx Protein Involved in Hepatitis B Virus Replication.* 2003. **77**(14): p. 7713-7719.

66. Gearhart, T.L. and M.J. Bouchard, *The Hepatitis B Virus X Protein Modulates Hepatocyte Proliferation Pathways To Stimulate Viral Replication.* 2010. **84**(6): p. 2675-2686.

67. Melegari, M., S.K. Wolf, and R.J. Schneider, *Hepatitis B Virus DNA Replication Is Coordinated by Core Protein Serine Phosphorylation and HBx Expression.* 2005. **79**(15): p. 9810-9820.

68. M Doria , N.K., R Lucito, R J Schneider, *The hepatitis B virus HBx protein is a dual specificity cytoplasmic activator of Ras and nuclear activator of transcription factors.* EMBO J, 1995. **2**(19): p. 10.

69. Leupin, O., et al., *Hepatitis B Virus X Protein Stimulates Viral Genome Replication via a DDB1-Dependent Pathway Distinct from That Leading to Cell Death.* 2005. **79**(7): p. 4238-4245.

70. Decorsière, A., et al., *Hepatitis B virus X protein identifies the Smc5/6 complex as a host restriction factor.* Nature, 2016. **531**(7594): p. 386-389.

71. Soucy, T.A., et al., *The NEDD8 Conjugation Pathway and Its Relevance in Cancer Biology and Therapy.* Genes & Cancer, 2010. **1**(7): p. 708-716.

72. Tuttleman, J.S., C. Pourcel, and J. Summers, *Formation of the pool of covalently closed circular viral DNA in hepadnavirus-infected cells.* Cell, 1986. **47**(3): p. 451-60.

73. Hantz, O., et al., *Persistence of the hepatitis B virus covalently closed circular DNA in HepaRG human hepatocyte-like cells.* Journal of General Virology, 2009. **90**(1): p. 127-135.

74. Tropberger, P., et al., *Mapping of histone modifications in episomal HBV cccDNA uncovers an unusual chromatin organization amenable to epigenetic manipulation.* Proceedings of the National Academy of Sciences, 2015. **112**(42): p. E5715-E5724.

75. Bourne, E.J., et al., *Quantitative analysis of HBV cccDNA from clinical specimens: correlation with clinical and virological response during antiviral therapy.* 2007. **14**(1): p. 55-63.

76. Werle–Lapostolle, B., et al., *Persistence of cccDNA during the natural history of chronic hepatitis B and decline during adefovir dipivoxil therapy1 ☆.* Gastroenterology, 2004. **126**(7): p. 1750-1758.

77. Allweiss, L. and M. Dandri, *The Role of cccDNA in HBV Maintenance.* Viruses, 2017. **9**(6): p. 156.

78. Lechardeur, D., et al., *Metabolic instability of plasmid DNA in the cytosol: a potential barrier to gene transfer.* Gene Therapy, 1999. **6**(4): p. 482-497.

79. Mason, W.S., et al., *The Amount of Hepatocyte Turnover That Occurred during Resolution of Transient Hepadnavirus Infections Was Lower When Virus Replication Was Inhibited with Entecavir.* 2009. **83**(4): p. 1778-1789.

80. Moriyama, T., et al., *Immunobiology and pathogenesis of hepatocellular injury in hepatitis B virus transgenic mice.* Science, 1990. **248**(4953): p. 361-364.

81. Kondo, Y., et al., *Vigorous response of cytotoxic T lymphocytes associated with systemic activation of CD8 T lymphocytes in fulminant hepatitis B.* Liver Int, 2004. **24**(6): p. 561-7.

82. Guidotti, L.G., et al., *Intracellular Inactivation of the Hepatitis B Virus by Cytotoxic T Lymphocytes.* Immunity, 1996. **4**(1): p. 25-36.

83. Franco, A., et al., *Pathogenetic effector function of CD4-positive T helper 1 cells in hepatitis B virus transgenic mice.* J Immunol, 1997. **159**(4): p. 2001-8.

84. Kakimi, K., et al., *Natural Killer T Cell Activation Inhibits Hepatitis B Virus Replication in Vivo.* 2000. **192**(7): p. 921-930.

85. Wieland, S.F., et al., *Expansion and contraction of the hepatitis B virus transcriptional template in infected chimpanzees.* Proceedings of the National Academy of Sciences, 2004. **101**(7): p. 2129-2134.

86. Lucifora, J., et al., *Specific and Nonhepatotoxic Degradation of Nuclear Hepatitis B Virus cccDNA.* Science, 2014. **343**(6176): p. 1221-1228.

87. Xia, Y., et al., *Interferon-γ and Tumor Necrosis Factor-α Produced by T Cells Reduce the HBV Persistence Form, cccDNA, Without Cytolysis.* Gastroenterology, 2016. **150**(1): p. 194-205.

88. Viganò, M., et al., *Treatment of hepatitis B: Is there still a role for interferon?* Liver International, 2018. **38**: p. 79-83.

89. Woo, A.S.J., R. Kwok, and T. Ahmed, *Alpha-interferon treatment in hepatitis B.* Ann Transl Med, 2017. **5**(7): p. 159.

90. Zhang, X., et al., *Preclinical development of TLR ligands as drugs for the treatment of chronic viral infections.* Expert Opin Drug Discov, 2012. **7**(7): p. 597-611.

91. Chisari, F.V., M. Isogawa, and S.F. Wieland, *Pathogenesis of hepatitis B virus infection.* Pathologie Biologie, 2010. **58**(4): p. 258-266.

92. Lanford, R.E., et al., *GS-9620, an Oral Agonist of Toll-Like Receptor-7, Induces Prolonged Suppression of Hepatitis B Virus in Chronically Infected Chimpanzees.* Gastroenterology, 2013. **144**(7): p. 1508-1517.e10.

93. Ligat, G., et al., *Targeting Viral cccDNA for Cure of Chronic Hepatitis B.* Current Hepatology Reports, 2020. **19**(3): p. 235-244.

94. Seth, R.B., L. Sun, and Z.J. Chen, *Antiviral innate immunity pathways.* Cell Research, 2006. **16**(2): p. 141-147.

95. Kenneth Murphy, C.W., *Janeway's Immunobiology, Ninth Edition.* Garland Science: New York,, 2016.

96. Luangsay, S., et al., *Early inhibition of hepatocyte innate responses by hepatitis B virus.* J Hepatol, 2015. **63**(6): p. 1314-22.

97. Megahed, F.A.K., X. Zhou, and P. Sun, *The Interactions Between HBV and the Innate Immunity of Hepatocytes.* Viruses, 2020. **12**(3): p. 285.

98. Sato, S., et al., *The RNA Sensor RIG-I Dually Functions as an Innate Sensor and Direct Antiviral Factor for Hepatitis B Virus.* Immunity, 2015. **42**(1): p. 123-132.

99. Guy, C.S., et al., *Intrahepatic Expression of Genes Affiliated with Innate and Adaptive Immune Responses Immediately after Invasion and during Acute Infection with Woodchuck Hepadnavirus.* 2008. **82**(17): p. 8579-8591.

100. Lucifora, J., et al., *Control of hepatitis B virus replication by innate response of HepaRG cells.* Hepatology, 2010. **51**(1): p. 63-72.

101. Fletcher, S.P., et al., *Transcriptomic analysis of the woodchuck model of chronic hepatitis B.* Hepatology, 2012. **56**(3): p. 820-830.

102. Wieland, S., et al., *Genomic analysis of the host response to hepatitis B virus infection.* Proceedings of the National Academy of Sciences, 2004. **101**(17): p. 6669-6674.

103. Christen, V., et al., *Inhibition of Alpha Interferon Signaling by Hepatitis B Virus.* 2007. **81**(1): p. 159-165.

104. Lutgehetmann, M., et al., *Hepatitis B virus limits response of human hepatocytes to interferon-alpha in chimeric mice.* Gastroenterology, 2011. **140**(7): p. 2074-83, 2083 e1-2.

105. Fisicaro, P., et al., *Early kinetics of innate and adaptive immune responses during hepatitis B virus infection.* Gut, 2009. **58**(7): p. 974-982.

106. Yang, P.L., et al., *Hydrodynamic injection of viral DNA: A mouse model of acute hepatitis B virus infection.* 2002. **99**(21): p. 13825-13830.

107. Okazaki, A., et al., *Severe necroinflammatory reaction caused by natural killer cell-mediated Fas/Fas ligand interaction and dendritic cells in human hepatocyte chimeric mouse.* 2012. **56**(2): p. 555-566.

108. Tjwa, E.T., et al., *Viral load reduction improves activation and function of natural killer cells in patients with chronic hepatitis B.* J Hepatol, 2011. **54**(2): p. 209-18.

109. Liaskou, E., et al., *Monocyte subsets in human liver disease show distinct phenotypic and functional characteristics.* Hepatology, 2013. **57**(1): p. 385-398.

110. Li, M., et al., *Kupffer Cells Support Hepatitis B Virus–Mediated CD8+ T Cell Exhaustion via Hepatitis B Core Antigen–TLR2 Interactions in Mice.* The Journal of Immunology, 2015. **195**(7): p. 3100-3109.

111. Hösel, M., et al., *Not interferon, but interleukin-6 controls early gene expression in hepatitis B virus infection.* Hepatology, 2009. **50**(6): p. 1773-1782.

112. Wu, J., et al., *Toll-like receptor-mediated control of HBV replication by nonparenchymal liver cells in mice.* 2007. **46**(6): p. 1769-1778.

113. Webster, G., *Incubation Phase of Acute Hepatitis B in Man: Dynamic of Cellular Immune Mechanisms.* Hepatology, 2000. **32**(5): p. 1117-1124.

114. Antonio Bertoletti, C.F., *Adaptive immunity in HBV infection.* Journal of Hepatology, 2016. **64**: p. s71-s83.

115. Roche, P.A. and K. Furuta, *The ins and outs of MHC class II-mediated antigen processing and presentation.* Nature Reviews Immunology, 2015. **15**(4): p. 203-216.

116. Henrickson, S.E., et al., *In Vivo Imaging of T Cell Priming.* Science Signaling, 2008. **1**(12): p. pt2-pt2.

117. Russell, J.H. and T.J. Ley, *LYMPHOCYTE-MEDIATEDCYTOTOXICITY.* Annual Review of Immunology, 2002. **20**(1): p. 323-370.

118. Christensen, J.E. and A.R. Thomsen, *Co-ordinating innate and adaptive immunity to viral infection: mobility is the key.* APMIS, 2009. **117**(5-6): p. 338-355.

119. Guidotti, L.G., *Viral Clearance Without Destruction of Infected Cells During Acute HBV Infection.* Science, 1999. **284**(5415): p. 825-829.

120. Guidotti, L.G. and F.V. Chisari, *NONCYTOLYTICCONTROL OFVIRALINFECTIONS BY THEINNATE ANDADAPTIVEIMMUNERESPONSE.* Annual Review of Immunology, 2001. **19**(1): p. 65-91.

121. Thimme, R., et al., *CD8+ T Cells Mediate Viral Clearance and Disease Pathogenesis during Acute Hepatitis B Virus Infection.* Journal of Virology, 2003. **77**(1): p. 68-76.

122. Wieland, S.F., et al., *Expansion and contraction of the hepatitis B virus transcriptional template in infected chimpanzees.* Proc Natl Acad Sci U S A, 2004. **101**(7): p. 2129-34.

123. Rehermann, B., et al., *The hepatitis B virus persists for decades after patients' recovery from acute viral hepatitis despite active maintenance of a cytotoxic T–lymphocyte response.* Nature Medicine, 1996. **2**(10): p. 1104-1108.

124. Penna, A., et al., *Long-lasting memory T cell responses following self-limited acute hepatitis B.* Journal of Clinical Investigation, 1996. **98**(5): p. 1185-1194.

125. Hoofnagle, J.H., *Reactivation of hepatitis B.* Hepatology, 2009. **49**(S5): p. S156-S165.

126. Shin, E.-C., P.S. Sung, and S.-H. Park, *Immune responses and immunopathology in acute and chronic viral hepatitis.* Nature Reviews Immunology, 2016. **16**(8): p. 509-523.

127. Jilbert, A.R., et al., *Characterization of age- and dose-related outcomes of duck hepatitis B virus infection.* Virology, 1998. **244**(2): p. 273-82.

128. Cote, P.J., et al., *Effects of age and viral determinants on chronicity as an outcome of experimental woodchuck hepatitis virus infection.* Hepatology, 2000. **31**(1): p. 190-200.

129. Lampertico, P., et al., *EASL 2017 Clinical Practice Guidelines on the management of hepatitis B virus infection.* Journal of Hepatology, 2017. **67**(2): p. 370-398.

130. Raffetti, E., G. Fattovich, and F. Donato, *Incidence of hepatocellular carcinoma in untreated subjects with chronic hepatitis B: a systematic review and meta-analysis.* 2016. **36**(9): p. 1239-1251.

131. Varbobitis, I. and G.V. Papatheodoridis, *The assessment of hepatocellular carcinoma risk in patients with chronic hepatitis B under antiviral therapy.* Clinical and Molecular Hepatology, 2016. **22**(3): p. 319-326.

132. Suk-Fong Lok, A., *Hepatitis B Treatment: What We Know Now and What Remains to Be Researched.* Hepatology Communications, 2019. **3**(1): p. 8-19.

133. Webster, G.J.M., et al., *Longitudinal Analysis of CD8+ T Cells Specific for Structural and Nonstructural Hepatitis B Virus Proteins in Patients with Chronic Hepatitis B: Implications for Immunotherapy.* Journal of Virology, 2004. **78**(11): p. 5707-5719.

134. Bengsch, B., B. Martin, and R. Thimme, *Restoration of HBV-specific CD8+ T cell function by PD-1 blockade in inactive carrier patients is linked to T cell differentiation.* J Hepatol, 2014. **61**(6): p. 1212-9.

135. Bowen, D.G., et al., *The site of primary T cell activation is a determinant of the balance between intrahepatic tolerance and immunity.* 2004. **114**(5): p. 701-712.

136. Bertolino, P., M.C. Trescol-Biemont, and C. Rabourdin-Combe, *Hepatocytes induce functional activation of naive CD8+ T lymphocytes but fail to promote survival.* Eur J Immunol, 1998. **28**(1): p. 221-36.

137. Boni, C., et al., *Characterization of Hepatitis B Virus (HBV)-Specific T-Cell Dysfunction in Chronic HBV Infection.* Journal of Virology, 2007. **81**(8): p. 4215-4225.

138. Yang, P.L., et al., *Immune effectors required for hepatitis B virus clearance.* Proceedings of the National Academy of Sciences, 2010. **107**(2): p. 798-802.

139. Das, A., et al., *Functional skewing of the global CD8 T cell population in chronic hepatitis B virus infection.* The Journal of Experimental Medicine, 2008. **205**(9): p. 2111-2124.

140. McNab, F., et al., *Type I interferons in infectious disease.* Nature Reviews Immunology, 2015. **15**(2): p. 87-103.

141. Ito, T., et al., *Differential Regulation of Human Blood Dendritic Cell Subsets by IFNs.* The Journal of Immunology, 2001. **166**(5): p. 2961-2969.

142. Lapenta, C., et al., *Potent Immune Response against HIV-1 and Protection from Virus Challenge in hu-PBL-SCID Mice Immunized with Inactivated Virus-pulsed Dendritic Cells Generated in the Presence of IFN-α.* Journal of Experimental Medicine, 2003. **198**(2): p. 361-367.

143. Montoya, M., et al., *Type I interferons produced by dendritic cells promote their phenotypic and functional activation.* Blood, 2002. **99**(9): p. 3263-3271.

144. Brinkmann, V., et al., *Interferon alpha increases the frequency of interferon gamma-producing human CD4+ T cells.* Journal of Experimental Medicine, 1993. **178**(5): p. 1655-1663.

145. Havenar-Daughton, C., G.A. Kolumam, and K. Murali-Krishna, *Cutting Edge: The Direct Action of Type I IFN on CD4 T Cells Is Critical for Sustaining Clonal Expansion in Response to a Viral but Not a Bacterial Infection.* The Journal of Immunology, 2006. **176**(6): p. 3315-3319.

146. Cousens, L.P., et al., *Two Roads Diverged: Interferon α/β– and Interleukin 12–mediated Pathways in Promoting T Cell Interferon γ Responses during Viral Infection.* Journal of Experimental Medicine, 1999. **189**(8): p. 1315-1328.

147. Marshall, H.D., et al., *IFN-αβ and Self-MHC Divert CD8 T Cells into a Distinct Differentiation Pathway Characterized by Rapid Acquisition of Effector Functions.* The Journal of Immunology, 2010. **185**(3): p. 1419-1428.

148. Tan, G., et al., *When Hepatitis B Virus Meets Interferons.* Frontiers in Microbiology, 2018. **9**.

149. Frucht, D.M., et al., *IFN-gamma production by antigen-presenting cells: mechanisms emerge.* Trends Immunol, 2001. **22**(10): p. 556-60.

150. Schroder, K., et al., *Interferon-γ: an overview of signals, mechanisms and functions.* Journal of Leukocyte Biology, 2004. **75**(2): p. 163-189.

151. Aaronson, D.S., *A Road Map for Those Who Don't Know JAK-STAT.* Science, 2002. **296**(5573): p. 1653-1655.

152. Platanias, L.C., *Mechanisms of type-I- and type-II-interferon-mediated signalling.* Nature Reviews Immunology, 2005. **5**(5): p. 375-386.

153. Kawakami, T., et al., *Possible involvement of the transcription factor ISGF3γ in virus-induced expression of the IFN-β gene.* FEBS Letters, 1995. **358**(3): p. 225-229.

154. Matsumoto, M., et al., *Activation of the Transcription Factor ISGF3 by Interferon-gamma.* Biological Chemistry, 1999. **380**(6): p. 699-703.

155. Takaoka, A., *Cross Talk Between Interferon-gamma and -alpha /beta Signaling Components in Caveolar Membrane Domains.* Science, 2000. **288**(5475): p. 2357-2360.

156. Janahi, E.M. and M.J. McGarvey, *The inhibition of hepatitis B virus by APOBEC cytidine deaminases.* Journal of Viral Hepatitis, 2013. **20**(12): p. 821-828.

157. Maher, S.G., et al., *IFN-α and IFN-λ differ in their antiproliferative effects and duration of JAK/STAT signaling activity.* Cancer Biology & Therapy, 2008. **7**(7): p. 1109-1115.

158. Pagliaccetti, N.E. and M.D. Robek, *Interferon-λ in the Immune Response to Hepatitis B Virus and Hepatitis C Virus.* Journal of Interferon & Cytokine Research, 2010. **30**(8): p. 585-590.

159. Phillips, S., et al., *Peg-Interferon Lambda Treatment Induces Robust Innate and Adaptive Immunity in Chronic Hepatitis B Patients.* Frontiers in Immunology, 2017. **8**.

160. Rehermann, B., et al., *Cytotoxic T lymphocyte responsiveness after resolution of chronic hepatitis B virus infection.* Journal of Clinical Investigation, 1996. **97**(7): p. 1655-1665.

161. Lau, G.K., et al., *Clearance of hepatitis B surface antigen after bone marrow transplantation: Role of adoptive immunity transfer.* 1997. **25**(6): p. 1497-1501.

162. Kosinska, A.D., T. Bauer, and U. Protzer, *Therapeutic vaccination for chronic hepatitis B.* Curr Opin Virol, 2017. **23**: p. 75-81.

163. Li, J., et al., *Research progress of therapeutic vaccines for treating chronic hepatitis B.* Human Vaccines & Immunotherapeutics, 2017. **13**(5): p. 986-997.

164. Pol, S., et al., *Specific vaccine therapy in chronic hepatitis B infection.* Lancet, 1994. **344**(8918): p. 342.

165. Hoa, P.T.L., et al., *Randomized Controlled Study Investigating Viral Suppression and Serological Response following Pre-S1/Pre-S2/S Vaccine Therapy Combined with Lamivudine Treatment in HBeAg-Positive Patients with Chronic Hepatitis B.* Antimicrobial Agents and Chemotherapy, 2009. **53**(12): p. 5134-5140.

166. Vandepapeliere, P., et al., *Therapeutic vaccination of chronic hepatitis B patients with virus suppression by antiviral therapy: a randomized, controlled study of co-administration of HBsAg/AS02 candidate vaccine and lamivudine.* Vaccine, 2007. **25**(51): p. 8585-97.

167. Al-Mahtab, M., et al., *Therapeutic potential of a combined hepatitis B virus surface and core antigen vaccine in patients with chronic hepatitis B.* Hepatology International, 2013. **7**(4): p. 981-989.

168. Mancini, M., et al., *DNA-mediated immunization in a transgenic mouse model of the hepatitis B surface antigen chronic carrier state.* 1996. **93**(22): p. 12496-12501.

169. Yang, S.H., et al., *Correlation of antiviral T-cell responses with suppression of viral rebound in chronic hepatitis B carriers: a proof-of-concept study.* 2006. **13**(14): p. 1110-1117.

170. Giel-Moloney, M., et al., *Recombinant HIV-1 vaccine candidates based on replication-defective flavivirus vector.* Scientific Reports, 2019. **9**(1).

171. Gomez, C.E., et al., *The HIV/AIDS Vaccine Candidate MVA-B Administered as a Single Immunogen in Humans Triggers Robust, Polyfunctional, and Selective Effector Memory T Cell Responses to HIV-1 Antigens.* 2011. **85**(21): p. 11468-11478.

172. Cavenaugh, J.S., et al., *Partially Randomized, Non-Blinded Trial of DNA and MVA Therapeutic Vaccines Based on Hepatitis B Virus Surface Protein for Chronic HBV Infection.* PLoS ONE, 2011. **6**(2): p. e14626.

173. Sallberg, M., et al., *Genetic immunization of chimpanzees chronically infected with the hepatitis B virus, using a recombinant retroviral vector encoding the hepatitis B virus core antigen.* Hum Gene Ther, 1998. **9**(12): p. 1719-29.

174. Volz, A. and G. Sutter, *Modified Vaccinia Virus Ankara*. 2017, Elsevier. p. 187-243.

175. Antoine, G., et al., *The complete genomic sequence of the modified vaccinia Ankara strain: comparison with other orthopoxviruses.* Virology, 1998. **244**(2): p. 365-96.

176. Antoine, G., et al., *Characterization of the vaccinia MVA hemagglutinin gene locus and its evaluation as an insertion site for foreign genes.* 1996. **177**(1-2): p. 43-46.

177. Blanchard, T.J., et al., *Modified vaccinia virus Ankara undergoes limited replication in human cells and lacks several immunomodulatory proteins: implications for use as a human vaccine.* 1998. **79**(5): p. 1159-1167.

178. Altenburg, A., et al., *Modified Vaccinia Virus Ankara (MVA) as Production Platform for Vaccines against Influenza and Other Viral Respiratory Diseases.* Viruses, 2014. **6**(7): p. 2735-2761.

179. Sutter, G., et al., *A recombinant vector derived from the host range-restricted and highly attenuated MVA strain of vaccinia virus stimulates protective immunity in mice to influenza virus.* 1994. **12**(11): p. 1032-1040.

180. Verheust, C., et al., *Biosafety aspects of modified vaccinia virus Ankara (MVA)-based vectors used for gene therapy or vaccination.* Vaccine, 2012. **30**(16): p. 2623-32.

181. Backes, S., et al., *Protein-prime/modified vaccinia virus Ankara vector-boost vaccination overcomes tolerance in high-antigenemic HBV-transgenic mice.* Vaccine, 2016. **34**(7): p. 923-32.

182. Biologicals, G., *TH HBV VV-001 Clinical study.* 2017.

183. Golding, H., S. Khurana, and M. Zaitseva, *What Is the Predictive Value of Animal Models for Vaccine Efficacy in Humans?* Cold Spring Harbor Perspectives in Biology, 2017: p. a028902.

184. Paul-Ehrlich-Instituts, G.B.d.B.f.A.u.M.u.d., *3. Bekanntmachungvzur klinischen Prüfung von Arzneimitteln am Menschen.* 2006.

185. Q7, I.G., *Good manufacturing practice for active pharmaceutical ingredients.* 2000: p. 1-49.

186. Q8, I.G., *Pharamceutical development.* 2006: p. 1-9.

187. Q9, I.G., *Quality risk management.* 2005: p. 1-19.

188. Dembek, C., U. Protzer, and M. Roggendorf, *Overcoming immune tolerance in chronic hepatitis B by therapeutic vaccination.* Curr Opin Virol, 2018. **30**: p. 58-67.

189. Donnelly, M.L.L., et al., *The 'cleavage' activities of foot-and-mouth disease virus 2A site-directed mutants and naturally occurring '2A-like' sequences.* Journal of General Virology, 2001. **82**(5): p. 1027-1041.

190. Donnelly, M.L.L., et al., *Analysis of the aphthovirus 2A/2B polyprotein 'cleavage' mechanism indicates not a proteolytic reaction, but a novel translational effect: a putative ribosomal 'skip'.* Journal of General Virology, 2001. **82**(5): p. 1013-1025.

191. Liu, Z., et al., *Systematic comparison of 2A peptides for cloning multi-genes in a polycistronic vector.* Sci Rep, 2017. **7**(1): p. 2193.

192. Kim, J.H., et al., *High cleavage efficiency of a 2A peptide derived from porcine teschovirus-1 in human cell lines, zebrafish and mice.* PLoS One, 2011. **6**(4): p. e18556.

193. Kremer, M., et al., *Easy and efficient protocols for working with recombinant vaccinia virus MVA.* Methods Mol Biol, 2012. **890**: p. 59-92.

194. Wunderlich, G. and V. Bruss, *Characterization of early hepatitis B virus surface protein oligomers.* Archives of Virology, 1996. **141**(7): p. 1191-1205.

195. Dembek, C. and U. Protzer, *Mouse models for therapeutic vaccination against hepatitis B virus.* Medical Microbiology and Immunology, 2015. **204**(1): p. 95-102.

196. Hwang, J.R. and S.G. Park, *Mouse models for hepatitis B virus research.* Lab Anim Res, 2018. **34**(3): p. 85-91.

197. Dion, S., et al., *Adeno-associated virus-mediated gene transfer leads to persistent hepatitis B virus replication in mice expressing HLA-A2 and HLA-DR1 molecules.* J Virol, 2013. **87**(10): p. 5554-63.

198. Lucifora, J., et al., *Detection of the hepatitis B virus (HBV) covalently-closed-circular DNA (cccDNA) in mice transduced with a recombinant AAV-HBV vector.* Antiviral Res, 2017. **145**: p. 14-19.

199. Guidotti, L.G., et al., *Viral clearance without destruction of infected cells during acute HBV infection.* Science, 1999. **284**(5415): p. 825-9.

200. Xia, Y., et al., *Interferon-gamma and Tumor Necrosis Factor-alpha Produced by T Cells Reduce the HBV Persistence Form, cccDNA, Without Cytolysis.* Gastroenterology, 2016. **150**(1): p. 194-205.

201. Soucy, T.A., et al., *An inhibitor of NEDD8-activating enzyme as a new approach to treat cancer.* Nature, 2009. **458**(7239): p. 732-736.

202. Pollicino, T., et al., *Hepatitis B virus replication is regulated by the acetylation status of hepatitis B virus cccDNA-bound H3 and H4 histones.* Gastroenterology, 2006. **130**(3): p. 823-37.

203. Espert, L., et al., *The exonuclease ISG20 mainly localizes in the nucleolus and the Cajal (Coiled) bodies and is associated with nuclear SMN protein-containing complexes.* J Cell Biochem, 2006. **98**(5): p. 1320-33.

204. Gongora, C., et al., *Molecular cloning of a new interferon-induced PML nuclear body-associated protein.* J Biol Chem, 1997. **272**(31): p. 19457-63.

205. Weiss, C.M., et al., *The Interferon-Induced Exonuclease ISG20 Exerts Antiviral Activity through Upregulation of Type I Interferon Response Proteins.* mSphere, 2018. **3**(5).

206. Wu, N., et al., *The interferon stimulated gene 20 protein (ISG20) is an innate defense antiviral factor that discriminates self versus non-self translation.* PLoS Pathog, 2019. **15**(10): p. e1008093.

207. Qu, H., et al., *Influenza A Virus-induced expression of ISG20 inhibits viral replication by interacting with nucleoprotein.* Virus Genes, 2016. **52**(6): p. 759-767.

208. Marasco, W.A., et al., *Spatial association of HIV-1tat protein and the nucleolar transport protein B23 in stably transfected Jurkat T-cells.* Archives of Virology, 1994. **139**(1-2): p. 133-154.

209. Jarboui, M.A., et al., *Nucleolar Protein Trafficking in Response to HIV-1 Tat: Rewiring the Nucleolus.* PLoS ONE, 2012. **7**(11): p. e48702.

210. Hirano, M., et al., *Direct Interaction between Nucleolin and Hepatitis C Virus NS5B.* Journal of Biological Chemistry, 2003. **278**(7): p. 5109-5115.

211. Callé, A., et al., *Nucleolin Is Required for an Efficient Herpes Simplex Virus Type 1 Infection.* Journal of Virology, 2008. **82**(10): p. 4762-4773.

212. Lindemann, M., et al., *Control of hepatitis B virus infection in hematopoietic stem cell recipients after receiving grafts from vaccinated donors.* Bone Marrow Transplantation, 2016. **51**(3): p. 428-431.

213. Kennedy, J.S. and R.N. Greenberg, *IMVAMUNE ® : modified vaccinia Ankara strain as an attenuated smallpox vaccine.* 2009. **8**(1): p. 13-24.

214. Askari, A., et al., *Prevalence of Hepatitis B Co-Infection among HIV Positive Patients: Narrative Review Article.* Iran J Public Health, 2014. **43**(6): p. 705-12.

215. Sheehy, S.H., et al., *Phase Ia Clinical Evaluation of the Plasmodium falciparum Blood-stage Antigen MSP1 in ChAd63 and MVA Vaccine Vectors.* Molecular Therapy, 2011. **19**(12): p. 2269-2276.

216. Chea, L.S., et al., *Novel MVA Vector Expressing Anti-apoptotic Gene B13R Delays Apoptosis and Enhances Humoral Responses.* Journal of Virology, 2018.

217. Cooney, E., *Safety of and immunological response to a recombinant vaccinia virus vaccine expressing HIV envelope glycoprotein.* 1991. **337**(8741): p. 567-572.

218. Song, F., et al., *Middle East respiratory syndrome coronavirus spike protein delivered by modified vaccinia virus Ankara efficiently induces virus-neutralizing antibodies.* J Virol, 2013. **87**(21): p. 11950-4.

219. Cottingham, M.G. and S.C. Gilbert, *Rapid generation of markerless recombinant MVA vaccines by en passant recombineering of a self-excising bacterial artificial chromosome.* J Virol Methods, 2010. **168**(1-2): p. 233-6.

220. Kugler, F., et al., *Generation of recombinant MVA-norovirus: a comparison study of bacterial artificial chromosome- and marker-based systems.* Virology Journal, 2019. **16**(1).

221. Chahroudi, A., et al., *Vaccinia Virus Tropism for Primary Hematolymphoid Cells Is Determined by Restricted Expression of a Unique Virus Receptor.* 2005. **79**(16): p. 10397-10407.

222. Altenburg, A.F., et al., *Modified Vaccinia Virus Ankara Preferentially Targets Antigen Presenting Cells In Vitro, Ex Vivo and In Vivo.* Sci Rep, 2017. **7**(1): p. 8580.

223. Veillette, A., *SLAM-Family Receptors: Immune Regulators with or without SAP-Family Adaptors.* Cold Spring Harbor Perspectives in Biology, 2010. **2**(3): p. a002469-a002469.

224. Erlenhoefer, C., et al., *CD150 (SLAM) Is a Receptor for Measles Virus but Is Not Involved in Viral Contact-Mediated Proliferation Inhibition.* Journal of Virology, 2001. **75**(10): p. 4499-4505.

225. Draper, S.J. and J.L. Heeney, *Viruses as vaccine vectors for infectious diseases and cancer.* Nature Reviews Microbiology, 2010. **8**(1): p. 62-73.

226. Wold, W.S. and K. Toth, *Adenovirus vectors for gene therapy, vaccination and cancer gene therapy.* Curr Gene Ther, 2013. **13**(6): p. 421-33.

227. Huang, H., et al., *Prophylactic and therapeutic HBV vaccination by an HBs-expressing cytomegalovirus vector lacking an interferon antagonist*. 2020, Cold Spring Harbor Laboratory.

228. Ferrari, C., et al., *Cellular immune response to hepatitis B virus-encoded antigens in acute and chronic hepatitis B virus infection.* J Immunol, 1990. **145**(10): p. 3442-9.

229. Rehermann, B., et al., *The cytotoxic T lymphocyte response to multiple hepatitis B virus polymerase epitopes during and after acute viral hepatitis.* 1995. **181**(3): p. 1047-1058.

230. Scheiblhofer, S., et al., *Influence of protein fold stability on immunogenicity and its implications for vaccine design.* Expert Review of Vaccines, 2017. **16**(5): p. 479-489.

231. Lin, Y.J., et al., *Hepatitis B Virus Nucleocapsid but Not Free Core Antigen Controls Viral Clearance in Mice.* 2012. **86**(17): p. 9266-9273.

232. Kim, J.H., et al., *High Cleavage Efficiency of a 2A Peptide Derived from Porcine Teschovirus-1 in Human Cell Lines, Zebrafish and Mice.* PLoS ONE, 2011. **6**(4): p. e18556.

233. Liu, Z., et al., *Systematic comparison of 2A peptides for cloning multi-genes in a polycistronic vector.* Scientific Reports, 2017. **7**(1).

234. Plummer, E.M. and M. Manchester, *Viral nanoparticles and virus-like particles: platforms for contemporary vaccine design.* Wiley Interdisciplinary Reviews: Nanomedicine and Nanobiotechnology, 2011. **3**(2): p. 174-196.

235. Horng, J.-H., et al., *HBV X protein-based therapeutic vaccine accelerates viral antigen clearance by mobilizing monocyte infiltration into the liver in HBV carrier mice.* Journal of Biomedical Science, 2020. **27**(1).

236. Chao, C.C.K., *Inhibition of apoptosis by oncogenic hepatitis B virus X protein: Implications for the treatment of hepatocellular carcinoma.* 2016. **8**(25): p. 1061.

237. Fu, S., et al., *Hepatitis B virus X protein in liver tumor microenvironment.* 2016.

238. Lin, Y.J., et al., *Hepatitis B virus core antigen determines viral persistence in a C57BL/6 mouse model.* 2010. **107**(20): p. 9340-9345.

239. Lin, Y.J., et al., *Hepatitis B Virus Nucleocapsid but Not Free Core Antigen Controls Viral Clearance in Mice.* Journal of Virology, 2012. **86**(17): p. 9266-9273.

240. Maruyama, T., et al., *The serology of chronic hepatitis B infection revisited.* 1993. **91**(6): p. 2586-2595.

241. Milich, D.R., et al., *Antibody production to the nucleocapsid and envelope of the hepatitis B virus primed by a single synthetic T cell site.* Nature, 1987. **329**(6139): p. 547-549.

242. Milich, D.R., et al., *Immune response to hepatitis B virus core antigen (HBcAg): localization of T cell recognition sites within HBcAg/HBeAg.* J Immunol, 1987. **139**(4): p. 1223-31.

243. Milich, D. and A. McLachlan, *The nucleocapsid of hepatitis B virus is both a T-cell-independent and a T-cell-dependent antigen.* 1986. **234**(4782): p. 1398-1401.

244. Julithe, R., G. Abou-Jaoude, and C. Sureau, *Modification of the Hepatitis B Virus Envelope Protein Glycosylation Pattern Interferes with Secretion of Viral Particles, Infectivity, and Susceptibility to Neutralizing Antibodies.* Journal of Virology, 2014. **88**(16): p. 9049-9059.

245. Mehta, A., et al., *Hepatitis B virus (HBV) envelope glycoproteins vary drastically in their sensitivity to glycan processing: Evidence that alteration of a single N-linked glycosylation site can regulate HBV secretion.* 1997. **94**(5): p. 1822-1827.

246. Suffner, S., et al., *Domains of the Hepatitis B Virus Small Surface Protein S Mediating Oligomerization.* Journal of Virology, 2018. **92**(11).

247. Bohm, W., et al., *Exogenous hepatitis B surface antigen particles processed by dendritic cells or macrophages prime murine MHC class I-restricted cytotoxic T lymphocytes in vivo.* J Immunol, 1995. **155**(7): p. 3313-21.

248. Schirmbeck, R., et al., *Processing of exogenous heat-aggregated (denatured) and particulate (native) hepatitis B surface antigen for class I-restricted epitope presentation.* J Immunol, 1995. **155**(10): p. 4676-84.

249. Ning, X., et al., *Common and Distinct Capsid and Surface Protein Requirements for Secretion of Complete and Genome-Free Hepatitis B Virions.* Journal of Virology, 2018. **92**(14): p. JVI.00272-18.

250. Sutter, G. and B. Moss, *Nonreplicating vaccinia vector efficiently expresses recombinant genes.* Proceedings of the National Academy of Sciences, 1992. **89**(22): p. 10847-10851.

251. Vanwolleghem, T., et al., *Re-evaluation of hepatitis B virus clinical phases by systems biology identifies unappreciated roles for the innate immune response and B cells.* Hepatology, 2015. **62**(1): p. 87-100.

252. Kusumoto, S., et al., *Reactivation of hepatitis B virus following rituximab-plus-steroid combination chemotherapy.* J Gastroenterol, 2011. **46**(1): p. 9-16.

253. Seto, W.-K., et al., *Hepatitis B Reactivation in Patients With Previous Hepatitis B Virus Exposure Undergoing Rituximab-Containing Chemotherapy for Lymphoma: A Prospective Study.* Journal of Clinical Oncology, 2014. **32**(33): p. 3736-3743.

254. Cyster, J.G. and C.D.C. Allen, *B Cell Responses: Cell Interaction Dynamics and Decisions.* Cell, 2019. **177**(3): p. 524-540.

255. Harwood, N.E. and F.D. Batista, *Early Events in B Cell Activation.* Annual Review of Immunology, 2010. **28**(1): p. 185-210.

256. Zhu, D., et al., *Clearing Persistent Extracellular Antigen of Hepatitis B Virus: An Immunomodulatory Strategy To Reverse Tolerance for an Effective Therapeutic Vaccination.* The Journal of Immunology, 2016. **196**(7): p. 3079-3087.

257. Michler, T., et al., *Knockdown of Virus Antigen Expression Increases Therapeutic Vaccine Efficacy in High-Titer Hepatitis B Virus Carrier Mice.* Gastroenterology, 2020. **158**(6): p. 1762-1775 e9.

258. Mueller, S.N. and R. Ahmed, *High antigen levels are the cause of T cell exhaustion during chronic viral infection.* Proceedings of the National Academy of Sciences, 2009. **106**(21): p. 8623-8628.

259. Cai, S., et al., *Serum hepatitis B core antibody levels predict HBeAg seroconversion in chronic hepatitis B patients with high viral load treated with nucleos(t)ide analogs.* Infection and Drug Resistance, 2018. **Volume 11**: p. 469-477.

260. Fan, R., et al., *Baseline quantitative hepatitis B core antibody titre alone strongly predicts HBeAg seroconversion across chronic hepatitis B patients treated with peginterferon or nucleos(t)ide analogues.* 2016. **65**(2): p. 313-320.

261. Wang, C.-T., *Models for predicting hepatitis B e antigen seroconversion in response to interferon-α in chronic hepatitis B patients.* 2015. **21**(18): p. 5668.

262. Yuan, Q., et al., *Total Hepatitis B Core Antigen Antibody, a Quantitative Non-Invasive Marker of Hepatitis B Virus Induced Liver Disease.* PLoS One, 2015. **10**(6): p. e0130209.

263. Ma, Z., et al., *Toward a Functional Cure for Hepatitis B: The Rationale and Challenges for Therapeutic Targeting of the B Cell Immune Response.* Frontiers in Immunology, 2019. **10**.

264. Caviglia, G.P., et al., *Quantitation of HBV cccDNA in anti-HBc-positive liver donors by droplet digital PCR: A new tool to detect occult infection.* J Hepatol, 2018. **69**(2): p. 301-307.

265. Chen, M.T., et al., *A function of the hepatitis B virus precore protein is to regulate the immune response to the core antigen.* Proceedings of the National Academy of Sciences, 2004. **101**(41): p. 14913-14918.

266. Gill, U.S. and N.E. McCarthy, *CD4 T cells in hepatitis B virus: "You don't have to be cytotoxic to work here and help".* Journal of Hepatology, 2020. **72**(1): p. 9-11.

267. Rivino, L., et al., *Hepatitis B virus–specific T cells associate with viral control upon nucleos(t)ide-analogue therapy discontinuation.* Journal of Clinical Investigation, 2018. **128**(2): p. 668-681.

268. Schuch, A., et al., *Phenotypic and functional differences of HBV core-specific versus HBV polymerase-specific CD8+ T cells in chronically HBV-infected patients with low viral load.* Gut, 2019. **68**(5): p. 905-915.

269. Kumar, B.V., T.J. Connors, and D.L. Farber, *Human T Cell Development, Localization, and Function throughout Life.* Immunity, 2018. **48**(2): p. 202-213.

270. Nolz, J.C., *Molecular mechanisms of CD8+ T cell trafficking and localization.* Cellular and Molecular Life Sciences, 2015. **72**(13): p. 2461-2473.

271. Protzer, U., M.K. Maini, and P.A. Knolle, *Living in the liver: hepatic infections.* Nature Reviews Immunology, 2012. **12**(3): p. 201-213.

272. Ye, B., et al., *T-cell exhaustion in chronic hepatitis B infection: current knowledge and clinical significance.* Cell Death & Disease, 2015. **6**(3): p. e1694-e1694.

273. Wherry, E.J. and R. Ahmed, *Memory CD8 T-Cell Differentiation during Viral Infection.* Journal of Virology, 2004. **78**(11): p. 5535-5545.

274. Hong, M. and A. Bertoletti, *Tolerance and immunity to pathogens in early life: insights from HBV infection.* Seminars in Immunopathology, 2017. **39**(6): p. 643-652.

275. Rehermann, B. and M. Nascimbeni, *Immunology of hepatitis B virus and hepatitis C virus infection.* Nature Reviews Immunology, 2005. **5**(3): p. 215-229.

276. Zhao, W., et al., *Clearance of HBeAg and HBsAg of HBV in mice model by a recombinant HBV vaccine combined with GM-CSF and IFN-α as an effective therapeutic vaccine adjuvant.* Oncotarget, 2018. **9**(76): p. 34213-34228.

277. Stern, A.C. and T.C. Jones, *The side-effect profile of GM-CSF.* Infection, 1992. **20**(2): p. S124-S127.

278.   Ramirez, J.C., M.M. Gherardi, and M. Esteban, *Biology of Attenuated Modified Vaccinia Virus Ankara Recombinant Vector in Mice: Virus Fate and Activation of B- and T-Cell Immune Responses in Comparison with the Western Reserve Strain and Advantages as a Vaccine.* 2000. **74**(2): p. 923-933.

279.   Volz, A., et al., *Rapid Expansion of CD8+ T Cells in Wild-Type and Type I Interferon Receptor-Deficient Mice Correlates with Protection after Low-Dose Emergency Immunization with Modified Vaccinia Virus Ankara.* 2014. **88**(18): p. 10946-10957.

280.   Brudno, J.N. and J.N. Kochenderfer, *Recent advances in CAR T-cell toxicity: Mechanisms, manifestations and management.* Blood Reviews, 2019. **34**: p. 45-55.

281.   Kim, J.H., et al., *Circulating serum HBsAg level is a biomarker for HBV-specific T and B cell responses in chronic hepatitis B patients.* Scientific Reports, 2020. **10**(1).

282.   Flisiak, R., J. Jaroszewicz, and M. Łucejko, *siRNA drug development against hepatitis B virus infection.* Expert Opinion on Biological Therapy, 2018. **18**(6): p. 609-617.

283.   Foster, J., et al., *Phase 1 study of pevonedistat (MLN4924) in combination with temozolomide (TMZ) and irinotecan (IRN) in pediatric patients with recurrent or refractory solid tumors (ADVL1615).* Journal of Clinical Oncology, 2019. **37**(15_suppl): p. e21521-e21521.

284.   Woo, A.S.J., R. Kwok, and T. Ahmed, *Alpha-interferon treatment in hepatitis B.* Annals of Translational Medicine, 2017. **5**(7): p. 159-159.

285.   Pardi, N., et al., *mRNA vaccines — a new era in vaccinology.* Nature Reviews Drug Discovery, 2018. **17**(4): p. 261-279.

286.   Chmielewska, A.M., et al., *Combined Adenovirus Vector and Hepatitis C Virus Envelope Protein Prime-Boost Regimen Elicits T Cell and Neutralizing Antibody Immune Responses.* 2014. **88**(10): p. 5502-5510.

287.   Korsholm, K.S., et al., *T-helper 1 and T-helper 2 adjuvants induce distinct differences in the magnitude, quality and kinetics of the early inflammatory response at the site of injection.* 2010. **129**(1): p. 75-86.

288.   De Beijer, M.T.A., et al., *Discovery and Selection of Hepatitis B Virus-Derived T Cell Epitopes for Global Immunotherapy Based on Viral Indispensability, Conservation, and HLA-Binding Strength.* Journal of Virology, 2019. **94**(7).

289.   Marr, L., et al., *Myristoylation increases the CD8+T-cell response to a GFP prototype antigen delivered by modified vaccinia virus Ankara.* Journal of General Virology, 2016. **97**(4): p. 934-940.

290.   Ura, T., K. Okuda, and M. Shimada, *Developments in Viral Vector-Based Vaccines.* Vaccines, 2014. **2**(3): p. 624-641.

291.   Paul, *Epigenetics and Genetics of Viral Latency.* Cell Host & Microbe, 2016. **19**(5): p. 619-628.

292.   Smith, H.C., et al., *Functions and regulation of the APOBEC family of proteins.* Seminars in Cell & Developmental Biology, 2012. **23**(3): p. 258-268.

293.   Bloom, K., et al., *Gene Therapy for Chronic HBV—Can We Eliminate cccDNA?* Genes, 2018. **9**(4): p. 207.

294.   Levrero, M., et al., *Control of cccDNA function in hepatitis B virus infection.* Journal of Hepatology, 2009. **51**(3): p. 581-592.

295.   Zhu, A., et al., *HBV cccDNA and Its Potential as a Therapeutic Target.* Journal of Clinical and Translational Hepatology, 2019. **7**(X): p. 1-5.

296.   Nassal, M., *HBV cccDNA: viral persistence reservoir and key obstacle for a cure of chronic hepatitis B.* Gut, 2015. **64**(12): p. 1972-1984.

297.   Bonvin, M., et al., *Interferon-inducible expression of APOBEC3 editing enzymes in human hepatocytes and inhibition of hepatitis B virus replication.* 2006. **43**(6): p. 1364-1374.

298.   Burns, M.B., et al., *APOBEC3B is an enzymatic source of mutation in breast cancer.* Nature, 2013. **494**(7437): p. 366-370.

299.   Salter, J.D., R.P. Bennett, and H.C. Smith, *The APOBEC Protein Family: United by Structure, Divergent in Function.* Trends in Biochemical Sciences, 2016. **41**(7): p. 578-594.

300. Chapman, J., et al., *The effect of APOBEC3B deaminase on double-stranded DNA*. 2019, Cold Spring Harbor Laboratory.

301. Silvas, T.V., et al., *Substrate sequence selectivity of APOBEC3A implicates intra-DNA interactions.* Scientific Reports, 2018. **8**(1).

302. Sekiba, K., et al., *Pevonedistat, a Neuronal Precursor Cell-Expressed Developmentally Down-Regulated Protein 8–Activating Enzyme Inhibitor, Is a Potent Inhibitor of Hepatitis B Virus.* Hepatology, 2019. **69**(5): p. 1903-1915.

303. Xie, M., et al., *Neddylation inhibitor MLN4924 has anti-HBV activity via modulating the ERK-HNF1α-C/EBPα-HNF4α axis.* Journal of Cellular and Molecular Medicine, 2020.

304. Hodgson, A.J., et al., *Hepatitis B virus regulatory HBx protein binding to DDB1 is required but is not sufficient for maximal HBV replication.* Virology, 2012. **426**(1): p. 73-82.

305. Murakami, S., *Hepatitis B Virus X Protein: Structure, Function and Biology.* Intervirology, 1999. **42**(2-3): p. 81-99.

306. Liu, N., et al., *HDM2 Promotes NEDDylation of Hepatitis B Virus HBx To Enhance Its Stability and Function.* Journal of Virology, 2017. **91**(16): p. e00340-17.

307. Sarantopoulos, J., et al., *Phase I Study of the Investigational NEDD8-Activating Enzyme Inhibitor Pevonedistat (TAK-924/MLN4924) in Patients with Advanced Solid Tumors.* Clinical Cancer Research, 2016. **22**(4): p. 847-857.

308. Swords, R.T., et al., *Pevonedistat (MLN4924), a First-in-Class NEDD8-activating enzyme inhibitor, in patients with acute myeloid leukaemia and myelodysplastic syndromes: a phase 1 study.* British Journal of Haematology, 2015. **169**(4): p. 534-543.

309. Sekiba, K., et al., *Inhibition of HBV Transcription From cccDNA With Nitazoxanide by Targeting the HBx–DDB1 Interaction.* Cellular and Molecular Gastroenterology and Hepatology, 2019. **7**(2): p. 297-312.

310. Schmidt, J., H.E. Blum, and R. Thimme, *T-cell responses in hepatitis B and C virus infection: similarities and differences.* 2013. **2**(3): p. e15.

311. Bowers, E.M., et al., *Virtual Ligand Screening of the p300/CBP Histone Acetyltransferase: Identification of a Selective Small Molecule Inhibitor.* 2010. **17**(5): p. 471-482.

312. Jin, Q., et al., *Distinct roles of GCN5/PCAF-mediated H3K9ac and CBP/p300-mediated H3K18/27ac in nuclear receptor transactivation.* The EMBO Journal, 2011. **30**(2): p. 249-262.

313. Tropberger, P., et al., *Regulation of Transcription through Acetylation of H3K122 on the Lateral Surface of the Histone Octamer.* Cell, 2013. **152**(4): p. 859-872.

314. Marcos-Villar, L., et al., *Epigenetic control of influenza virus: role of H3K79 methylation in interferon-induced antiviral response.* Scientific Reports, 2018. **8**(1).

315. Dandri, M., *Epigenetic modulation in chronic hepatitis B virus infection.* Seminars in Immunopathology, 2020. **42**(2): p. 173-185.

316. Zhang, D., et al., *Histone deacetylases and acetylated histone H3 are involved in the process of hepatitis B virus DNA replication.* Life Sci, 2019. **223**: p. 1-8.

317. Liu, F., et al., *Alpha-Interferon Suppresses Hepadnavirus Transcription by Altering Epigenetic Modification of cccDNA Minichromosomes.* PLoS Pathogens, 2013. **9**(9): p. e1003613.

318. Ramos, J.C. and I.S. Lossos, *Newly Emerging Therapies Targeting Viral-Related Lymphomas.* Current Oncology Reports, 2011. **13**(5): p. 416-426.

319. Pederson, T., *The Nucleolus.* Cold Spring Harbor Perspectives in Biology, 2011. **3**(3): p. a000638-a000638.

320. Ritossa, F.M., et al., *On the chromosomal distribution of DNA complementary to ribosomal and soluble RNA.* Natl Cancer Inst Monogr, 1966. **23**: p. 449-72.

321. Andersen, J.S., et al., *Nucleolar proteome dynamics.* Nature, 2005. **433**(7021): p. 77-83.

322. Pendle, A.F., *Proteomic Analysis of the Arabidopsis Nucleolus Suggests Novel Nucleolar Functions.* 2004. **16**(1): p. 260-269.

323. Kobayashi, J., et al., *Nucleolin Participates in DNA Double-Strand Break-Induced Damage Response through MDC1-Dependent Pathway.* 2012. **7**(11): p. e49245.

324. Tsekrekou, M., K. Stratigi, and G. Chatzinikolaou, *The Nucleolus: In Genome Maintenance and Repair.* International Journal of Molecular Sciences, 2017. **18**(7): p. 1411.

325. Salvetti, A. and A. Greco, *Viruses and the nucleolus: the fatal attraction.* Biochim Biophys Acta, 2014. **1842**(6): p. 840-7.

326. Espert, L., et al., *The exonuclease ISG20 mainly localizes in the nucleolus and the Cajal (Coiled) bodies and is associated with nuclear SMN protein-containing complexes.* 2006. **98**(5): p. 1320-1333.

327. Degols, G., P. Eldin, and N. Mechti, *ISG20, an actor of the innate immune response.* Biochimie, 2007. **89**(6-7): p. 831-5.

328. Zheng, Z., L. Wang, and J. Pan, *Interferon-stimulated gene 20-kDa protein (ISG20) in infection and disease: Review and outlook.* Intractable & Rare Diseases Research, 2017. **6**(1): p. 35-40.

329. Imam, H., et al., *Interferon-stimulated gene 20 (ISG20) selectively degrades N6-methyladenosine modified Hepatitis B Virus transcripts.* PLOS Pathogens, 2020. **16**(2): p. e1008338.

330. Leong, C.R., et al., *Interferon-stimulated gene of 20 kDa protein (ISG20) degrades RNA of hepatitis B virus to impede the replication of HBV in vitro and in vivo.* Oncotarget, 2016. **7**(42): p. 68179-68193.

331. Liu, Y., et al., *Interferon-inducible ribonuclease ISG20 inhibits hepatitis B virus replication through directly binding to the epsilon stem-loop structure of viral RNA.* PLOS Pathogens, 2017. **13**(4): p. e1006296.

332. Couté, Y., et al., *ISG20L2, a Novel Vertebrate Nucleolar Exoribonuclease Involved in Ribosome Biogenesis.* Molecular & Cellular Proteomics, 2008. **7**(3): p. 546-559.

333. Gongora, C., *A unique ISRE, in the TATA-less human Isg20 promoter, confers IRF-1-mediated responsiveness to both interferon type I and type II.* Nucleic Acids Research, 2000. **28**(12): p. 2333-2341.

334. Gongora, C., et al., *Molecular Cloning of a New Interferon-induced PML Nuclear Body-associated Protein.* Journal of Biological Chemistry, 1997. **272**(31): p. 19457-19463.

335. Espert, L., et al., *The exonuclease ISG20 mainly localizes in the nucleolus and the Cajal (Coiled) bodies and is associated with nuclear SMN protein-containing complexes.* Journal of Cellular Biochemistry, 2006. **98**(5): p. 1320-1333.

336. Margolin, W., *The Price of Tags in Protein Localization Studies.* 2012. **194**(23): p. 6369-6371.

337. Espert, L., et al., *ISG20, a New Interferon-induced RNase Specific for Single-stranded RNA, Defines an Alternative Antiviral Pathway against RNA Genomic Viruses.* Journal of Biological Chemistry, 2003. **278**(18): p. 16151-16158.

338. Wang, S.-H., et al., *Intracellular localization and determination of a nuclear localization signal of the core protein of dengue virus.* 2002. **83**(12): p. 3093-3102.

339. Wu, N., et al., *The interferon stimulated gene 20 protein (ISG20) is an innate defense antiviral factor that discriminates self versus non-self translation.* PLOS Pathogens, 2019. **15**(10): p. e1008093.

340. Suslov, A., et al., *Hepatitis B Virus Does Not Interfere With Innate Immune Responses in the Human Liver.* Gastroenterology, 2018. **154**(6): p. 1778-1790.

341. Liebler, D.C. and L.J. Zimmerman, *Targeted Quantitation of Proteins by Mass Spectrometry.* Biochemistry, 2013. **52**(22): p. 3797-3806.

342. Hayano, T., et al., *Proteomic Analysis of Human Nop56p-associated Pre-ribosomal Ribonucleoprotein Complexes.* Journal of Biological Chemistry, 2003. **278**(36): p. 34309-34319.

343. Michalak, T. and A. Nowoslawski, *Hepatitis B virus in nucleoli of liver cells.* N Engl J Med, 1977. **297**(14): p. 787-8.

344. Selzer, L. and A. Zlotnick, *Assembly and Release of Hepatitis B Virus.* Cold Spring Harbor Perspectives in Medicine, 2015: p. a021394.

345. Sonntag, F., K. Schmidt, and J.A. Kleinschmidt, *A viral assembly factor promotes AAV2 capsid formation in the nucleolus.* Proceedings of the National Academy of Sciences, 2010. **107**(22): p. 10220-10225.

346. Ning, B. and C. Shih, *Nucleolar Localization of Human Hepatitis B Virus Capsid Protein.* Journal of Virology, 2004. **78**(24): p. 13653-13668.

347. Gallucci, L. and M. Kann, *Nuclear Import of Hepatitis B Virus Capsids and Genome.* Viruses, 2017. **9**(1): p. 21.

348. Okuwaki, M., et al., *Function of nucleophosmin/B23, a nucleolar acidic protein, as a histone chaperone.* FEBS Letters, 2001. **506**(3): p. 272-276.

349. Irmisch, A., et al., *Smc5/6 maintains stalled replication forks in a recombination-competent conformation.* 2009. **28**(2): p. 144-155.

350. Macpherson, I. and M. Stoker, *Polyoma transformation of hamster cell clones--an investigation of genetic factors affecting cell competence.* Virology, 1962. **16**: p. 147-51.

351. Henle, G., et al., *STUDIES ON PERSISTENT INFECTIONS OF TISSUE CULTURES.* Journal of Experimental Medicine, 1958. **108**(4): p. 537-560.

352. Himly, M., et al., *The DF-1 Chicken Fibroblast Cell Line: Transformation Induced by Diverse Oncogenes and Cell Death Resulting from Infection by Avian Leukosis Viruses.* Virology, 1998. **248**(2): p. 295-304.

353. Graham, F.L., et al., *Characteristics of a Human Cell Line Transformed by DNA from Human Adenovirus Type 5.* Journal of General Virology, 1977. **36**(1): p. 59-72.

354. Aden, D.P., et al., *Controlled synthesis of HBsAg in a differentiated human liver carcinoma-derived cell line.* Nature, 1979. **282**(5739): p. 615-616.

355. Marion, M.J., O. Hantz, and D. Durantel, *The HepaRG cell line: biological properties and relevance as a tool for cell biology, drug metabolism, and virology studies.* Methods Mol Biol, 2010. **640**: p. 261-72.

356. Protzer, U., et al., *Antiviral activity and hepatoprotection by heme oxygenase-1 in hepatitis B virus infection.* Gastroenterology, 2007. **133**(4): p. 1156-65.

357. Kosinska, A.D., et al., *Synergy of therapeutic heterologous prime-boost hepatitis B vaccination with CpG-application to improve immune control of persistent HBV infection.* Scientific Reports, 2019. **9**(1).

358. Gripon, P., et al., *Nonlinear partial differential equations and applications: Infection of a human hepatoma cell line by hepatitis B virus.* Proceedings of the National Academy of Sciences, 2002. **99**(24): p. 15655-15660.

359. Xia, Y., et al., *Analyses of HBV cccDNA Quantification and Modification.* Methods Mol Biol, 2017. **1540**: p. 59-72.

Acknowledgements

First and foremost, I would like to thank Prof. Dr. Protzer for giving me the opportunity to do my PhD thesis in her research group and for allowing me the freedom of exploring a broad range of projects and methods. I am especially grateful for my inclusion into the TherVacB vaccine development team, giving me the opportunity to work on a highly translational and clinically relevant project. I furthermore want to thank her for her extensive support throughout the years, on both, a personal, as well as a scientific level.

I would also like to thank my second supervisor, Prof. Dr. Sattler for taking an interest in my projects and for supporting me with helpful advice on protein-DNA interactions. I especially want to thank him and Dr. Alisha Jones for the excellent cooperation in the context of the ISG20 project

Special thanks go to the two Postdocs who mentored me during by PhD: Dr. Katrin Singethan, who first introduced me to virology and from whom I absorbed not only a broad range of techniques but also a fascination for unusual research topics, and Dr. Daniela Stadler who guided me on my travels through the world of HBV molecular biology with all its associated challenges with high amounts of patience and scientific knowledge and who proof-red this thesis.

Equally, I thank Dr. Anna Kosinska for all her work in the MVA-HBVac project and her extensive support during the writing of our paper. Without her, her great knowledge in immunology and her expert skills in conducting *in vivo* experiments, this thesis would not have been possible.

Lastly, I wanted to thank all my colleagues and friends from the institute who made the last four years of my life into a very enjoyable, if sometimes stressful, time. Julia, for always being there and for her extensive support through the whole HBVac project as well as the day-to-day lab life. Romina, for organizing the whole lab-life and preventing its drop into anarchy as well as for her criticism and encouragement to use more colors in my presentations. Andreas, for the many scientific (and non-scientific) discussions, for the great working atmosphere during the RNA mouse-screening project and of course for proof-reading this thesis. I would also like to thank all the other recent and former people of our institute (unfortunately there are too many to name them all), without you my time here would not have been the same.

Mein besonderer Dank gilt meiner Familie, die mich über die letzten Jahre (und Jahrzehnte) immer unterstützt und ermutigt hat. Vielen, vielen Dank dafür, dass ihr immer für mich da seid, auch wenn ich mich viel zu selten melde. Zu guter Letzt möchte ich mich bei Enikö bedanken, dafür das sie mich für die letzten zwei Jahre begleitet und unterstützt hat. Durch dich ist mein Leben deutlich bunter geworden und dafür bin ich dir zutiefst dankbar.